Simulation of heat and mass transfer in spray drying

J. van der Lijn

Simulation of heat and mass transfer in spray drying

Abstract

A survey is given of heat and mass transfer around droplets in spray dryers and the diffusional transport inside them. A calculational model is developed which includes variable diffusion coefficients in the drying liquid and swelling or shrinking of droplets. Calculations for droplets containing soluble solids show how the drying histories of droplets are influenced by three extreme patterns of air circulation and spray dispersion, and by droplet inflation. The influence of these factors on the properties of spray-dried liquid foods are discussed. Furthermore diffusion equations for binary systems are surveyed and diffusion coefficients for super-saturated aqueous maltose solutions are reported.

Descriptors: droplets, drying of foods, diffusion equations, diffusion of sugars, maltose.

Stellingen

1. Een voorspelling van het droogverloop van druppels in een verstuivings-
   droger zal pas mogelijk zijn, als meer bekend is over de menging van
   lucht en druppels in de droger.

   Dit proefschrift

2. Het door Verhey op grond van experimenten veronderstelde droogverloop
   van druppels in een verstuivingsdroger is plausibel. Het is echter, in
   tegenstelling tot zijn stelling daarover, niet in strijd met een beschrij-
   ving van het massatransport in de drogende druppels onder de aanname van
   moleculaire diffusie.

   J.G.P.Verhey – stelling nr. 4 bij
   Vacuolenvorming bij het verstuivingsdrogen.
   proefschrift Wageningen, 1973

3. De veronderstelling van Rulkens, dat aromaverliezen tijdens het verstui-
   vingsdrogen in belangrijke mate op zouden treden tijdens de periode van
   druppelvorming, waarbij ten gevolge van hoge turbulentie de weerstand
   voor stoftransport in de vloeistoffase verwaarloosbaar zou zijn, is aan-
   vechtbaar op grond van het door hem zelf gevonden geringe effect van de
   relatieve vluchtigheid van de aromacomponenten op de retentie.

   W.H.Rulkens – Retention of volatile trace components
   in drying aqueous carbohydrate solutions.
   proefschrift Eindhoven 1973

4. De door Ladisch vermelde recirculatie van drooglucht om aromaverlies
   te beperken is zelden zinvol.

   G.Ladisch – Die Ernährungswirtschaft/Lebensmittel-
   technik 9.704 (1968)

5. Bij opgaven van de grootteverdeling van een mobiele disperse fase
   wordt ten onrechte zelden aangegeven of de locale verdeling danwel de
   verdeling in het per tijdseenheid passerende materiaal bedoeld wordt.

6. De verzamelingen van *algemene* oplossingen van warmte- en stoftransport-
   problemen in de gebruikelijke handboeken kunnen aanmerkelijk in bruikbaar-
   heid toenemen als naast analytische oplossingen meer numerieke oplossingen
   opgenomen worden.

   > *H.S.Carlslaw & J.C.Jaeger - Conduction of heat in*
   > *solids. Oxford, 1959*
   > *J.Crank - The mathematics of diffusion. Oxford, 1956.*
   > *A.V.Luikov - Analytical heat diffusion theory.*
   > *New York, 1968*

7. Het overheidstoezicht op levensmiddelen zal aan effectiviteit winnen, als
   het zich meer dan thans richt op kwaliteitsbeheersing en risicobeperking
   tijdens de productie. Daartoe dient het principe van toezicht op de fabri-
   cage in de Warenwet meer uitgewerkt te worden en de Keuringsdiensten van
   Waren zouden meer technologisch geschoold personeel aan moeten stellen.

8. Aan de risico's verbonden aan (fysische) processen bij de produktie van
   levensmiddelen wordt in het algemeen te weinig aandacht besteed in verhou-
   ding tot de risico's verbonden aan het gebruik van chemische hulpstoffen
   (additieven).

9. Het toestaan van de aanwezigheid van additieven in een voedingsmiddel als
   deze er in zijn gebracht via grondstoffen die aan de normen voldoen
   (carry-over), is een automatisme, dat in de plaats treedt van de gebruike-
   lijke afweging van nut en risico van de additieven.

10. Omdat de werkelijkheid oneindig genuanceerder is dan enig model ervan, is
    elk model van de werkelijkheid falsificeerbaar. Wetenschap is danook de
    kunst van het simplificeren.

11. De hope des vaderlands is niet te veel hope des vaderlands.

> *J.van der Lijn*
> *dissertatie Simulation of heat and mass transfer*
> *in spray drying*

Contents

Dankwoord

Curriculum vitae

De auteur werd geboren op 16 oktober 1942 te Amsterdam. Hij haalde in 1959 het diploma HBS-B aan het Spinoza Lyceum aldaar en begon in het zelfde jaar zijn studie aan de Landbouwhogeschool te Wageningen. Na in juni 1963 het kandidaatsexamen te hebben afgelegd, behaalde hij in april 1966 het diploma landbouwkundig ingenieur. Het ingenieursexamen omvatte de vakken technologie, kennis van levensmiddelen, fysische- en colloïdchemie en bedrijfsleer. Nadien was hij werkzaam als wetenschappelijk medewerker aan het Unilever Research Laboratorium Duiven (1966–1967) en aan het Centre for Industrial Research of the National Council for Research and Development, Haifa, Israël (1967–1970). Vervolgens trad hij in dienst bij de Afdeling Levensmiddelentechnologie van de Landbouwhogeschool, waar hij als wetenschappelijk assistent het promotie-onderzoek verrichtte (1970–1973). Sinds september 1973 is hij werkzaam als procestechnoloog bij Douwe Egberts Jacobs International Research.

List of symbols most commonly used

A = amplitude	m
A = area	m^2
a_w = water activity	—
$Bi = h'R/\lambda$ = Biot number	—
$Bi_m = k'R/D$ = Biot number for mass transfer	—
c = molar density	mole/m^3
c_i = molar concentration of i	mole/m^3
c_p = molar heat capacity	J/mole·K
C = heat capacity of droplet	J/K
D = diffussion coefficient; diffusivity	m^2/s
ΔE = activation energy	J/mole
F = rate of transport	kg/s
$Fo = Dt/R^2$ = Fourier number	—
Gr = Grashof number	—
h = heat transfer coefficient	W/m^2·K
H_i = partial molar enthalpy	J/mole
i = integer variable	—
j = integer variable	—
J = molar flux	mole/m^2·s
k = mass transfer coefficient	m/s
k_i = source term	kg/m^3·s
K_i = source term	mole/m^3·s
Kn = Knudsen number, Eqn (10)	—
l = distance	m
L = heat of evaporation	J/mole
M = number mean molecular weight, Eqn (A.5)	kg/mole
M_t = loss of volatile from a droplet	kg
M_i = molecular weight of component i	kg/mole
n = integer variable	—
n = refractive index	—
$Nu = 2h'R/\lambda'$ = Nusselt number	—
P = pressure	Pa
P_i = partial pressure	Pa
Pe = Peclet number, Eqn (6)	—
$Pr = \rho'c_p v'/h'$ = Prandtl number	—
q = heat flux	W/m^2
Q = rate of atomization	kg/s
r = radius	m

R = gas constant   J/mole·K
R = radius at the droplet surface   m
R_{is} = radius of bubble in droplet   m
R_{os} = radius of surroundings of droplet   m
$Re = 2Rv/v'$ = Reynolds number   —
s = transformed diffusion coefficient, Eqn (34)   mol^2/m^4·s
$Sc = v/D$ = Schmidt number   —
$Sh = 2k'R/D'$ = Sherwood number   —
t = time   s
T = temperature   K or °C
u = dissolved solids based concentration, Eqn (32)   —
$\bar{v}_i$ = partial specific volume   m^3/kg
V_i = partial molar volume   m^3/mole
v = velocity   m/s
T_{wb} = wet-bulb temperature   K or °C
x = mole fraction   —
x = liquid load in spray   —
x = distance coordinate   m
y = distance   m
z = transformed distance coordinate Eqn (33)   mole
Z = z coordinate at the droplet surface   mole

α = half atomization angle   —
α_n = roots of Eqn (31)   —
β = dispersion angle of spray   —
γ_w = activity coefficient   —
θ_T = correction term in Eqn. (20)   —
λ = mean free path   m
λ = heat conductivity   W/m·K
λ_n = roots of Eqn (15)   —
v = kinematic viscosity   m^2/s
ρ = density   kg/m^3
ρ_i = partial density (concentration)   kg/m^3
φ = ratio between diffusional and conductive heat flow Eqn (21)   —
ω = mass fraction   —

Subscripts:
$_s$ = at the droplet surface
$_s$ = sugar (Appendix B)
$_{is}$ = at the surface of the bubble inside the droplet
$_\infty$ = at infinite distance
$_\infty$ = in the bulk of the continuous phase
$_\infty$ = after infinite time
$_o$ = initial
$_w$ = water
$_r$ = reference component

$_i$ = of component i

$_j$ = of component j

$_{1,2}$ = of component 1 or 2 in binary system

$_L$ = liquid

$_G$ = gas

$_{sat}$ = saturated, in equilibrium with pure water at the same temperature

Superscripts:

$'$ = in the continuous phase, gas phase

^{m} = relative to/in barycentric coordinates (see Appendix A)

* = relative to/in mole centred coordinates (see Appendix A)

^{r} = relative to/in reference component fixed coordinates (see Appendix A)

^{0} = relative to/in volume fixed coordinates (see Appendix A)

^{s} = relative to/at the surface

^{is} = relative to/at the bubble surface

$^\cdot$ = at high mass fluxes

^{c} = by conduction

^{d} = by diffusion

Bold type symbols indicate vector quantities but in specified geometries no vector notation has been used.

1 Introduction

Spray drying is a unit-operation of great importance in chemical engineering. The unit-operation is widely used in the food industry. The most important commodity in the food industry which is spray-dried, is skim milk, but also the spray drying of many other liquid foods such as fruit juices and vegetable extracts, coffee and tea extracts and other dairy products such as whey, is of economic importance. Also in the chemical industry the operation is frequently used. Examples of spray-dried products from this industry are washing powders (detergents, enzymatic powders) as well as a variety of dried salts, polymers, pigments and catalysts. Extensive surveys of products which can be spray dried are presented by Masters (1968, 1972).

A reason for the application of spray-drying is that it is one of the most practical methods, by which a solution of solids in water can be dehydrated to a solid final product. Other methods for the removal of water from such solutions, such as freeze-drying, are usually much more expensive whereas a method like liquid-liquid extraction requires the use of solvents which is often undesirable. Furthermore with spray-drying powders of desired functional properties can often be produced, and therefore it is also frequently used for products which could be dehydrated more cheaply by other methods, such as drum-drying or dewatering followed by drying of solids.

Both spray-drying economics and the product properties are strongly dependent on the physical process of heat and mass transport inside and around the evaporating droplets. Processs economics depend not only on the overall heat balances for the spray-drying process but also on the rates of transfer which determine the size of equipment. Product properties such as the bulk density of the powder, the extent of chemical conversion and enzyme inactivation, and the retention of aromas, are as a rule affected by the conditions inside the droplets during spray drying.

Hence, extensive knowledge of the drying process and of the conditions inside the drying droplets is desirable for improving the product properties, for optimization of spray drying economics and for improved design of spray-drying equipment. This knowledge should ideally be obtained from direct measurements in a spray dryer.

Measuring local humidities, temperatures and velocities inside a spray dryer and especially inside the drying droplets is hardly possible. In the absence of information from direct measurement one must therefore rely on other sources:

1

1. Some information about the temperature and concentration histories can be obtained from changes in product properties such as those caused by chemical conversion, if the dependence of the rates of change on temperature and concentration are already known from model studies (see e.g. Verhey, 1973). This empirical approach, although very convincing because the results are obtained during actual drying, does usually not explain the results. Furthermore, the changes observed are the result of a continuous process over the whole drying period and a quantitative differentiation of the process with regard to time is extremely difficult.

2. Drying characteristics of the material to be dried can be measured under optimum laboratory conditions and can be used in simulation models to calculate the drying histories of droplets under spray-drying conditions. The drying characteristics can be found by the measurement of diffusion coefficients and their dependence on temperature and water concentrations (Appendix B) or alternatively by the interpretation of a few simple drying experiments (Kerkhof, 1975; Schoeber & Thijssen, 1975).

Various models can be postulated and depending on the assumptions made different product properties will be predicted. Comparison of the calculated results with the results in actual spray-drying may show whether a model is realistic. Such an integrated theoretical and empirical approach can yield a better understanding of the process.

We should be careful, however, when drawing conclusions because several theories (several physical models) may lead to similar results. Hence, a good fit of a limited number of practical results is not yet a proof of the validity of the model. Another limitation of the theoretical approach is that the actual drying behaviour in a spray-dryer is so complex, that assumptions must be made to simplify the calculation of the temperature and drying histories of the droplets, even if fast computers are available. Such assumptions may be arbitrary. A sensitivity analysis can show, however, which assumptions play a vital role in determining the performance of the dryer and which are relatively insignificant. Thus, the analysis can reduce the computation time needed for calculations, and can also indicate the issues, which are to be studied most urgently in the practical situation.

This second approach was adopted in this report.

Extensive knowledge of some of the fundamental physical phenomena taking place in spray dryers, such as atomization and heat and mass transfer of droplets of pure liquids is available (Marshall, 1954; Dombrowski & Munday, 1968; Masters, 1972). Some authors have made calculations on the spray-drying of droplets of pure liquids (Sjenitzer, 1952, 1962; Dickinson & Marshall, 1968; Adler & Lyn, 1971; Parti & Palansz, 1974). Other authors have studied the drying of droplets containing dissolved solids, but then it was necessary to use major simplifications about the concentration pattern of the solute in the droplets; in particular it was necessary to assume a surface layer consisting of saturated solution with a constant surface vapour concentration (Arni, 1959: Charlesworth & Marshall, 1960; Baltas & Gauvin, 1969). Calculations on the drying of droplets

containing dispersed solids have been made with similar simplifications (Dlouhy & Gauvin, 1960; Krüger, 1973) or with the assumption of a simple fixed relation between the average and the surface concentrations (Stein, 1972). Kerkhof & Schoeber (1973) reviewed the modelling of the drying behaviour of droplets in spray-dryers.

When I began these investigations in 1970, no calculations were available, however, on droplets containing dissolved solids in which the diffusional transfer inside the droplet was fully included. Such calculations require much time to compute the concentration distribution inside a droplet.

One aim of this study was to provide a calculational model which would give a reasonable description of the spray-drying of liquid foods containing dissolved solids and which would therefore take diffusion inside the droplets into account. Some of the results of this study have already been applied by van der Lijn et al. (1972), Schoeber (1973), Rulkens (1973), Kerkhof & Schoeber (1973), Kerkhof (1974, 1975, 1975b), Schoeber & Thijssen (1975), van der Lijn (1976).

The physical modelling of the drying of droplets in spray dryers is discussed in Chapter 2.

The original aim of my investigation was to use the physical models to study the inflation of droplets in spray dryers. However, it was found that the mixing in spray dryers has such a crucial effect on the drying behaviour of droplets that it had to be examined first. This subject is treated in Chapter 3. Consequently, the problem of droplet inflation received only limited attention. The results are presented in Chapter 4. Finally, some remarks on the link between the theoretical models and actual drying practice are made in Chapter 5.

Various physical properties and especially diffusion coefficients had to be determined over a wide range of temperatures and soluble solids concentrations so that the calculations be relevant to actual spray-drying and could be tested in actual drying systems. These measurements, constituted an important part of the actual work. However the results are given in Appendix B because they do not belong to the central theme of this report. Part of the necessary basic diffusion theory, on which the calculations were based, is given in Appendix A for the same reason.

2 Physical models for heat and mass transfer of droplets

2.1 Introduction

The spray-drying process is one of a large family of processes in which a liquid is finely dispersed in a gas, usually with a nozzle or a rotary atomizer. At the outlet of the nozzle or atomizer a liquid film is formed which disintegrates into small droplets. The droplets move at an initial velocity of about 100 m/s. During and after formation they exchange heat, mass and momentum with the surrounding gas. This investigation is not concerned with the phenomena during the atomization of the liquid and is limited to heat and mass transfer *after* the formation of droplets. The exchange of momentum, although important in spray-drying practice and for spray-dryer design, is included in this study only for the estimation of heat and mass transfer.

Similar situations of heat and mass transfer in aerocolloidal systems may be found in the evaporation or condensation of droplets in clouds, in the spraying of pesticides, in fuel injection in diesel engines, in rocket propulsion, in gas turbines, in spray-cooling. As a result there has been a vast amount of literature published about transfer in sprays. Several surveys are available (Sideman, 1966; Resnick & Gal-Or, 1967; Gal-Or et al., 1969; Tavlarides et al., 1970). A bibliography on the older literature on sprays (Pennsylvania State Bibliography; de Juhasz, 1959) and two monographs on aerocolloidal systems may also be referred to (Fuchs, 1959; Hidy & Brock, 1970).

In the majority of these related fields, the transfer in sprays involves the evaporation of a (more or less) pure liquid into a gas. Hence, no marked concentration changes or gradients occur in the dispersed phase. As a result, mass transfer is completely governed by resistance to transfer in the continuous phase. Transfer under such conditions has been well studied. The results of those studies can be also used here to describe the heat and mass transfer outside a droplet. This subject is discussed in Section 2.2.

The purpose of the spray-drying operation is to separate a volatile liquid (usually water) from a non-volatile solid. Hence, by the nature of the process, the average concentration of the non-volatile component in the disperse phase increases and can pass through a wide range during the process. The subject of non-stationary mass transfer inside droplets is discussed in Section 2.3.

Various mechanisms may be distinguished when studying the resistance to mass transfer inside a droplet:
– The first mechanism is the formation of a solid crust at the surface of a droplet, followed by the flow of liquid through the more or less porous crust. This

4

mechanism may occur in the drying of inorganic salt solutions. By crystallization a crust forms at the surface and essentially saturated solution flows outwards through the crust. This mechanism was studied by Charlesworth & Marshall (1960). Sometimes this mechanism also occurs in the drying of slurries of finely dispersed solids.

– A second mechanism may be the formation of a rigid matrix such as a crust, through which water vapour is transported. Thus a drying front penetrates into the drying material. Extensive literature exists about the drying of capillary-porous materials (Luikov, 1964). This mechanism will usually occur as a continuation of the first mechanism.

– A third mechanism is the diffusional transport of water in a homogenous liquid phase. Concentration gradients exist in the liquid phase and the volatile component evaporates from the surface of the liquid.

– A fourth mechanism is transfer by convection in the liquid phase

All of these mechanisms may occur during actual spray-drying. Especially transfer by convection will be important during and immediately after droplet formation. Transport through a solid crust is very common in easily crystallizing materials such as inorganic salt solutions. Transfer of water vapour through dry solids often occurs in the last stages of drying. Crystallization is usually not very spontaneous because of the composition of liquid foods and a rigid matrix will often be formed at a late stage of drying. Therefore mass transfer by diffusion is thought to be the more important mechanism during the drying of many liquid foods. Sometimes as in the drying of coffee extract, the droplets remain liquid up to a late stage of the drying and cool down to a glass-like structure afterwards. Often the dried product has an amorphous or glass-like structure. Hence, if there is no important convection in the liquid the drying process can reasonably be described in terms of molecular diffusion.

A description in terms of diffusion in a liquid can sometimes also be applied when the droplets are not entirely liquid. Often a skin is formed on the surface of a droplet but the formation of a skin of concentrated liquid on a drying surface does not always behave like a solid crust. Therefore, the assumption of molecular diffusion does not exclude the presence of glass-like skin.

When small amounts of finely dispersed non-volatile material (fibres, fat) are present, the system can be described in the same terms of liquid diffusion, if the effect of tortuosity is included in the estimation of an effective diffusion coefficient.

With larger amounts of fibrous material, or dispersed material of larger size, or materials which do not remain in perfect solution (e.g. salts, proteins), a more complex mechanism results.

This investigation is restricted to a treatment of the internal mass transfer in terms of binary liquid diffusion and the calculations are based on the physical properties of supersaturated solutions of maltose in water. These solutions are considered as a model for liquid foods because they show a characteristic drying pattern with steep concentration gradients in the liquid phase. Unavoidably the results of a study with a model component do not apply to all liquid foods. However they are applicable to an important group among them.

5

The combination of the transfer in and outside the droplets into an overall physical model is described in Section 2.4.

2.2 Transfer between a droplet and a gas phase

2.2.1 Droplet velocities relative to air

Droplets emanating from a centrifugal pressure nozzle or a rotary atomizer move at high velocities relative to stationary coordinates. During their residence in the dryer this velocity is reduced to a final velocity, which is approximately the sum of the stationary falling velocity in still air, the velocity of the air, and sometimes the velocity attained in the centrifugal field of a rotary air motion. Knowledge about droplet trajectories can be used to design drying equipment so that wall deposits are avoided but here we shall only apply it to calculate heat and mass transfer to the moving droplets.

Trajectories of single droplets relative to stationary air or to air of known velocity can be calculated on the basis of the known drag coefficients for rigid spheres and their dependence on the Reynolds number of the spheres. Many data on the relation between the drag coefficient and the Reynolds number are available (Bird et al., 1960; Perry, 1973; Ihme, 1972). Trajectory calculations based on these relations are also well known (Lapple & Shephard, 1940; Coulson & Richardson, 1968).

Usually these calculations neglect the effect, on the drag coefficient of deceleration of the droplets, and of evaporation, as well as deviations from rigidity of the sphere. Ingebo (1956) gave data for evaporating and accelerating droplets which do not deviate too much from those for rigid spheres in steady motion. Hughes & Gilliland (1952), however, stated that the drag coefficients during an acceleration period are much larger than those for steady motion at the same Reynolds number. Quantification of the effects is difficult at present. Bailey et al. (1970) cited work of Eisenklam (1966) according to which the mass transfer rate affects the drag coefficient in a similar way as the rate of heat transfer discussed in Section 2.2.3.

Internal circulation in droplets is known to reduce the drag. This effect is often very marked in liquid-liquid systems. The effect of internal circulation on the drag coefficient in liquid in gas systems is as a rule negligible because of the high viscosity ratio of liquid and gas (Levich, 1962; Hadamard, 1911). Furthermore the presence of surface active materials in almost all practical systems greatly reduces internal circulation. Hughes & Gilliland (1952) concluded that 'drops in gases are rarely circulating.' Hence the assumption of a rigid sphere for the calculation of droplet velocities as a part of heat and mass transfer calculations appears justified apart from possibly a very short period immediately after droplet formation (Eqn 27).

Up to here motion of the drying air in a spray dryer has been ignored. The velocity of the drying air can have effect, however, on the relative velocity between droplets and air and, thus, on the transfer coefficients calculated from Eqns (2) and (18).

The velocities of the droplets relative to (equipment) fixed coordinates are usually known at the moment of atomization. Overall air velocities in spray-dryers are as a rule also known and these velocities are usually much smaller than the

6

initial droplet velocities. Local air velocities, however, can be much higher than the overall velocities over a cross-section of the dryer. So is it known that the droplets maintain high velocities for much longer times than would be expected from calculations for the drag in still air (Masters, 1972). The deceleration in the vicinity of the atomizing device appears to be very limited (Kerkhof & Schoeber, 1973). The difference between trajectories calculated for the deceleration of droplets in still air and the actual trajectories can be explained by the velocity of the air which is entrained in the stream of droplets emanating from the atomizer. In drying practice this situation may lead to wall deposits.

Momentum transfer from the stream of droplets to the drying air causes high air velocities in the surroundings of the droplets, and a certain pumping effect of the resulting jet (Marshall, 1954). Air entrainment in sprays was studied by Benatt & Eisenklam (1969) and Briffa & Dombrowski (1966). The velocity distributions in sprays at larger distances from the atomizer of a spray-dryer and the effects on drying histories was studied by Baltas & Gauvin (1969). However, knowledge is still far from complete as to how momentum is distributed within a spray pattern over spray droplets and entrained air (Masters, 1972).

Drawing accurate quantitative conclusions about the relative velocities which should be used in drying calculations is therefore impossible with present knowledge.

2.2.2 Mass transfer

Mass transfer from a stationary sphere to unbounded surroundings has already been analysed by Maxwell (1890). Later Langmuir (1918) arrived at similar results with the experimental data of Morse (1910): the rate of mass loss from a small sphere is proportional to the radius of the sphere and the difference between the concentration at the surface and that at an infinite distance from the surface. Hence, the flux from the surface is inversely proportional to the radius

$$J = \frac{D}{R}(c_s - c_\infty) \tag{1}$$

The same is expressed by

$$Sh = 2 \tag{1a}$$

The influence on heat and mass transfer coefficients of the motion of single spheres relative to a stationary continuous phase has been studied extensively. Many surveys on correlations between the Nusselt and Sherwood numbers on the one hand and the Reynolds, Prandtl, Schmidt, and Péclet numbers on the other hand are available (Acrivos & Taylor, 1962; Sideman & Shabtai, 1964; Pritchard & Biswas, 1967; Rowe et al., 1965; Sideman, 1966). It should be remembered, however, that the majority of these correlations apply to systems with a liquid continuous phase (low Re, high Pe). Few of the correlations are useful for liquid in air systems. Generally accepted correlations for mass transfer from single spheres in a gas stream were first given by Frössling (1938) and later with slightly different coefficients by Ranz & Marshall (1952) (Eqn 2).

7

$$Sh = 2 + 0.6\,Re^{\frac{1}{2}}Sc^{\frac{1}{3}} \tag{2}$$

However, some effects can cause deviations from the Sherwood numbers predicted by Eqns (1) and (2).

Effect of unsteady state   The use of Eqns (1) and (2) assumes a condition of steady state. As a rule the conditions during spray drying deviate from the steady state because of:
– the initial change in conditions at the start of the transfer operation,
– change in the droplet radius,
– change in the moisture concentration at the droplet surface,
– change in the moisture concentration in the air far from the surface.
Strictly Eqns (1) and (2) are not valid for these conditions. It is possible, however, to assume 'quasi steady state' conditions if such changes occur relatively slowly. Then Eqns (1) and (2) can be applied for the conditions at a given moment.

The assumption of quasi-steady behaviour is reasonable if changes in any of the parameters involved are small during the time needed for the relaxation of a change, t_{rel} (Buikov, 1962; Fuchs, 1959; Hidy & Brock, 1970) where t_{rel} is defined by

$$t_{rel} \equiv \frac{R^2}{D} \tag{3}$$

Furthermore, the effect on non-steady state conditions will be small for high Péclet numbers, because relaxation will be quicker if transport takes place through a thin boundary layer.

Fuchs (1959) discussed the evaporation of a stationary droplet in an infinite medium with boundary conditions:

$$c = c_\infty \quad \text{for} \quad r > R; \qquad t = 0 \tag{4a}$$
$$c = c_s \quad \text{for} \quad r = R; \qquad t > 0 \tag{4b}$$

Owing to the sudden change at $t = 0$ a flux which is higher than that according to the steady state calculations develops, but reduces gradually to the steady rate as

$$J = J_\infty \left(1 + \frac{R}{\sqrt{\pi D t}}\right) \tag{5}$$

in which the radius of the droplet is assumed constant. The time required to approach the steady state flux up to 10 and 1 %, would amount to 0.1 and 10 % of the time needed for the complete evaporation of a water droplet in dry air at 20 °C, respectively. Although this example indicates that the transient effect may be neglected for water drops at low temperatures, it should be realized that the corresponding times would be 1 and 100 % of the time needed for complete evaporation in dry air at a wet-bulb temperature of 45 °C because of the higher surface vapour concentration and higher rate of evaporation. Such drying conditions are not uncommon in spray drying. (The use of Eqn 5 is no longer correct under such conditions because of the decreasing radius.)

Brian & Hales (1969) gave figures for deviations from the steady state Nusselt (Sherwood) numbers due to shrinking or growing of spheres. They found little effect of a change in radius, provided a radial Péclet number defined by

$$Pe = \frac{2R}{D}\frac{dR}{dt} \tag{6}$$

is much smaller than the Nusselt number. Fuchs showed that the effect of a changing radius on the Sherwood number is also negligible for a low partition coefficient when the radius changes as a result of evaporation only. This observation is in agreement with the results of Brian & Hales because

8

$$\frac{dR}{dt} = \frac{J}{c} \approx \frac{D}{R} \frac{c_s' - c_\infty'}{c} \frac{Sh}{2} \tag{7}$$

and, hence

$$Pe/Sh = \frac{c_s' - c_\infty'}{c} \tag{8}$$

Thus, the effect of the change in droplet diameter on the Sherwood number may usually be ignored for evaporating droplets at moderate pressures. A change in radius of a droplet due to inflation might have some effect on the Sherwood number, but droplets in spray dryers usually inflate at a stage when the evaporation rates are mainly determined by the internal transport (Chapter 4).

Fuchs (1959) also described the effect of a continuous change in surface vapour concentration on the evaporation rate:

$$J^s = \frac{D}{R} c_s'(t) \left(1 + \frac{R}{\sqrt{\pi D t}} + 2 \frac{dc_s'}{dt} \frac{t}{c_s'} \frac{R}{\sqrt{\pi D t}} \right) \tag{9}$$

from which it follows, that an approximation to the quasi-stationary state is only possible if the surface concentration changes sufficiently slowly. A change in the surface vapour concentration may be due to a change in solute concentration inside the droplet. Usually the water activity at the surface remains approximately one over a wide range of concentrations in the liquid. During drying a rather sudden change in water activity may occur at lower water concentrations in the liquid, but the change in the equilibrium vapour concentration at the surface is less marked due to a simultaneous rise in droplet temperature. Changes in the liquid concentrations during the drying process are discussed in Section 2.3. It should be remembered, however, that the effect of a sudden change in surface vapour concentration is rather small because such a change takes place at a moment when the evaporation rates start to be determined by the internal transport.

Data on the relaxation of a change in the vapour concentrations in the bulk of the continuous phase are not available.

Effect of deviations from continuum theory The diffusion theory used in the derivation of Eqn (1) assumes the applicability of continuum theory. For low pressure gases and small diffusion distances this assumption may lead to erroneous results. The use of continuum theory for transfer to aerosols is considered justified if the Knudsen number

$$Kn = \frac{\lambda}{R} < 0.05 \tag{10}$$

(Hidy & Brock, 1970). If we take the mean free path of nitrogen at 273 K and 1 bar as indicative -6×10^{-8} m (Moore, 1963) – this would mean that continuum theory may be applied to droplets larger than 1.2×10^{-6} m radius. Usually droplets in spray-drying are 10–100 times larger. Fuchs (1959) and Okuyama & Zung (1967) found, however, contrary to these results significant deviations from the Maxwell equation due to gas kinetic effects for droplets as large as 100 μm.

Effect of a net mass flow Eqn (1) is not valid when diffusion evokes a net mass flow. If we assume that no air is absorbed by the droplet, for higher mass transfer rates we can use a flux equation based on reference component centred coordinates (Appendix A). The fluxes relative to air-fixed coordinates equal the fluxes in a droplet-centred frame of reference

$$J = J^r = -c_r D \frac{d(c/c_r)}{dr} = +cD \frac{d}{dr} \ln(1-x) \tag{11}$$

Integration between $r = R$ and $r = \infty$ and introduction of the boundary conditions $x = x_s$

9

and $x = x_\infty$ yields for constant molar concentration and constant diffusion coefficient the following expression for the flux

$$J^s = +\frac{cD}{R} \ln \frac{1-x_\infty}{1-x_s} = kc \ln \frac{1-x_\infty}{1-x_s} \tag{12}$$

We find the deviation from the Maxwell equation due to the net mass flux from the surface by comparing Eqn (12) to Eqn (1). At a wet-bulb temperature of about 45 °C and a water activity of one, the mole fraction in the vapour at the surface is about 0.1. When we assume dry air at an infinite distance, we find a discrepancy between Eqn (1) and Eqn (12) of about 5 %. The difference diminishes as soon as the surface vapour pressure is reduced because of a decrease in the water concentration in the liquid phase. The same is true when the water vapour concentration far from the surface increases. The correction made in Eqn (12) can identically be applied to the mass transfer coefficients predicted by Eqn (2).

Effects of variable coefficients It has been assumed that the values of the molar density and of the diffusion coefficient are independent of the position in the drying air. Under isothermal and isobaric conditions the assumption of constant molar density is correct for ideal gas mixtures. The diffusion coefficient in gases too is usually fairly insensitive to changes in the composition. In non-isothermal systems, neither the molar density nor the diffusion coefficient are constant. The diffusion coefficient in the boundary layer around a droplet may vary by a factor 2 under spray-drying conditions and the molar concentration by a factor 1.5. It is common practice to choose some mean value for the whole boundary layer. The choice is often arbitrary. Complete integration of the diffusion equation is therefore preferable but this is much more elaborate.

Soret effect Cross effects known from irreversible thermodynamics have been neglected. It can be shown, however, that under normal drying conditions in spray drying the Soret effect gives a deviation of less than one percent.

Effect of free convection Free convection for a single sphere in a semi-infinite medium is given by the semi-empirical relation (Ranz & Marshall, 1952)

$$Sh = 2 + 0.6 \, Gr^{\frac{1}{4}} Sc^{\frac{1}{3}} \tag{13}$$

Introduction into this relation of the properties of air at 100 °C and assumption of a constant temperature difference of 100 °C between the droplet and the air yields a deviation of the mass flux from that predicted by $Sh = 2$, ranging from 1.3 % for droplets of 10 μm through 4.6 % for droplets of 50 μm to 7.5 % for droplets of 100 μm diameter. For the determination of these figures only the effect of temperature gradients has been included in the Grashof number. The concentration gradients have an opposite but minor effect on the Grashof number. Obviously, the relative effect of free convection decreases as the effect of forced convection increases.

Effect of a non-infinite medium Droplets inside a spray do not evaporate in an infinite medium. The presence of other droplets in the surroundings creates an equipotential plane around a droplet, through which no transfer takes place. If the plane is situated far away from the droplet, the deviation from Eqn (1) will be small. If the equipotential plane is nearer to the droplet, deviations are due to two reasons. The first is that the water vapour concentration in the space enclosed by the plane rises. This effect has been mentioned on page 8.
A second reason is that the diffusion equation cannot be integrated from the surface to infinity but must be integrated to the boundary indicated by the equipotential plane. In general the deviation caused by this effect is limited when the plane is located at a distance of more than 10 times the radius of the droplet.

Fuchs (1959) stated that a drop in a spray evaporates approximately at the rate it would have in a vessel with non-absorbing walls and a volume equal to the average volume surrounding each drop in the system. For this situation a general solution is available for non-stationary evaporation. If we assume the radius of droplet and cell, the surface vapour concentration, the diffusion coefficient and the molar density to be constant and the initial concentration to be uniform throughout the cell, the concentration in the vapour is given by

$$c = c_s + \frac{1}{r} \sum_{n=1}^{\infty} (c_0 - c_s) \frac{2R \sin\left[\lambda_n(r-R)\right] \exp\left(-\lambda_n^2 Dt\right)}{\lambda_n \{ R_{os} \sin^2\left[\lambda_n(R_{os}-R)\right] - R \}} \tag{14}$$

in which λ_n are the roots of

$$\lambda_n R_{os} = \tan\left[\lambda_n(R_{os}-R)\right] \tag{15}$$

The evaporation rate is given by

$$\mathcal{J} = -D\frac{dc}{dr}\bigg|_{r=R} = \frac{D}{R}(c_s - c_0) \sum_{n=1}^{\infty} \frac{2R \exp\left(-\lambda_n^2 Dt\right)}{R_{os} \sin^2\left[\lambda_n(R_{os}-R)\right] - R} \tag{16}$$

The system described here is called the *cellular model* and is described more extensively in Section 2.4.3 and Appendix C.

The effect of the presence of other droplets on the heat and mass transfer coefficients will decrease with increasing Reynolds number because of the thinner boundary layer. It should be kept in mind, however, that the other droplets may have some influence on the values of the driving forces.

Effect of internal circulation and oscillations   According to Fuchs (1959) the outside heat and mass transfer coefficients may nearly double with internal circulation. As discussed above with regard to transfer of momentum, however, internal circulation probably can be neglected.

Oscillations inside droplets can also increase the outside transfer coefficients. Immediately after atomization droplets are oscillating. Stable oscillations occur only at very high Reynolds numbers and therefore the effect of oscillation may be neglected for most of the drying period (see also Eqn 27).

Effect of turbulence   Galloway & Sage (1967) noticed that 'the many data presented in the literature and laid down in correlations such as Eqns (2) and (18) constitute and extensive, in some cases repetitive but often conflicting collection.' They mentioned some factors which bring about this variation. Special attention is drawn to the influence of turbulence of the main stream. Keey (1972) noticed, however, that the droplet diameters in spray-dryers are much smaller than the measured scale of turbulence. According to this line of reasoning, the droplets may respond to all components of the turbulence. The effect of the free stream turbulence would therefore be limited. Contrary to this opinion it can be stated that moving droplets do not follow the components of the turbulence and that for that reason free-stream turbulent perturbation of the laminar boundary flow may occur. Furthermore, the inertia of a droplet in a turbulent flow causes a relative velocity at every change in the local air velocity. Such a relative motion will influence the transfer coefficients. No quantification is available, however.

Local variation of transfer coefficients   Marshall (1954) reported on the observations of Frössling that Eqn (2) indicates only average mass transfer coefficients for moving spheres. The local variations of these coefficients are given in Fig. 1. It should be noted that these local variations may lead to serious deviations from radial symmetry of concentration fields inside the droplets (see also Section 2.3.1). Also the non-sphericity of the equipotential plane around a droplet, through which no transfer takes place causes local variations of the transfer coefficients.
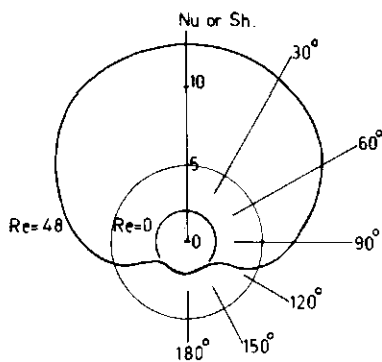
11

.

Fig. 1. Local variation of the Nusselt or Sherwood number around the surface of a sphere as a function of the angle from the front stagnation point. $Re = 0$ and $Re = 48$ (after Frössling, 1938).

2.2.3 Heat transfer

Heat transfer to stagnant droplets can be described analoguously to Eqn (1) using

$$Nu = 2 \tag{17}$$

Heat transfer to droplets moving relative to air can be described by the equation (Ranz & Marshall, 1952)

$$Nu = 2 + 0.6 \, Re^{\frac{1}{2}} Pr^{\frac{1}{3}} \tag{18}$$

Some effects can cause deviations from the Nusselt numbers predicted by Eqns (17) and (18). The same limitations as described for mass transfer are valid.

Effect of radiation Additionally we must assume that no heat is transferred by radiation. This assumption seems reasonable. Fuchs showed that radiation may be neglected at ambient temperatures for droplets smaller than 100 μ m radius. The influence of radiation may rise, however, to 8 % of the heat transferred by conduction for the same droplets at 200 °C. Only for droplets smaller than 15 μm is the effect less than 1 % at this temperature. On the other hand, radiation is seldom of importance in industrial equipment, where radiation is a wall effect with limited depth of penetration, and the majority of the droplets are screened by other droplets. This argument depends, however, on the size of the equipment and on the droplet load of the air. It also ignores the fact that droplets may have different temperatures.

The effect of the mass flux on the heat flux The effect of mass efflux on the rates of mass and heat transfer is limited in the case of evaporation of water at moderate evaporating conditions. Frazier & Hellier (1969) stated, that the Ranz & Marshall equations yield too high values of the Nusselt and Sherwood numbers for evaporation of fuel droplets in gases at high temperatures. Mass transfer does indeed cause a decrease in the heat transfer rate as well as in the apparent mass transfer coefficient, but Crosby & Stewart (1970) showed that application of the correction predicted by the boundary layer theory (Bird et al., 1960) gives acceptable results. The correction according to this theory is given by

$$q^{\cdot} = \Theta_T h (T_s - T_\infty) \tag{19}$$

in which θ_T is the correction term for the effect of the mass flux

12

$$\Theta_T = \frac{\varphi}{e^\varphi - 1} \approx 1 - \varphi/2 \tag{20}$$

with

$$\varphi = \frac{J c_p}{h} \tag{21}$$

It can be shown that the same equation which was derived for a thin boundary layer is also valid for the transfer around a stationary sphere in an infinite medium. The right hand side of Eqn (20) is obviously valid only for small values of φ.

An approximate value of the correction term is obtained by replacing the mass flux term by the heat flux divided by the heat of evaporation (allowable if – as in the case of water – the heat flux is almost entirely used for evaporation of the volatile)

$$\Theta_T \approx 1 - \frac{J c_p}{2h} \approx 1 - \frac{q c_p}{2Lh} \approx 1 - \frac{c_p \Delta T}{2L} \tag{22}$$

Because of the large value of the heat of evaporation, the term is small for water evaporating at moderate temperatures, but increases with increasing temperature difference

$$\frac{c_p \Delta T}{2L} \approx 4 \times 10^{-4} \Delta T \tag{23}$$

Values of this dimensionless group for other systems than water-air were given by Bailey et al. (1970). Hoffman & Ross (1972) gave a more theoretical and detailed study of the phenomena involved.

If desired the coupled heat and diffusion equations describing the transport in the air can also be solved. This approach has the advantage that transient effects, and those of the non-infinite medium and of variable coefficients can be included. Details are worked out in Section 2.4.3 and in Appendix B.

2.2.4 Discussion and conclusions

There is some inaccuracy in the calculation of heat and mass transfer during the period of decreasing relative velocity of the droplets because the accurate relative velocities are not known. Fortunately the fractional water loss during the period of decreasing relative velocity is relatively low (Sjenitzer, 1952; Kerkhof & Schoeber, 1973) and therefore the effect of the assumptions made on the predicted total drying history is limited. Furthermore Biot numbers for mass transfer are high even for low Sherwood numbers, and after a short time the drying is fully governed by internal diffusion in the droplets. Which relative velocity is assumed can affect, however, the calculated time until a dry surface layer forms. This time period often determines the functional properties of the product. The relative velocities also affect the droplet temperature after the formation of a dry skin.

For the main part of the drying process, transfer coefficients can be based on the final velocities of the droplets which are due to gravitational, centrifugal and inertia forces. The Nusselt and Sherwood numbers of water droplets at their stationary falling velocities in air are given in Fig. 2 as a function of their diameter.

It can be concluded that the accuracy of calculations of heat and mass transfer coefficients is limited by many unknowns. Many corrections can, however, be
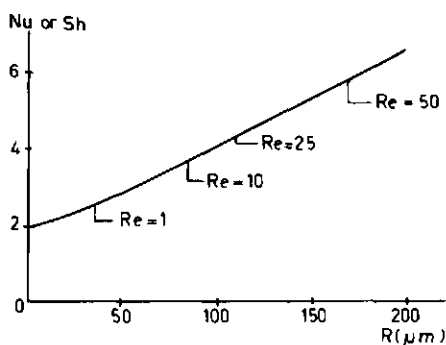
13

Fig. 2. Nusselt or Sherwood number for spheres at their stationary falling velocity in air at 20 °C as a function of their diameter (droplet density 1000 kg/m³).

included in the calculations. For engineering purposes such minor corrections are often not warranted if the general trends provide sufficient understanding of the process involved. In this study we shall accept some inaccuracy because – as we shall see – errors in the estimation of the conditions of the continuous phase (Chapter 3) are larger than the, say 10 % error in the transfer coefficients under discussion here.

2.3 Transport inside a droplet

In this paragraph we will discuss the diffusional transport inside a droplet. The diffusion equation and some limitations of its use are discussed in Section 2.3.1 Some relevant solutions of the diffusion equation are given in Section 2.3.2. A numerical method for the solution of the diffusion equation in situations for which no analytical solutions are available, is developed in Section 2.3.3. Heat transport inside a droplet will not be discussed because it is assumed that resistance to heat transport in the systems under consideration is entirely located outside the droplets:

$$Bi = 0 \tag{24}$$

Hence, there are no temperature gradients inside the droplets. This assumption is justified because the Biot number is very small indeed for the systems studied (Kerkhof & Schoeber, 1973).

2.3.1 The diffusion equation

In Section 2.1 we defined our physical system as one in which mass is transported in the disperse phase by binary diffusion in a homogeneous liquid. Such transport is usually described by the diffusion equation for spherical symmetric systems

$$\frac{\partial c_w}{\partial t} = \frac{1}{r^2} \frac{\partial}{\partial r} \left\{ r^2 D(c_w, t) \frac{\partial c_w}{\partial r} \right\} \tag{25a}$$

It is shown in Appendix A that this diffusion equation is only valid when there is no volume contraction or expansion and no net flow of volume. If volume

14

contraction and droplet inflation are absent there is no net flow of volume (relative to the centre of the droplet). It is shown in Appendix B. 1.2 that volume contraction is indeed negligible for sugar solutions over a wide range of concentrations. Inflation, however, is very common in spray drying. It would be more correct therefore to describe diffusion in our droplets by the diffusion equation in reference component fixed coordinates (Appendix A)

$$\frac{D^r}{Dt}(c_w/c_r) = \frac{1}{c_r r^2}\frac{\partial}{\partial r}\left\{r^2 c_r D(c_w, t)\frac{\partial}{\partial r}(c_w/c_r)\right\} \tag{25b}$$

Initial and boundary conditions to diffusion equations (25a) and (25b) are

$$c_w = c_{w,0} \text{ at } 0 \leqslant r \leqslant R; \quad t = 0 \tag{26a}$$

$$\frac{\partial c_w}{\partial r} = 0 \text{ at } r = 0; \quad t \geqslant 0 \tag{26b}$$

$$c_r D(c_w, t)\frac{\partial}{\partial r}(c_w/c_r) = J^s(c_w, R, t) \text{ at } r = R(t); \quad t > 0 \tag{26c}$$

The flux J^s in the latter boundary condition can be calculated with Eqn (2) for the determination of the mass transfer coefficient and by using sorption isotherm data for the determination of the water vapour concentration at the surface.

If the water concentration at the surface is a known function of the time, boundary condition (26c) can be replaced by

$$c_w = c_{w,s}(t) \text{ at } r = R(t); \quad t > 0 \tag{26d}$$

in which $c_{ws}(t)$ is the known water concentration. If droplets inflate, the boundary condition (26b) should be replaced by

$$c_r D(c_w, t)\frac{\partial}{\partial r}(c_w/c_r) = J^{is}(c_w, R_{is}, t) \text{ at } r = R_{is}(t); \quad t > 0 \tag{26e}$$

The solution of both Eqn (25a) and (25b) with boundary conditions (26) is complicated by the following factors:
1. The differential equation has a highly non-linear character because the diffusion coefficient, which depends on the water concentration c_w and on the temperature of the droplet (in Eqn (25a) and (25b) indicated as a time dependence) can vary by several magnitudes. The effect of the water concentration and the temperature on the diffusion coefficient in maltose solutions are given in Appendix B.1.1.
2. Boundary conditions (26c), (26d) and (26e) are given at a position moving relative to fixed space coordinates. If not net volume production or contraction occurs inside the droplet as a result of inflation or of concentration changes, the volume of the droplet decreases by the volume of water evaporating from the droplet surface and the radius decreases accordingly. If net volume expansion or contraction do occur, the volume of the droplet will be affected by these effects and by the loss of volume due to water evaporation.
3. Boundary conditions (26c) and (26d) are time and concentration dependent. This character is caused by
– the non-linear sorption isotherms of many liquid foods and the change in water

vapour pressure with changing temperature (time) (Appendices B. 1.3 and B.2),
– the change in mass transfer coefficient due to velocity changes of the droplet
(Section 2.2.2),
– the change in outside driving force due to changes in the conditions of the
drying air as drying progresses.
The latter factor will be discussed in detail in Chapter 3.

For these reasons the analytical solution of diffusion equations (25) with
boundary conditions (26) is restricted to very simple situations (Section 2.3.2). For
a vast number of practical drying problems we shall have to use numerical
methods such as described in section 2.3.3.

Before dealing with the analytical and numerical solutions of the diffusion
equations, however, we must discuss a number of restrictions on the use of Eqns
(25a) and (25b).

Assymetric concentration profiles   Diffusion equations (25) assume the presence of spheri-
cal symmetry. Small liquid droplets will usually be approximately spherical. Deviations
from spherically symmetric concentration profiles may occur, however, in droplets moving
relative to air because the front will evaporate more rapidly than the rear. Variations of the
local Nusselt numbers are given in Fig. 2. If the droplets rotate, alternate periods of high and
low local Nusselt-numbers may be expected. Then deviations from the spherically symmetric
concentration profiles which are predicted if the average Nusselt-number is used for the
whole surface, will be small. Charlesworth & Marshall (1960) indicated, however, that
temporarily higher evaporation rates at a given point of the droplet could cause a higher
local specific gravity. As a result, the droplet will tend to move with that point as a
permanent front stagnation point. Spray-dried powders do indeed sometimes show a
clearly asymmetric structure.

Often the surface has a ribbed appearance. Bends are frequently formed when the
droplets shrink after the prior formation of a firm surface layer. The use of the diffusion
equations for spherical symmetry is therefore restricted to the first stages of drying.
However, many spray-dried powders show a clearly spherical form and many others
do not deviate all that much from sphericity, so that Eqn (25a) and (25b) were used in this
study.

Internal circulation and droplet oscillations   Transfer inside droplets can be enhanced by
internal circulation and droplet oscillations. 2–5 fold increases in the rate of transfer have been
reported for fully developed streamline circulation (Kronig & Brink, 1950) and up to 20
fold increases for oscillations (Marsh & Heidegger, 1965).

Circulation of the Hadamard-Rybczinski type is expected to increase with increasing
droplet size and a higher ratio of the viscosities of the continuous and dispersed phases.
Droplets of the size common in spray dryers will, therefore, circulate extremely slowly, if at
all. Fully developed streamline flow will certainly never be found. Kerkhof & Schoeber
(1973) discussed the effect of the presence of surface active material on the internal
circulation of droplets and concluded that droplets will at most circulate internally for a
short period after atomization.

Stable oscillations can occur at high Reynolds numbers ($Re > 1000$) but they are never
important in spray drying. Unstable oscillations can occur as a result of atomization.
Hughes & Gilliland (1952) reported on the Rayleigh equation for the decay of oscillations.
In the absence of eddies within the droplet and neglecting any effect of the continuous
phase, the damping effect of the viscosity is given by

$$A = A_0 \exp(-5\nu t/R^2) \tag{27}$$

The relative importance of the oscillation period has not been well-studied but from Eqn

16

(27) and an estimation of the drying times of droplets of the same size, it seems reasonable to expect that the decay of the oscillations is rapid relative to the decay of the amount of water in a droplet.

Surfactants are well known for reducing the evaporation from water surfaces. Deryagin (1966), for example, studied the sorption of cetyl alcohol on the surface of a water droplet and found a marked reduction of the evaporation rate at the moment a saturated monolayer was formed. Snead & Zung (1968) reported a reduction of the evaporation rate by as much as several hundred times. Huang & Kintner (1969) summarized the results given in the literature about the effect of surfactants on the mass transfer to and from droplets as follows:
– The mass transfer coefficients are reduced by surface active agents.
– Oscillations and other surface disturbances are damped.
– Convection sweeps the surfactant to the rear stagnation point. Hadamard-circulation yields a stagnation ring, which moves forward as the surfactant accumulates at the rear.
– The drag is increased.
– A quasi-steady interfacial barrier results in an interfacial resistance to mass transfer.
    The effect of the surfactants normally present in liquid foods is unknown. They are likely to cause some reduction of evaporation rates, but it is not expected that a tight monolayer will often be formed.

Deviations from continuum theory Diffusion Eqns (25) are based on continuum theory. Hence they are only valid if the scale on which the diffusion phenomena take place is a large one compared with the molecular dimensions. The dimensions of droplets in spray drying are very much larger than the molecular dimensions, but sometimes very steep concentration gradients may be expected on the surface. Even the local concentration cannot be defined clearly if very steep concentration gradients are predicted by the diffusion theory over distances of the order of molecules.
    Steep gradients are always present at the surface after an instantaneous change in the conditions at the start of the·diffusional process. Those conditions are transient, however, and pass into a situation with less steep gradients.
    Extremely steep gradients are also predicted when the diffusion coefficients vary by several orders as a result of changes in liquid concentration. Such variations frequently occur in carbohydrate solutions. The gradients can be expected over a skin at the surface of a drying droplet and may remain for an important part of drying. Because of the problem of defining the concentration in such a skin, it is impossible to predict the diffusivity inside the skin or its permeability accurately. However, the prediction of drying rates will not be much affected, because of the limited thickness of the skin.

2.3.2 General solutions of the diffusion equation

Limitation to mass transfer outside the droplet If transport of the water inside the droplet does not limit the transfer, the concentration may be regarded as homogeneous throughout the droplet. Then no solution of the diffusion equation is needed because the concentration in the droplet can be calculated from a mass balance over the droplet. Knowledge about the transfer process outside the droplet and the equilibrium water vapour pressure at the surface as a function of the water concentration inside the droplet suffice to determine the value of the drying rates. Sjenitzer (1952) indicated that a hygrometric chart can be used for the graphical determination of the driving forces.
    A common measure of the validity of the assumption of easy internal mass transport is

17

$$Bi_m \ll 1 \qquad (28)$$

A rough estimation of the magnitude of the parameters involved shows, however, that condition (28) is generally not fulfilled for the systems considered in this study. Hence, significant concentration gradients will usually build up inside the droplet.

Limitation to mass transfer inside the droplet   The assumption that the resistance to mass transfer is situated entirely in the liquid phase can be expressed in terms of the Biot number as

$$Bi_m = \infty \qquad (29)$$

Here the liquid at the surface is in equilibrium with the drying air. If the conditions in the drying air and the temperature of the droplet remain constant, we can use boundary condition (26d) with the surface concentration as a constant. If we assume furthermore that the dimensions of the droplet do not change during drying, (26d) becomes

$$c_w = c_{w,s} = \text{constant} \qquad \text{at } r = R; \quad t > 0 \qquad (26f)$$

Solutions of diffusion equation (25a) with a constant diffusion coefficient and boundary conditions (26a), (26b), (26f) are available in the handbooks (Carlslaw & Jaeger, 1959; Crank, 1956; Luikov, 1968). For a shrinking sphere no general solutions are available.

Although the assumption of easy external mass transport may be true during at least part of the drying, the analytical solution does not give a good representation of the drying of a droplet in a spray-dryer.

First, the droplet temperature changes. This temperature is determined by the equilibrium between heat and mass transfer between droplet and air. The Biot number for heat transfer will never be large. Therefore, even if the conditions in the air remain constant, the temperature of the droplets changes because of the changing rate of evaporation. A change in the temperature causes changes in the diffusion coefficients and theoretically also in the water concentration of the liquid at the surface, which is in equilibrium with the drying air. Deviations from the theoretical situation in which these are constant result.

Secondly, the conditions of the outside air usually change during the process. Hence, the surface concentration, which is in equilibrium with the air, will also change. An exception to this rule is the example of perfectly mixed air (described in Chapter 3) in which the conditions of the air remain constant throughout the process.

Vapour concentration proportional to concentration in the liquid phase   If the equilibrium vapour concentration is proportional to the concentration of the volatile component in the liquid phase, solutions for the convective heating of a sphere can be applied. Solutions for various values of Bi and for constant radius are given by Luikov (1968) and others.

These solutions can rarely be used in the systems studied because the above

18

mentioned proportionality is seldom valid over a wide range of concentrations. As shown in Appendix B.1.3, the water activity (and therefore also the molar vapour concentration) is proportional to the mole fraction in the liquid phase over a wide range of concentrations. Hence, the concentrations in both phases would only be proportional if the total molar density in the liquid were a constant, which is clearly not so.

Constant flux at the surface Assumption of a constant drying rate is very usual in drying calculations. It results frequently from a constant water activity of an aqueous system over a wide range of water concentrations at the surface. A solution of Eqn (25a) is available with a constant diffusion coefficient and with boundary conditions (26a–c), in which the flux J^s, the molar density c_r and the radius R are constant. Concentration profiles inside the sphere are given by

$$c_{w,0} - c_w = \frac{3J^s t}{R} + \frac{J^s(5r^2 - 3R^2)}{10DR} - \frac{2J^s R^2}{Dr} \sum_{n=1}^{\infty} \frac{\sin(\alpha_n r/R)}{\alpha_n^2 \sin \alpha_n} \exp(-Dt\alpha_n^2/R^2) \qquad (30)$$

In which α_n are the positive roots of:

$$\tan \alpha = \alpha \qquad (\alpha \cot \alpha = 1) \qquad (31)$$

In taking c_r and R as constant it has been assumed implicitly that diffusion takes place relative to a stationary surface. This assumption may be valid in the presence of a rigid matrix through which a solvent is diffusing, but it is not true for a homogeneous liquid with a retreating surface. Solutions of Eqns (25a) and (26a–c) for a variable solute concentration c_r in Eqn (26c) but a constant radius were given by Charlesworth & Marshall (1960) and by Schlünder (1964).

Obviously, a variable solute concentration and a constant radius in boundary condition (26c) are contradictory and, hence, solution of the equations yields only approximate results. Van der Lijn (1976) gave a general numerical solution of Eqn (25) and boundary conditions (26a–c) for a constant diffusion coefficient and a change of the droplet volume equal to the partial volume of the water lost. Then the surface flux was not taken as a constant but was defined by a constant driving force at the outside of the droplet and a constant Sherwood number. Therefore the flux increased with decreasing radius. These assumptions are even slightly more realistic in drying droplets than the assumption of a constant flux. Kerkhof (1975) gave correlations between the duration of the constant rate period and the flux which are also valid for non constant diffusion coefficients.

The assumption of a constant flux at the surface, although usual in drying calculations does not describe very well the drying of carbohydrate solutions inside a spray dryer, because:

– Carbohydrate solutions show an equilibrium water vapour pressure which is a monotonously decreasing function of the solute concentration, and the rate of evaporation from the surface changes gradually as a result of a decreasing driving force as the liquid concentration at the surface falls. The change in the surface vapour concentration also affects the temperature of the droplet and with it the diffusion coefficient.

– A change in the droplet radius causes both a decrease in the surface area of the

droplet and an increase in the heat and mass transfer coefficients.

– The water vapour concentration in the bulk of the drying air usually changes during the process.

– Even if the water flux at the surface were to remain constant for a certain time, it would start to vary as soon as the surface water concentration drops to zero or to the value at which the liquid is in equilibrium with the drying air. However, the above-mentioned calculations can be useful in a limited number of situations to estimate the duration of and the amount of water evaporated during a 'constant rate period.' Examples of such estimations were given by Kerkhof (1975) and Van der Lijn (1976).

Conclusion None of the general solutions available from the literature can give an effective description of the drying of droplets in a spray dryer, mainly because of the variable diffusion coefficients, the shrinking of droplets and the time dependence of the boundary conditions of the diffusion equation.

2.3.3 Numerical methods of solving the diffusion equation

In the absence of suitable analytical solutions to the diffusion equation for a drying sphere, we need to use numerical methods for solving the given problem. The usual methods which solve the diffusion equation by using a grid in distance and time space, are not convenient because they require a complicated interpolation procedure to locate the moving phase boundary between grid points. A further complication is, that the highly variable diffusion coefficients cause very steep concentration gradients near the surface. Therefore a very dense grid is required there. It is logical in such situations to try to save computer time by designing an unequally spaced grid. With a moving boundary, a dense grid would be needed throughout the whole region across which the moving boundary could possibly traverse, but such an approach would take too much computer time. Alternatively the grid could be adjusted during the computations, but this would also be very elaborate.

For these reasons I decided to use transformed coordinates in which the moving boundary is immobilized. The diffusion equation (25b) can be conveniently transformed in solute fixed coordinates by defining the following new variables:
– the reference component related concentration

$$u \equiv c_w/c_r \tag{32}$$

– the reference component fixed distance coordinate

$$z \equiv \int_0^{r'} c_r r^2 \, dr \tag{33}$$

– the transformed diffusion coefficient

$$s \equiv D(c_w)c_r^2 = D(u)/(uV_w + V_r)^2 \tag{34}$$

Diffusion equation (25b) reads in terms of these new variables:

20

$$\frac{\partial u}{\partial t} = \frac{\partial}{\partial z}\left(r^4 s \frac{\partial u}{\partial z}\right) \tag{35}$$

in which the radius r is defined as

$$r = \left\{\int_0^{z'} 3(uV_w + V_r)dz\right\}^{\frac{1}{3}} \tag{36}$$

As the increments of z contain constant amounts of the non-volatile solute, the boundary conditions are defined at fixed values of z. Initial and boundary conditions (26a–d) read in the new coordinates

$$u = u_0 \quad \text{for} \quad 0 < z < Z; \quad t = 0 \tag{37a}$$

$$\frac{\partial u}{\partial z} = 0 \quad \text{for} \quad z = 0; \quad t > 0 \tag{37b}$$

$$-r^2 s \frac{\partial u}{\partial z} = J^s(u, t) \quad \text{for} \quad z = Z; \quad t > 0 \tag{37c}$$

$$u = u_s(t) \quad \text{for} \quad z = Z; \quad t > 0 \tag{37d}$$

Eqn (35) with boundary conditions (37a–c) or (37a, b and d) can be solved with standard techniques for the solution of parabolic partial differential equations. In principle many finite difference approximations may be used, provided that a reasonable estimate is made of the non-linear coefficient and that provisions are made for the unequally spaced grid points. Care must be taken to write the difference analogue of Eqn 35 with the coefficient inside the brackets. Attempts to place the coefficient outside the brackets and to differentiate it analytically lead to a form with r to the first order times the first derivative and r to the fourth order times the second derivative. This form results in instability, especially at the lower values of r.

For the calculations reported here an implicit difference scheme was used. Details about the method of calculation were given by van der Lijn et al. (1972).

A major problem in the application of difference schemes to highly non-linear partial differential equations is that it is often extremely difficult to prove stability and convergence to a true solution. Here too there is no such proof. For that reason the numerical method was tested by comparing the results in one example with the analytical solution of Eqn (25) with boundary conditions (26a, b and f) in another case with Eqn (30). Results with a 20-point grid were accurate within 1 %. Furthermore no substantial effects could be detected when the grid-point spacing or the number of grid-points, both in distance and in time were modified. Therefore these solutions seem reliable.

2.4 Models for transfer in spray dryers

2.4.1 Concepts for the modelling of spray drying

This section describes three different types of models for the drying in a spray dryer. One (using transfer units) is mainly empirical. The two other types

21

discussed are based on the analytical description of the transport inside a droplet and the transfer between a droplet and its surroundings.

Transfer units Sjenitzer (1952) introduced the concept of transfer units into spray-drying. This concept is mainly suitable for cocurrent or countercurrent phase contacting, although axial dispersion may be included. The units indicate the size of apparatus required to accomplish a transfer process of standard difficulty. On the basis of the desired inlet and outlet conditions of both phases and the equilibrium curves the required number of transfer units can be calculated. The dryer height or volume required per transfer unit must be estimated empirically.

Transfer units are, however, useful only if they can be linked to some dimension of the equipment. Therefore it is desirable that the transfer mechanism and the transfer coefficients and equilibrium lines remain more or less constant throughout the process. This condition is not satisfied if, as in spray-drying, the transport coefficients depend on the previous drying history. Hence, the concept of the transfer unit, which is extremely useful in many other phase contacting operations, has only little practical value for spray drying.

Cellular models The concept of cellular models is based on the exchange between one droplet and restricted (spherical) surroundings. The dimensions of the spherical surroundings are such that an amount of air is contained equal to the average amount of air surrounding each drop in a spray. The mass transport and the changes in the concentrations in the liquid phase can be described by the diffusion equation (Eqns 25a and 25b).

The coupled heat and mass transport and the changes in the conditions in the air can be found by simultaneous solution of the heat and diffusion equations. An example of the application of the cellular model is given in Section 2.4.3. Details of the calculations are given in Appendix C.

Cellular models were also used by Gal-Or & Hoelscher (1966) for a well mixed continuous phase. They assumed the droplet (bubble) to be in contact with its cell for the average residence time of the dispersed phase, after which the continuous phase was assumed to be well mixed before a new droplet (bubble) was introduced. Zung (1967a) used the model for the calculations of life times of clouds. First the droplets would evaporate until equilibrium within their cell was reached, after which evaporation was assumed to take place only from the cells at the outside boundary of the cloud.

An advantage of cellular models is, that they account for the effect of the limited dimensions of the air with which a droplet exchanges heat and mass as a result of the presence of other droplets (see Section 2.2). The model also accounts for the inherently transient nature of the transfer process in both phases.

A disadvantage of cellular models is that they neglect long range mixing altering the conditions in the air, because of the assumption that the droplet exchanges heat and mass only with a restricted environment. Therefore the use of these models is almost restricted to stagnant sprays or to perfectly cocurrently moving air and droplets.

Continuum models Cellular models assume exchange between droplets and their adjacent air only, and these sub-systems are considered to be independent of the rest of the spray. Alternatively, the continuous phase can be considered as a continuum, in which changes in the conditions are caused by turbulent mixing, by diffusion, by convection and by evaporation. The conditions of the continuous phase are determined by drawing a heat and mass balance over an arbitrary control volume in which evaporation is accounted for by a source term in the mass balance and a heat sink in the heat balance. The rate of evaporation of droplets can in general be calculated by the methods commonly used to estimate the rates of transfer of single droplets in an infinite medium (Section 2.2).

Adler & Lyn (1971) calculated the steady evaporation and mixing of a spray in a gaseous swirl. They included the droplet trajectories in their calculations but used simplified concentration, temperature and velocity profiles in the spray: these profiles were assumed to be homogeneous over the width of the spray, which was calculated by the Prandtl mixing length theory.

An advantage of continuum models is that the effect of long range mixing can be accounted for relatively simply. Sometimes the admixing of dry air can simply be included in the mass and heat balance over a control of volume. If the conditions of the air vary with the location, the temperature and concentration profiles can be found by solving the equations for the mixing of the continuous phase. The evaporation must be included as a mass source and a heat sink which can be dependent on the local air conditions and the droplet number density.

A disadvantage of continuum models is that they neglect the effects which were mentioned as an advantage of the cellular models. Therefore these models should preferably be used in more dilute systems only. The results of the calculations on one example of spray drying done either with a continuum model or a cellular model, are compared in Section 2.4.3.

With the necessity of introducing simplifications to keep calculation time within acceptable limits, the relative simplicity of continuum models is preferred to the slightly more sophisticated cellular models. Furthermore the greater flexibility of the continuum models is a distinct advantage. In the calculations in Chapters 3 and 4 a (rather simple) continuum model is used.

2.4.2 Description of the model used in the calculations

The assumptions made and the equations used in the calculations, in this report are:
– Exchange of mass and heat was assumed to take place between a droplet and an unbounded continuum (continuum model). The transfer processes are limited by diffusional resistances inside as well as outside the droplet $(0 < Bi < \infty)$ and by heat conduction through a boundary layer surrounding the droplet.
– The internal mass transfer was described by Eqn (25b) and was worked out with the transformations of Eqns (32–35).
– Boundary conditions (37a–c) were used. Eqn (37c) reads more specifically

$$-r^2 s \frac{\partial u}{\partial z} = k\bar{c}' \ln \frac{1-x'_{\text{bulk}}}{1-x'_s} \tag{38}$$

in which the correction for high transfer rates (Eqn 11) was used. The average molar concentration in the gas phase is given by the Gas Law

$$\bar{c}' = \frac{P}{RT} \tag{39}$$

The value of the transfer coefficient was calculated from Eqn (2) using arithmetic average values of the temperatures and concentrations in the boundary layer to determine transport coefficients and molar concentration. If local equilibrium is assumed at the surface, the mole fraction of water in the gas phase at the surface can be calculated from the sorption isotherm by

$$x'_s = \frac{p_w}{P} = a_{w,s}(u, T) \frac{p_{\text{sat}}(T)}{P} \tag{40}$$

The mole fraction of water in the bulk of the continuous phase depends on the mixing pattern in the dryer. The subject of mixing is discussed in Chapter 3. The values used for the properties of the bulk air are given there.
– The droplet was assumed to be of uniform temperature at any given moment. The temperature was calculated by a heat balance over the droplet

$$\frac{C}{4\pi R^2} \frac{\partial T}{\partial t} = LsR^4 \frac{\partial u}{\partial z}\bigg|_{z=Z} + \Theta_T h (T_\infty - T_s) \tag{41}$$

In this equation the correction term Θ_T is given by Eqn (20) and the heat transfer coefficient is calculated with Eqn (18). Hence, radiation was neglected.
– In Chapter 4 the situation of a gas bubble being inside the droplet is considered. The initial condition (37a) has then to be slightly adapted:

$$u = u_0 \quad \text{for} \quad Z_{\text{is}} < z < Z; \quad t = 0 \tag{42a}$$

and the boundary condition at the inner interface is given by a mass balance over the bubble

$$r^4 s \frac{\partial u}{\partial z} = Z_{\text{is}} \frac{\partial u'}{\partial t} \quad \text{for} \quad z = Z_{\text{is}}; \quad t > 0 \tag{42b}$$

u' in this formula can be calculated from the sorption isotherm with Eqn (40) together with the transformation formula

$$u' = \frac{x'_w}{1 + x'_w} \tag{43}$$

Z_{is} is a given amount of inert gas (in moles) inside the bubble. The gradients at the inner surface will usually be extremely flat, because of the low rates of internal evaporation. Then boundary condition (42b) can more conveniently be replaced by

$$\frac{\partial u}{\partial z} = 0 \quad \text{for} \quad z = Z_{\text{is}}; \quad t > 0 \tag{42c}$$

24

Solution of the diffusion equation requires the calculation of the radius. The radius at the bubble surface R_{is} is given by

$$\frac{4}{3}\pi \dot{R}_{is}^{3} = Z_{is}(1+u')\frac{RT}{P} \tag{44}$$

in which we used the Gas Law.

The model described before in general terms was worked out using the physical properties of the homogeneous binary system maltose-water for the disperse phase and the system air-water vapour for the continuous phase. These properties are given in Appendix B. The following assumptions were made throughout the calculations but are not essential to the model.
– The initial water content in the liquid phase equals 50 % (w/w).
– The partial molar volumes of the components of the liquid phase are constant (Appendix B).
– The heat of evaporation equals the heat of evaporation of pure water at the droplet temperature.
– The Nusselt and Sherwood numbers equal two.
– The system is isobaric, pressure 10^5 Pa.

2.4.3 Discussion of the model used in the calculations

The factors determining the evaporation of a droplet in a spray have been discussed in Sections 2.2 and 2.3. The effect of the conditions in the continuous phase on heat and mass transfer will still be discussed in Chapter 3. In this section we shall consider the consequences of using a model based on a single droplet for simulating the evaporation of a spray with size distributed droplets. The results for one example obtained with a continuum or a cellular model will be compared (see Section 2.4.1).

Size distribution of the droplets The model used is based on the evaporation of one single droplet. Hence, it is assumed implicitly that a calculation made for one droplet can be indicative of the evaporation of a spray with size distributed droplets. There are many different opinions in the literature as to whether such a simplification should be allowed. This disagreement is partially because the conclusions were based on different situations.

– During the evaporation of a spray of a pure liquid the individual droplets grow smaller. However, the average droplet size in the spray can decrease but can also increase during some parts of the evaporation process because the smaller droplets disappear. Hence, in such situations the evaporation of a single droplet is unlikely to be representative of the total process.
Dickinson & Marshall (1968) made a computational study of the evaporation rates of size distributed sprays of pure liquids. They assumed perfectly cocurrent flow of air and droplets. Very different times were required for the evaporation of sprays with different size distributions but the same Sauter diameter (volume/surface average diameter). They concluded, therefore, that the mean diameter could not adequately characterize the evaporative behaviour of a non-uniform spray.
On the other hand, the change in the droplet diameter is limited if the droplets consist for an appreciable part of non-volatile material. Then the droplet size-distribution is more

25

or less retained during the drying process and the average droplet size will decrease slightly.

– In cocurrently moving air and droplets the conditions of the drying air change during the drying. Hence the smaller droplets, which evaporate at a much higher rate and lose most of their water in a shorter time than the larger droplets, dry under different conditions of the air. One of the consequences is that smaller droplets containing dissolved solids may reach much higher temperatures than larger ones. This temperature behaviour is shown qualitatively in Fig. 3. In such situations the behaviour of an 'average' droplet may be indicative, but does not give a precise prediction of the behaviour of the spray.

Drying rates of a spray are predicted more accurately, however, by the behaviour of one droplet if the conditions of the drying air do not change appreciably during the drying process. This is so if the drying air is well mixed (Chapter 3). Under such conditions and for identical Sherwood and Nusselt numbers each droplet reaches an identical relative water content at the same Fourier number. Therefore, the evaporation rate of a spray can be obtained by summation of the evaporation rates of each of the size classes which are known as a function of the Fourier number.

– Droplets at high Péclet numbers show Nusselt and Sherwood numbers proportional to the square root of the Reynolds number and because the velocity for stationary fall is often proportional to the square of the radius, the Nusselt and Sherwood numbers are proportional to the radius. Droplets at low Péclet numbers, however, show a constant Nusselt and Sherwood number. Hence, drying rates can also show different dependencies on the droplet radius for different Péclet numbers. The disagreement in the literature about the best average diameter (surface-mean (Arni, 1959) volume-mean (Gal-Or & Hoelscher, 1966), Sauter (volume-surface) (Pita, 1969; Adler & Lyn, 1971)) can partially be explained by these differences.

– Separation effects are caused by quicker sedimentation of the larger droplets in gravitational or centrifugal fields. As a result, droplets of different sizes may dry in separate zones of the dryer. Planovskii et al. (1970) calculated drop trajectories in cocurrent, countercurrent and mixed flow regions. Droplets were larger than those usually encountered in spray
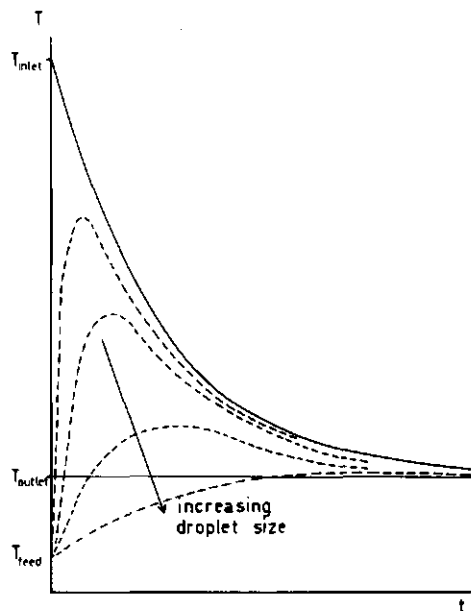

Fig. 3. Qualitative representation of the temperature histories of droplets of various sizes and air for perfectly cocurrent spray drying.

26

drying practice. Different sizes reached different heights in the dryer and, hence, the transfer and the conditions of the drying medium were determined by the differences in trajectories. Similar separation effects are observed during the deceleration near the atomizer.

– Small droplets can be regarded as completely entrained, i.e. their stationary falling velocity relative to the air is negligible compared with the overall velocity of the air as well as its turbulent movements. Consequently in every zone of the dryer these droplets have residence times equal to those of the air in which they are entrained. Larger droplets may show a distinct movement relative to the air. As a result the residence time of large droplets in the various zones of the dryer will be shorter for downward airflow and longer for upward airflow. Hence, the size distribution of the spray at a given point may differ from the size distribution of the droplets passing the same point per unit time. The overall evaporation rates will be affected both by the relative abundance of droplets of a given size and by the difference in drying history for such a group because of different residence times in the previous zones.

From the above discussion, it will be clear, that the size distribution of droplets in a spray must be taken into account to make accurate calculations on drying. Calculations which are based on one droplet size such as those in this study can only be of an indicative nature. It should be noted, however, that the computational effort is approximately proportional to the number of size classes considered. The extra computer time required to include the size distribution of a spray was not warranted for this study. Nor would it have guaranteed better results because of the many unknowns in other aspects of the calculations.

Comparison of results obtained with a cellular or a continuum model As discussed in Section 2.4.1, the use of a continuum model ignores the transient character of the concentration and temperature fields in the continuous phase and assumes exchange between a droplet and an unbounded medium. These inaccuracies can be avoided by solving the coupled heat and diffusion equations describing the transport in air in a cellular model. Below we shall evaluate the effect of this simplification by comparing the two models.

The equations describing the transport in the cellular model are given in Appendix C.

Drying histories according to the cellular model described in Appendix C and according to the continuum model described in Section 2.4.2 are given in Fig. 4 and 5. Drying conditions were:

– $Nu = 2$
– perfectly cocurrent drying (see Chapter 3)
– initial air temperature of 250 °C
– initially dry air
– initial liquid concentration 50 % water
– weight ratio between air and water 21 (final temperature after adiabatic equilibration 70 °C).

In the cellular model the drying rate initially will be higher than that in the continuum model, as may be expected from the initially steep gradients. The surface water concentration decreases more rapidly in the cellular model as a result of the higher transfer rates and the temperature rises more quickly to the temperature of the bulk air. Eventually, however, the drying and cooling rate of
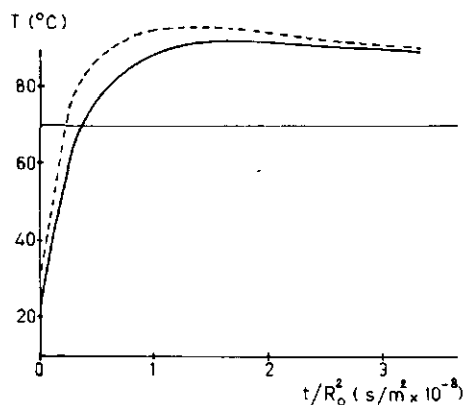
27

Fig. 4. Effect of the model on the calculated temperature history of a droplet. Cocurrent airflow, inlet temperature 250 °C, outlet temperature 70 °C; cellular model (---) and continuum model (——).
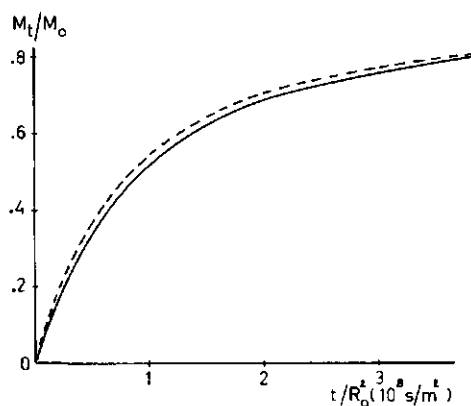

Fig. 5. Effect of the model on the calculated course of water loss from a droplet. Cocurrent airflow, inlet temperature 250 °C, outlet temperature 70 °C; cellular model (---) and continuum model (——).

the droplet-air system are fully determined by the diffusional transport inside the droplet. The calculation for the cellular model give a slightly higher maximum droplet temperature.

Hence, it may be concluded that the simplifications made in the continuum model lead to distinct deviations from actual drying rates. Yet the improvement of the calculations by the cellular model will seldom justify the extra calculational effort and loss of flexibility. Furthermore the deviations are small compared with the differences in drying history due to the mixing effects discussed in Chapter 3.

2.4.4 Testing the calculational model experimentally

The experiments described in this section were intended to check the methods and assumptions used in the theoretical calculations. Theoretical calculations may easily lead to strong deviations from reality. Reasons for such deviations are:
– The assumptions made in the physical model may have been too rigorous to yield a good approximation of the actual behaviour.

28

– The parameters used in the model were obtained from measurements which did not completely cover the range of conditions during drying. Especially the diffusion coefficients have been extrapolated to low water concentrations for which no measurements were available.

– The method of calculation could not be proved to be valid.

Section 2.3.3 described a check of the method of calculation. After the check of the model for single droplets described here, a final check of the models by actual spray drying experiments would have been desirable but was not made because of the experimental difficulties involved.

Droplets   Experiments were done with spheres of 3 to 4 mm diameter consisting of water or a maltose-water solution (23, 52 % (w/w) maltose) to which 1 % (w/w) of agar-agar had been added. Spheres were produced by preparing a warm agar solution of the desired water-maltose composition, pipetting and transferring it into a mixture of petroleum ether and chloroform of approximately the same density. As soon as a droplet of the desired size had formed at the tip of the pipette, the droplet was removed by tapping lightly against the pipette. The droplet remained suspended until it became rigid upon cooling down in the solvent. The suspended state was attained most easily if there was a slight vertical concentration (density) gradient in the solvent.

The experimental apparatus is shown schematically in Fig. 6. Electrically heated air flowed upwards through a 2.5″-pipe packed with steel wool, subsequently passing through a venturi throat nozzle of 2″ diameter to ensure an upward air flow of homogeneous velocity distribution. The spheres were suspended from a 45 μm chromel P-constantan thermocouple, with the weld in the centre of the sphere. The spheres were suspended by pressing them on to the thermocouple, which easily cut through the gel and were placed in the flow of hot air. Drying conditions were limited to moderate temperatures (air temperatures below 80 °C) because with too high droplet temperatures liquefaction of the gel would result and the sphere would fall from the thermocouple. The moisture content of the air was 4.9 g water/kg air.

Temperature histories of the droplets were recorded and compared with those calculated with the continuum model for droplets of the same solid concentrations
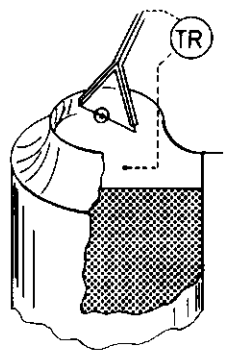

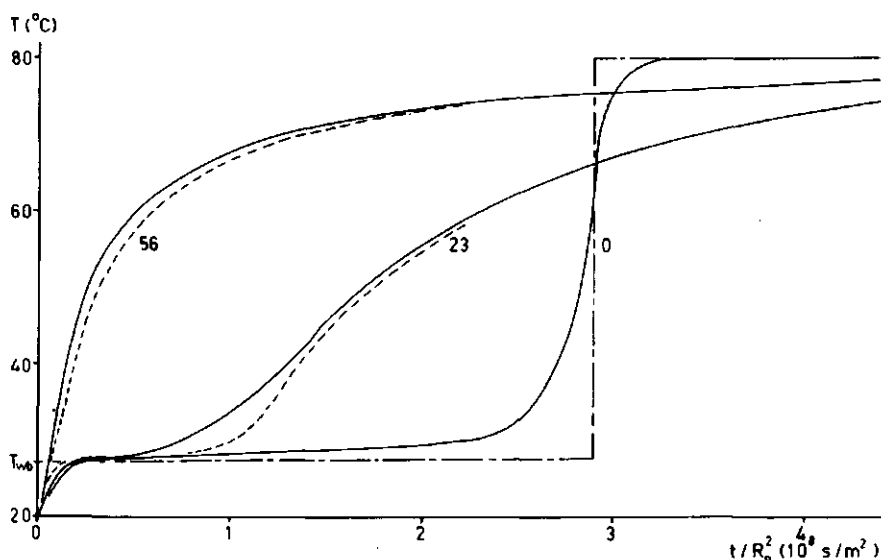Fig. 6. Diagram of the experimental apparatus.

29

Fig. 7. Experimental (———), calculated (– – –) and theoretical (– · –) temperature histories of droplets containing various amounts of maltose (%-w/w).

as in the experiment. Nusselt and Sherwood numbers were calculated with Eqns (22) and (23). Calculations were based on the physical properties of maltose as given in Appendix B.1.

Results and discussion Both experimental and theoretical temperature histories of droplets of various solid contents in drying air at 80° C are given in Fig. 7. The theoretical prediction is rather accurate at the high solid concentration. The temperatures of droplets with lower initial solids concentrations start to rise more rapidly than predicted by the theory. This behaviour can be explained by the fact that the droplets were in a fixed position with one side exposed towards the air flow. Hence, this front stagnation point would dry more rapidly and tend to attain a higher temperature, while the rear of the droplet would still be wet. The temperature of the droplet will be higher than the wet bulb temperature as soon as the evaporative flux from any point of the surface is less than that of a free water surface in the same air. This may explain the typically less flat character of the experimental temperature curves approaching the end of the 'constant rate period.' Obviously the presence of the agar-agar and conduction through the thermocouple also have some effect. The effect of conduction through the thermocouple was estimated by a method described by Trommelen & Crosby (1970) and was found to add 2 % to the total heat flux.

Conslusion The model seems to predict drying behaviour well especially for drying stages in which the drying process is fully governed by diffusion inside a droplet. For the earlier stages of drying a better fit would have been obtained if drying had progressed approximately uniformly at all sides of the droplet.

30

3 Effect of mixing in spray dryers on the drying history

3.1 Introduction

The rate of evaporation of droplets in a cloud is determined by the mass transfer coefficient and by the difference in water vapour concentration at the droplet surface and in the bulk of the continuous phase.

The effect of various parameters on the transfer coefficient has received ample attention in the literature on spray drying and has been extensively discussed in Section 2.2. The values of the driving forces for mass and heat transfer in actual spray-drying, however, received hardly any attention. The vapour concentration at the droplet surface is a function of the droplet temperature and of the liquid concentration at the droplet surface. This factor depends on the sorption isotherm which is known for many products and can readily be measured (Appendix B. 1.3). But to determine the driving forces and to calculate the drying history of a droplet we must also know the exact conditions of the bulk of the drying air surrounding the droplet.

It is not yet possible to measure temperatures of the drying air and vapour concentrations in the air inside an evaporating cloud with reasonable accuracy. Therefore we can at best predict changes in the initial air conditions by adding up the effects of the evaporation inside the cloud and those of the admixing of air from other regions of the dryer. Admixing results from convection throughout the dryer and from turbulent diffusivity.

The actual flow patterns in spray dryers are complex and variable. Extensive studies on the general design of spray dryers and flow patterns inside them are available (Marshall, 1954; Masters, 1972).

The overall flow pattern in a spray dryer is usually described as cocurrent or counter-current. These terms give no indication, however, of the local flow-pattern especially in the regions of the most intensive heat and mass transfer. Therefore as a rule, the process cannot be considered as the ideal phase contacting operation of the same name known from the chemical engineering literature. Many calculations presented in spray-drying literature, for instance, assume cocurrent flow of air and droplets in which the flow of droplets generated by the atomizer is instantaneously and homogeneously mixed with the flow of air.

Briffa (1967) showed, however, that during atomization a gradually diverging spray is formed. Baltas & Gauvin (1969a) found that the axial injection of a spray into the airstream of a cocurrently operating spray dryer results in peaked velocity profiles, steep gradients in the spatial concentration of the spray and, to a lesser extent, in the humidity of the air. They studied the radial dispersion of vapour and droplets under the influence of turbulent diffusivity and concluded that 'the

31

assumption of complete radial uniformity so prevalent in prediction techniques which have appeared in the literature so far, is quite unsound'. Cox (1962) made a computational and experimental study of the mixing efficiency of air and spray near a pressure nozzle. Experimentally he found that saturated air can be present.

Another type of mixing than radial dispersion of the spray must be mentioned. Especially in short-type dryers considerable vertical mixing of the drying air can take place. Such mixing can be caused by circulation induced by the centrifugal atomizer (Masters & Mohtadi, 1967). Buckham & Moulton (1955) found considerable vertical mixing inside a cocurrent spray dryer. They thought this mixing was due to:
– the effect of the high velocity of the inlet airstream,
– localized volume contraction caused by cooling of the spray and by heat losses through the chamber walls.
The injection of the spray itself also causes vertical mixing.

These flow and mixing patterns have a considerable influence on the conditions of the drying air surrounding the droplets. As a result of uneven distribution of the droplets over the drying air the temperature of the air in the vicinity of the atomizer will be more moderate than with even dispersion. Overall mixing of air will also create more moderate drying conditions in the air entrance region.

Few studies on the relations between these mixing patterns and the heat and mass transfer during drying can be found in the literature. Baltas & Gauvin (1969a) and Adler & Lyn (1971) included turbulent spray dispersion in their calculations of heat and mass transfer in sprays. Buckham & Moulton (1955) compared actual temperature distributions in a cocurrent flow spray-dryer with those in two idealized situations of vertical mixing:
– Complete mixing of the drying air.
– Perfectly cocurrent air flow.
Actual results were found to be in between these extremes. Van der Lijn et al. (1972) calculated the effect of these extreme mixing situations on the drying of droplets with internal resistance to mass transfer. Kerkhof & Schoeber (1973) made a similar comparison of drying in ideally cocurrent, countercurrent and perfectly mixed air.

In this study the effects of the air-mixing and spray-dispersion patterns on heat and mass transfer are discussed for various inlet air temperatures and water to air ratios. Effects of the mixing pattern on other important factors in spray drying such as wall deposits and scorching are omitted. Only three extreme cases of gas phase mixing are considered. These extremes do not occur as such in actual drying situations, but by studying them we hope to improve our understanding of the processes involved. Some features of all of these extreme patterns will, however, occur. To what extent they occur depends on the particular spray dryer and on the product which is dried, and will be briefly discussed in Chapter 5.

3.2 Drying histories for perfectly mixed air

One extreme case of gas phase mixing is characterized by complete mixing of the bulk of the continuous phase throughout the dryer. Air of inlet conditions is

supposed to be instantaneously mixed up with the gas phase already present in the dryer. Hence, the temperature and humidity of the bulk of the air which surrounds the droplets are constant during the entire drying process. They are equal to the temperature and humidity of the outlet air. The conditions of the air can be calculated on the basis of mass and energy balances over the whole spray-dryer.

Although the bulk phase is perfectly mixed, it is assumed that the conditions of the gas phase adjacent to the droplets are determined by diffusion or conduction through a stagnant boundary layer. The conditions of the drying air for the calculations reported here are given in Table 1. The air temperatures and humidity are such as would result if the dryer is operated adiabatically, if hot completely dry air at the inlet temperature were introduced and the droplets reached equilibrium inside the dryer. These conditions are only equal to the outlet air conditions if the residence time in the dryer is sufficiently long. This assumption has been made.

Temperature histories of droplets in perfectly mixed air are given in Fig. 8 and the course of the water loss in Fig. 9. The drying histories may be summarized as follows:
– If the droplets are introduced in the dryer at a temperature below the dew point of the air, moisture condenses until the dew point is reached. A rapid rise in the temperature of the droplet occurs because of condensation and conduction.
– When the dew point temperature has been reached, the temperature rises more slowly because from then on the droplets start evaporating. Thus, heat influx is partially used as heat of evaporation. The droplets approach T_{wb} (wet-bulb temperature) and remain near this temperature until the surface water concentration falls to such a value that the equilibrium water vapour pressure deviates significantly from the vapour pressure of pure water at the same temperature.
– The surface water concentration continues to fall. Hence, the evaporation rate decreases and the temperature of the droplets rises until eventually equilibrium between the droplets and the air is reached.

For a system in which the equilibrium water vapour pressure is a monotonously decreasing function of the soluble solids content, such as maltose solutions, an absolutely constant rate period will not occur. After a rapid rise to T_{wb} the

Table 1. Conditions of the air in the situations studied.

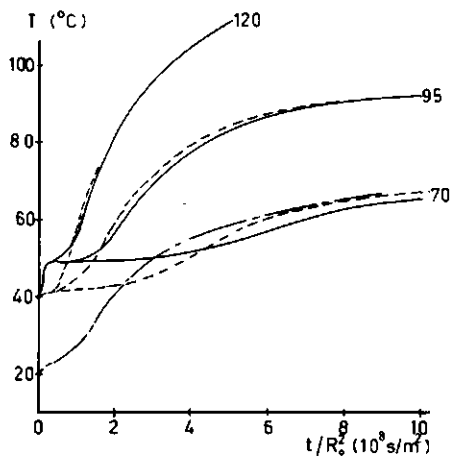| Dry air inlet temperature (°C)	Feed rate (50 % d.s.) (kg/kg air)	Outlet (adiabatic equilibration) temp. (°C)	Outlet (adiabatic equilibration) humidity (kg water/kg air)
250	0.1412	70	0.0706
	0.1166	95	0.0583
	0.0952	120	0.0476
175	0.0780	70	0.0390
	0.0576	95	0.0288
	0.0370	120	0.0185

Fig. 8. Temperature histories for droplets in perfectly mixed air. Numbers on the curves indicate (outlet) air temperatures (°C). Inlet temperatures 250 °C (——), 175 °C (---) and 70 °C (- · -).
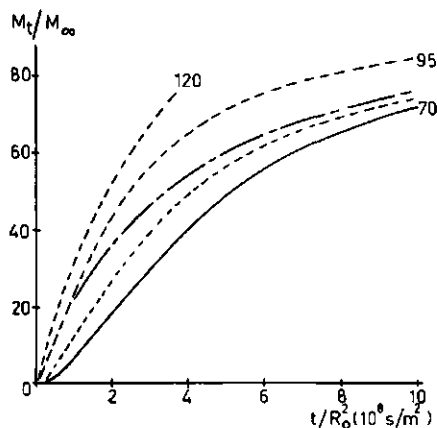
Fig. 9. Course of water loss for droplets in perfectly mixed air. Specifications as in Fig. 8.

temperature usually increases only slowly. This slow change is in accordance with the small decrease in equilibrium relative humidity of maltose solutions with decreasing water content at the initial concentration level assumed.

The droplets attain nearly equal T_{wb} for various outlet temperatures but constant inlet temperatures, as may be seen from Fig. 8 and as follows from the fact that the psychrometric ratio is approximately one for water vapour in air. Furthermore the drying rates are higher at higher outlet temperatures and, therefore, the droplet temperatures start to rise significantly above T_{wb} at an earlier stage.

The effect of the inlet temperature on the temperature histories of the droplets, the well mixed air (outlet air) temperature being constant, is also shown in Fig. 8. The higher inlet temperatures, obviously lead to higher wet bulb temperatures at the same air temperature. For wet droplets, which necessarily have temperatures near T_{wb} of the air, the driving forces for heat transfer and evaporation are therefore lowest for the highest inlet temperatures. Hence, drying is slower (Fig. 9) and the near wet bulb temperature will be maintained for a longer time. The temperature history curves for various inlet temperatures in Fig. 8 do indeed intersect.

Usually, the near wet bulb temperatures are reached quickly because of condensation. In situations in which no condensation can occur, for example because the dew point of the drying air is too low, the picture may be quite different. Fig. 8 includes an example of dry air at 70 °C. The drying rates are higher than in the other examples. The droplet is warmed up by heat conduction while it is already evaporating, and before T_{wb} is reached the surface concentration has already fallen so much that the temperature will continue its steep rise,
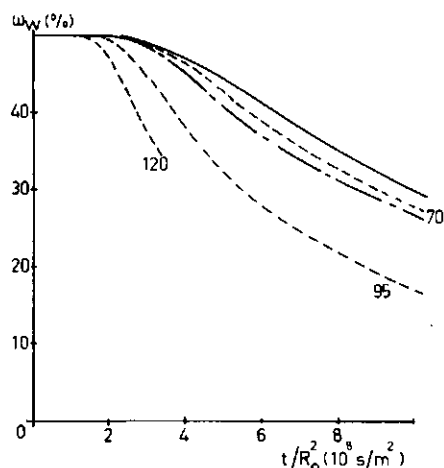
34

Fig. 10. Concentration histories in the centre of a droplet in perfectly mixed air. Specifications as in Fig. 8.
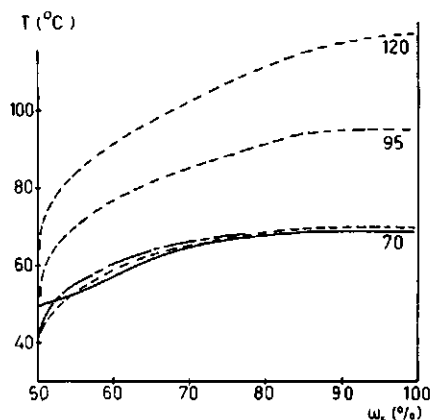
Fig. 11. Concentrations in the centre of a droplet and coincident droplet temperatures for perfectly mixed air. Specifications as in Fig. 8.

without remaining near T_{wb}.

The concentration history in the centre of a droplet is drawn in Fig. 10. The combinations of droplet temperature and the concentration in the centre of a droplet during the drying sequence, which might be of importance for the determination of chemical reaction rates, are shown in Fig. 11 for various conditions of the inlet and outlet air.

3.3 Drying histories for perfectly cocurrent dryer operation

For a perfectly cocurrent spray-dryer operation it is assumed that the flow of wet droplets generated by the atomizer is instantaneously mixed with the inlet airflow. After this initial mixing, both air and droplets move in plug flow through the dryer. Heat and mass exchange take place between the droplets and the cocurrently moving air. The conditions of the air gradually change because of the transfer processes. The system of air and droplets is assumed to behave adiabatically and the air conditions can be calculated on the basis of mass and energy balances over an arbitrary control volume of air with dispersed droplets. The conditions of the drying air at the inlet and after adiabatic equilibration are again given in Table 1.

The calculated temperature histories for droplets in perfectly cocurrent air are given in Fig. 12 and the course of water loss is summarized in Fig. 13. The simultaneous behaviour of the temperatures of a droplet and its surrounding air is shown in Fig. 14.

The drying histories may be summarized as follows:
– After mixing of the droplets with hot dry air, there is usually no condensation on the droplets. The droplets are heated by conduction and the temperature rises rapidly because of the large difference in temperature with the surrounding air.
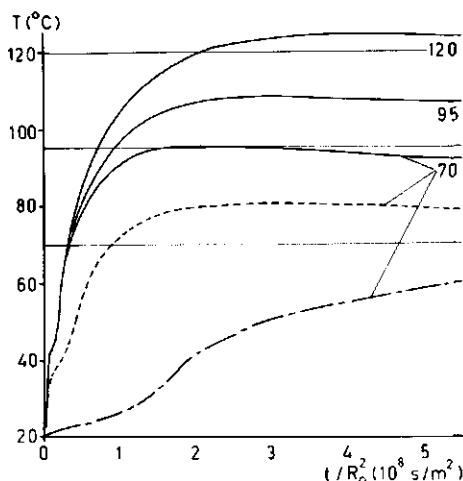
35

Fig. 12. Temperature histories of droplets for perfectly cocurrent dryer operation. Numbers on curves indicate outlet temperatures. Inlet temperatures 250 °C (——) and 175 °C (- - -) and 70 °C (—·—).
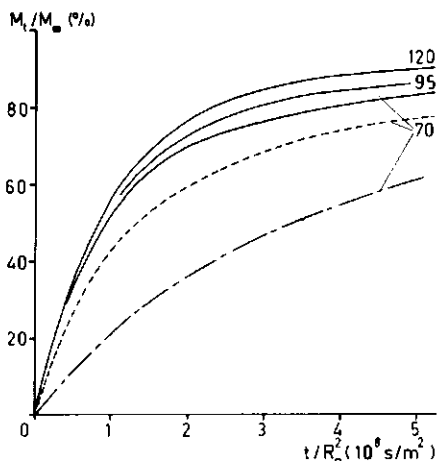
Fig. 13. Course of water loss of droplet for perfectly cocurrent dryer operation. Specifications as in Fig. 12.

– The rate of temperature rise slows down slightly when the temperature approaches the air T_{wb}. No period of near T_{wb} occurs, however, because of a rapid fall in surface concentration.

– The surface water concentration continues to fall. Hence the evaporation rate decreases and the temperature of the droplets approaches the temperature of the surrounding air which is at that moment still clearly above the outlet temperature.

– The temperature of the surrounding air decreases as a result of continued evaporation from the droplet and the temperature of the droplets passes
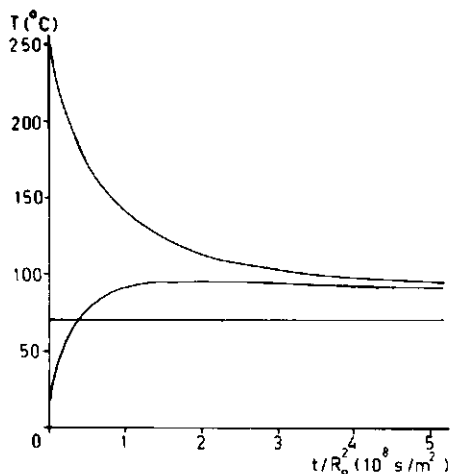

Fig. 14. Temperature history of a droplet and its surrounding air for perfectly cocurrent dryer operation. Inlet temperature 250 °C, outlet temperature 70 °C.

36

Table 2. Dimensionless maximum droplet temperature $((T_{max} - T_{feed})/(T_{outlet} - T_{feed}))$ as a function of inlet and outlet temperatures (cocurrent airflow) ($T_{feed} = 20 °C$).

Outlet temperature (°C)	Inlet temperature (°C)		
	175	200	250
70	1.30	1.36	1.52
95	1.08	1.11	1.17
120	1.03	1.03	1.03

through a maximum, while the surface concentration rises slightly as a result of the rising relative humidity of the air.

From Fig. 12 it follows that the higher inlet temperatures and the lower outlet temperatures cause a more pronounced maximum of the droplet temperature. The relative rise in temperature above the outlet temperature is shown in Table 2. Although not studied explicitly it is clear that droplets of different sizes in one spray will reach different temperatures. This is represented in Fig. 3.

The drying rate of droplets during the first stages of drying depends mainly on the inlet air conditions. Hence, the initial behaviour of droplets under constant inlet and varying outlet conditions is identical. This effect is shown in Figs 12 and 13. Differentiation in droplet behaviour starts as soon as the air conditions have changed markedly as a result of water evaporation. The drying rate of droplets at equal outlet temperatures but various inlet temperatures is higher at the higher inlet temperatures. The difference is also shown in Fig. 13.

The concentration history at the centre of the droplets is given in Fig. 15 for various inlet and outlet conditions. The concentration histories of Fig. 15 together
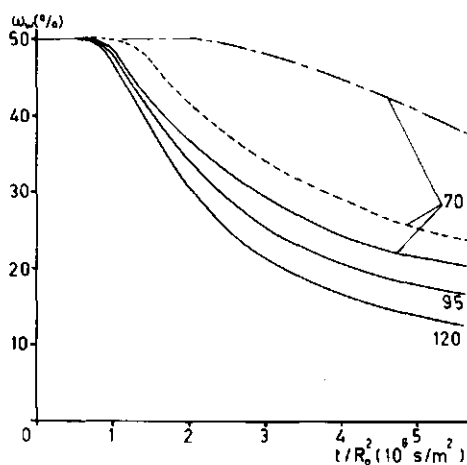

Fig. 15. Concentration histories in the centre of a droplet for perfectly cocurrent dryer operation. Specifications as in Fig. 12.
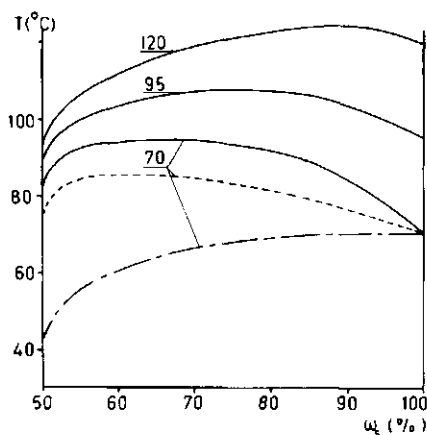
37

T (°C)

120

95

70

100

80

60

40

50   60   70   80   90   100

ω (%)

Fig. 16. Concentrations in the centre of a droplet and coincident droplet temperatures for *perfectly cocurrent dryer operation*. Specifications as in Fig. 12.

with the temperature histories of Fig. 12 yield a set of combinations of temperatures and concentrations at the centre of the droplets during the drying process. These data are given in Fig. 16.

3.4 Drying histories for gradual spray dispersion

As stated in Section 3.1 the assumption about perfectly cocurrent spray-drying that droplets are instantaneously mixed with the drying air is not realistic. In fact, the droplets generated by the atomizer are not mixed instantaneously with the *total* amount of inlet air.

Initially a spray is formed consisting of the droplets and a minor part of the inlet air. Exchange takes place within this spray, but because the ratio of air to liquid is far lower than for perfectly cocurrent drying, the air becomes saturated after some evaporation has taken place. The spray is then gradually diluted with the remaining air which is still at inlet conditions. The conditions of the air in an arbitrary volume inside the spray are thus determined by the combined effects of evaporative cooling and the entrainment of hot air in the spray.

The extreme situation that the admixing takes place in a very short time compared with the time needed for evaporation would be identical with a perfectly cocurrent dryer operation.

In another extreme example spray dilution would take place very slowly. Hence, the droplets are approximately in equilibrium with the surrounding air and the admixing of air is the mechanism controlling the drying rate. The droplets may be considered of homogeneous concentration and temperature and the conditions of the air are directly related to the droplet concentration and temperatures by the sorption isotherms of the droplet material.

Furthermore, the conditions of the air are determined by the adiabatic cooling of the air-droplet system due to evaporation. Possible conditions of the air are indicated by an adiabatic cooling line in the psychrometric chart. The equilibrium condition is given by the intersection point of this line with the equi-concentration lines in the same chart, which indicate the set of air conditions in equilibrium with
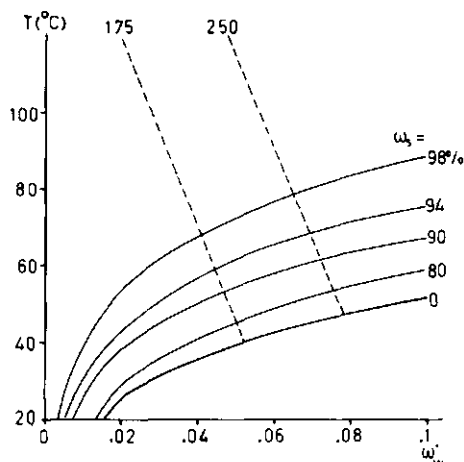
38

Fig. 17. Psychrometric chart indicating air conditions in equilibrium with maltose solutions of indicated concentrations (equiconcentration lines) (——) and adiabatic cooling lines (– – –) for two inlet temperatures.
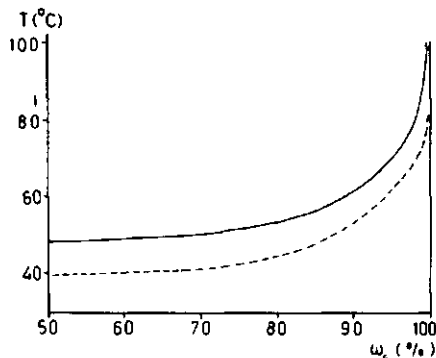
Fig. 18. Concentrations in the centre of a droplet and coincident droplet temperatures for gradual spray dispersion in for two inlet temperatures.

a solution of a given concentration. Both types of lines are shown schematically in Fig. 17. If we only assume that spray dispersion takes place slowly compared with equilibration inside the spray, additional data on the rate of mixing would be required to give water loss and temperature histories. Because the choice of such data would be arbitrary with no reliable data on spray dispersion in actual spray-dryers available, drying histories are omitted here. As with perfectly cocurrent operation and perfectly mixed air, it is, however, possible to give the combinations for droplet temperatures and concentrations during drying. They are shown in Fig. 18.

A rough calculation on the rate of spray dispersion in actual spray-drying is given in Chapter 5.

3.5 Comparison of drying histories for various mixing patterns

Drying histories in the three extreme drying situations discussed in the preceding sections show remarkable differences. A comparison of the temperature histories is given in Fig. 19 and the courses of water loss for equal inlet and outlet air conditions are compared in Fig. 20. Part of the drying histories for slow spray-dispersion, although stated as arbitrary, are indicated in Fig. 19 and 20, because changes of temperature and concentration are slow relative to the rates of change in the other two examples and, the droplet conditions will therefore remain approximately constant during the short period under consideration.

The highest droplet temperatures are reached in a perfectly cocurrent dryer operation. They are reached at an early stage of drying and can be well above the
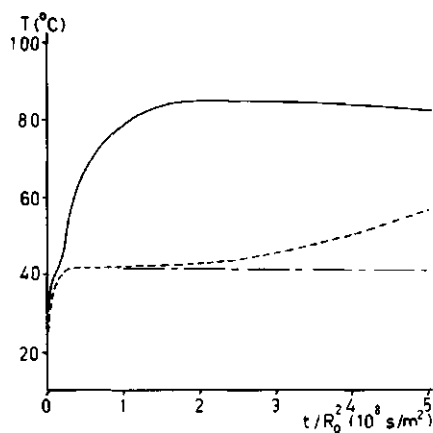
39

Fig. 19. Temperature histories of drying droplets for perfectly cocurrent dryer operation (———), perfectly mixed air (– – –) and gradual spray dispersion (– · –). Inlet temperature 175 °C, outlet temperature 70 °C.
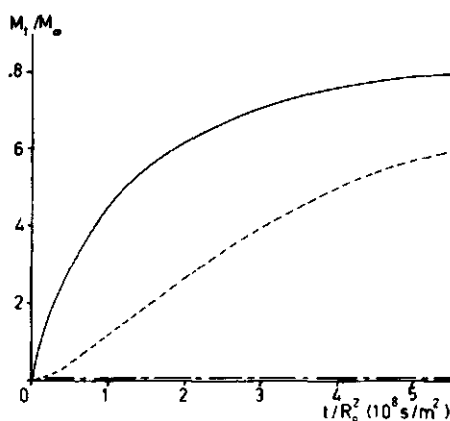
Fig. 20. Course of water loss from drying droplets for perfectly cocurrent dryer operation, perfectly mixed air and gradual spray dispersion. Specifications as in Fig. 19.

outlet temperature (Table 2). With a gradual spray-dispersion and in perfectly mixed air the droplets reach the maximum temperature at the outlet.

The drying rates for a perfectly cocurrent dryer operation are always higher than the rates for perfectly mixed air. It is interesting to note that for a constant outlet temperature in the perfectly cocurrent situation, the drying rate increases with increasing inlet temperature and for perfectly mixed air the drying rate decreases with increasing inlet temperature.

The way in which temperature history and concentration history are interlinked is of practical interest for the calculation of the effect of drying on chemical reaction, droplet inflation, etc. The combinations of water concentrations and temperatures in the centre of a droplet for the various mixing patterns are compared in Fig. 21. At equal concentrations in the droplet centre, the droplet temperature is always highest under perfectly cocurrent conditions and lowest if spray-dispersion takes place extremely slowly. However the time required to reach a certain average concentration in a droplet is always shorter in cocurrent drying and longest for slow spray-dispersion.

In a perfectly cocurrent dryer operation, the concentration profiles at the surface of the droplets are very steep because of high evaporation rates. In perfectly mixed air, drying rates are lower and the concentration profiles are less steep. In this situation more water has evaporated before a given surface water concentration is reached. This effect is of practical relevance to the retention of aroma components during drying. (Kerkhof et al., 1972; Kerkhof, 1975). The concentration profiles for both situations are compared in Fig. 22. The amounts of water evaporated before an arbitrary water surface concentration of 15 % (w/w) is reached are compared in Table 3.
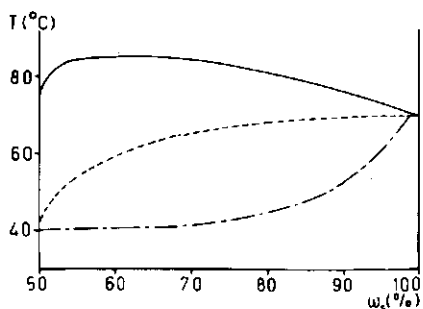
40

Fig. 21. Concentrations in the centre of a droplet and coincident droplet temperatures for perfectly cocurrent dryer operation, perfectly mixed air and gradual spray dispersion. Specifications as in Fig. 19.
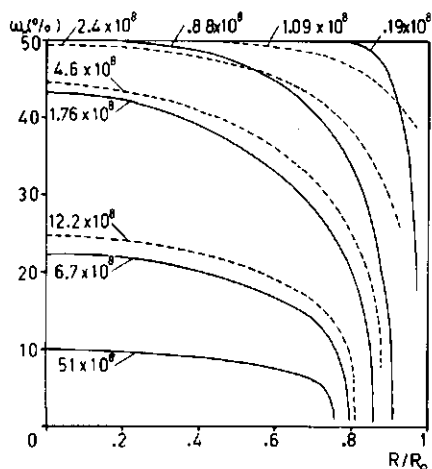
Fig. 22. Concentration profiles inside a drying droplet for perfectly cocurrent dryer operation (——) and perfectly mixed air (---). Inlet temperature 175 °C, outlet temperature 70 °C. Numbers on curves indicate values of t/R_o^2.

Table 3. The effect of the inlet and outlet temperatures and airflow pattern on the water loss (M_t/M_o) until a surface concentration of 15% (w/w) is reached.

	Inlet temperature (°C)	Outlet temperature (°C)		
		70	95	120
Perfectly cocurrent airflow	250	0.12	0.12	0.12
	175	0.16	0.13	0.12
Perfectly mixed air	250	0.53	0.38	0.30
	175	0.44	0.30	0.23

3.6 Conclusion

In many respects the drying process strongly depends on the way in which air and droplets are brought into contact. Quick mixing of a spray with the total air flow gives results which are quite different from those obtained for gradual dispersion. Similarly the results obtained when the total bulk of the air is well mixed differ greatly from those obtained when it flows cocurrently with the droplets. *Hence, the spray-dryer design and the spray dispersion and air flow pattern which result from it will have a strong influence on all product properties which depend on the drying process.* This subject deserves much more attention than it has received until now.

41

4 Droplet inflation

4.1 Introduction

Spray-dried particles are usually hollow.
– Hollowness may result from the presence of dispersed gases in the liquid feed or from gases which are entrapped in the liquid feed during atomization.
– Hollow particles may result from the presence of a vapour impervious film which is inflated when moisture or other dissolved volatiles vaporize within the droplet.
– Voids (or vacuoles) result from the formation of a rigid crust through which moisture is transported to the surface. In porous particles the volume of the evaporated water will be replaced by air flowing back into the voids. If the surface is impervious, a vacuum will result inside the droplet.

Verhey (1973) showed that the inclusion of air during atomization is very usual during spray drying, thus supporting the first explanation. He also measured the vacuum present in spray-dried particles immediately after drying, thus indicating the formation of a rigid impervious crust at some stage of the drying. He showed furthermore, that solid milk powder particles can be formed if inclusion of air during atomization is avoided.

From his results it can be concluded that no spontaneous nucleation occurs under the moderate drying conditions in his experiments. Thus, the second explanation can only be valid after the prior formation of a small vapour bubble either by spontaneous nucleation as a result of more severe drying conditions or as a result of the presence of other dissolved volatiles which create a higher super-saturation.

4.2 Calculational model

The fact that an air bubble is often present inside a droplet can be used as a basis for the calculation of the drying histories of inflating droplets. It was assumed that there was one central air bubble which at any given moment was in equilibrium with the liquid at the internal interface. Hence, the volume and the gas composition of the bubble could be calculated as functions of the liquid composition and the temperature of the liquid at the interface. The model used has been described in Section 2.4.2. Eqns (42) and (44) in particular are relevant here.

To keep the calculations simple the bubble pressure was assumed to be atmospheric. This assumption can be inaccurate because:
– Surface tension causes a pressure inside the droplet which is slightly higher than

the outside pressure.

– Viscous forces increase internal pressure during bubble growth and reduce internal pressure during bubble shrinkage.

Yet these calculations may give a good impression of the combined effects of air inclusion and internal evaporation during the first stages of drying when the droplet (skin) is still plastic. For some thermoplastic products this period can extend over a major part of the drying process. As soon as the droplet hardens to form a very viscous or even rigid shell the model presented can no longer describe the phenomena.

As we concluded in Chapter 3 the drying behaviour of droplets strongly depends on the air flow pattern. This is also true for droplet inflation. The calculations which we made on the inflation of droplets assumed the presence of perfectly cocurrent air flow. In this air flow pattern high droplet temperatures can be reached at a moment the droplets are still internally wet. Thus, the best conditions for bubble growth (ballooning) during drying are created and the effect of the presence of an entrapped air bubble will be largest. The assumed conditions of the drying air were the same as those used for the calculations on drying in the absence of droplet inflation (Table 1, page 33) and therefore allow comparison.

4.3 Results and discussion

The temperature histories of droplets with and without a central air bubble are compared in Fig. 23 for various outlet temperatures. Fig. 24 shows the course of water loss under the same conditions and Fig. 25 shows the calculated bubble sizes if a gas nucleus is present initially.

The figures indicate that the presence of entrapped air has a limited effect when the outlet temperature is low, but increases with rising outlet temperature. When the outlet temperature is low, the droplet temperature remains well below the
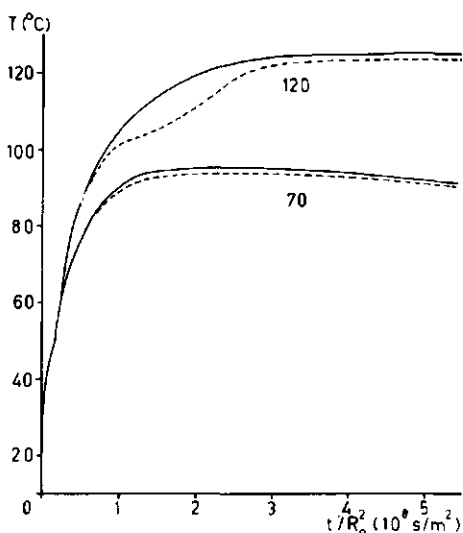
Fig. 23. Temperature histories of droplets with (– – –) and without (——) a central air bubble. Perfectly cocurrent airflow, inlet temperature 250 °C, $R_{is,0}/R_0 = 0.2$. Numbers on curves indicate outlet temperatures.
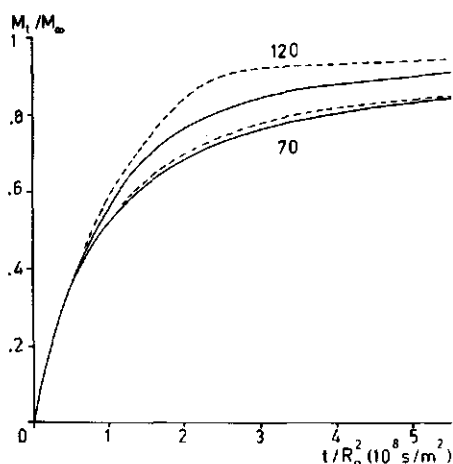
Fig. 24. Course of water loss for droplets with and without a central air bubble. Specifications as in Fig. 23.
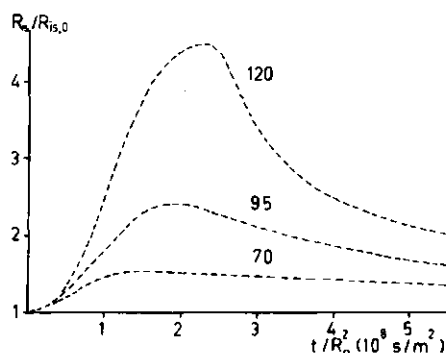
Fig. 25. Variation of the size of an entrapped air bubble with the time. Specifications as in Fig. 23.

boiling point of the liquid in the droplet, the internal evaporation is limited and for that reason only a slight growth of the bubble radius occurs.

At a high outlet temperature the droplet temperature rises well above the boiling point of the liquid in the droplet if no internal evaporation takes place (because of the absence of spontaneous nucleation inside the droplets). In the presence of a gas necleus, however, considerable internal evaporation and a rapid increase in bubble radius occurs.

The bubble radius increases maximally about five times and the volume about hundred times the original value for an outlet temperature of 120 °C. The volume increased only about three times the original volume at an outlet temperature of 70 °C.

The effect of inflation on the drying histories starts to be important at the moment the droplet temperature approaches the boiling point of the liquid. At that moment the rate of evaporation becomes much larger than the rate would have been in the absence of inflation, mainly because of an increase of the concentration gradients. The faster evaporation causes a lower temperature.

The effect of the presence of a bubble on the combinations of droplet temperatures and water concentrations at the wettest point inside the droplet is represented in Fig. 26 for various outlet temperatures. The effect is again small for temperatures well below the boiling point.

Fig. 27 shows the effect on the temperature histories of drying droplets of varying the amount of air entrapped in the droplet. The effect on the course of water loss is given in Fig. 28 and the effect on the relative increase in bubble radius is given in Fig. 29. All other conditions remaining the same, drying takes place more quickly, the droplet temperatures are lower and the relative increase in bubble diameter is smaller for the larger amounts of entrapped air. Small bubbles cause a droplet temperature which is slightly below the boiling point of

44
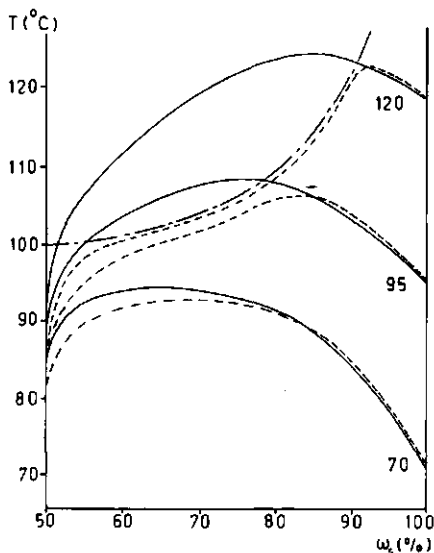
Fig. 26. Concentrations in the wettest point of a droplet and coincident droplet temperatures with and without an entrapped air bubble. Specifications as in Fig. 23.
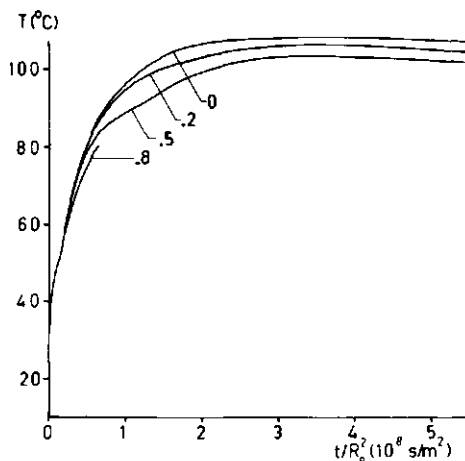
Fig. 27. Effect of the amount of entrapped air on the temperature history of a drying droplet. Perfectly cocurrent dryer operation, inlet temperature 250 °C, outlet temperature 95 °C. Numbers on curves indicate values of $R_{is,0}/R_0$.

Fig. 28. Effect of the amount of entrapped air on the course of water loss. Specifications as in Fig. 27.

Fig. 29. Effect of the amount of entrapped air on the variation of the size of an entrapped air bubble with time. Specifications as in Fig. 27.

45

Fig. 30. Effect of the amount of entrapped air on the concentrations in the wettest point of a droplet and the coincident droplet temperatures. Specifications as in Fig. 27.
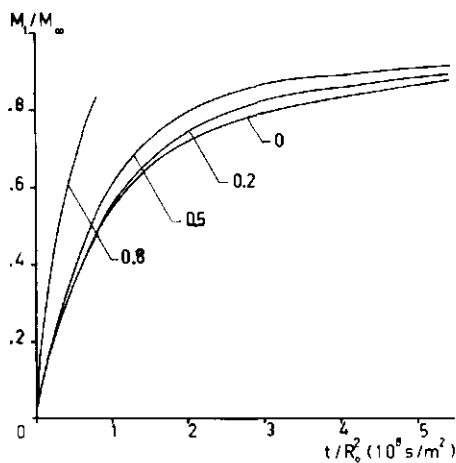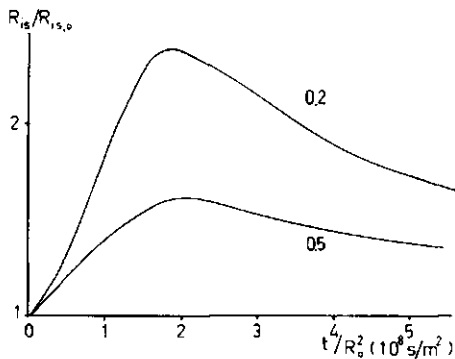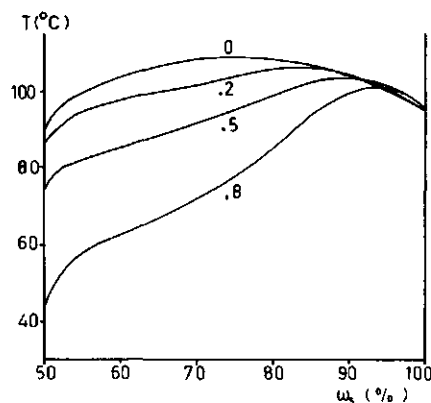
the liquid. Larger bubbles cause the temperature to be markedly lower.

Hence, droplet inflation is clearly a combined effect of the partial air and water vapour pressures. The smallest amounts of entrapped air hardly contribute to the total pressure and the effect of the entrapped air is limited to avoiding superheating of the droplet.

The relations between the droplet temperature and the concentration at the wettest point in droplets with various amounts of entrapped air are given in Fig. 30. At equal concentrations the temperature of droplets with the largest amounts of entrapped air is markedly lower (except at the very end of the drying). This result is caused by the combination of quicker drying and lower droplet temperatures during the course of drying.

4.4 Inflation and product properties

The calculations described give the history of the bubble inside a drying droplet for the hypothetical situation, that the droplet remains plastic during the whole drying process. Actual drying products turn rigid at some stage of the drying. According to Charlesworth & Marshall (1960) the final diameter of a spray-dried particle equals the diameter at the moment the crust is complete. This is especially true for products which form a rigid crust such as most inorganic salts. The skin formed around some other products such as instant coffee powder remains plastic over prolonged periods (Sivetz & Foote, 1963).

Charlesworth & Marshall gave a schematic survey of the various alternative physical changes in drying droplets depending on the presence or absence of inflation and on the stage of formation and the character of the solid crust. No general rules can be given about the effect of inflation on the final droplet (and bulk) volume of the product without knowledge of the flowing properties of the material in the droplet and its dependence on water concentration and temperature. It is important whether crystallization can add to the rigidity of the particle. Particles which attain rigidity from a glass-like structure will harden when the water concentration or temperature fall below given values. Various alternative examples of inflation and rigidification are shown in Fig. 31.

46
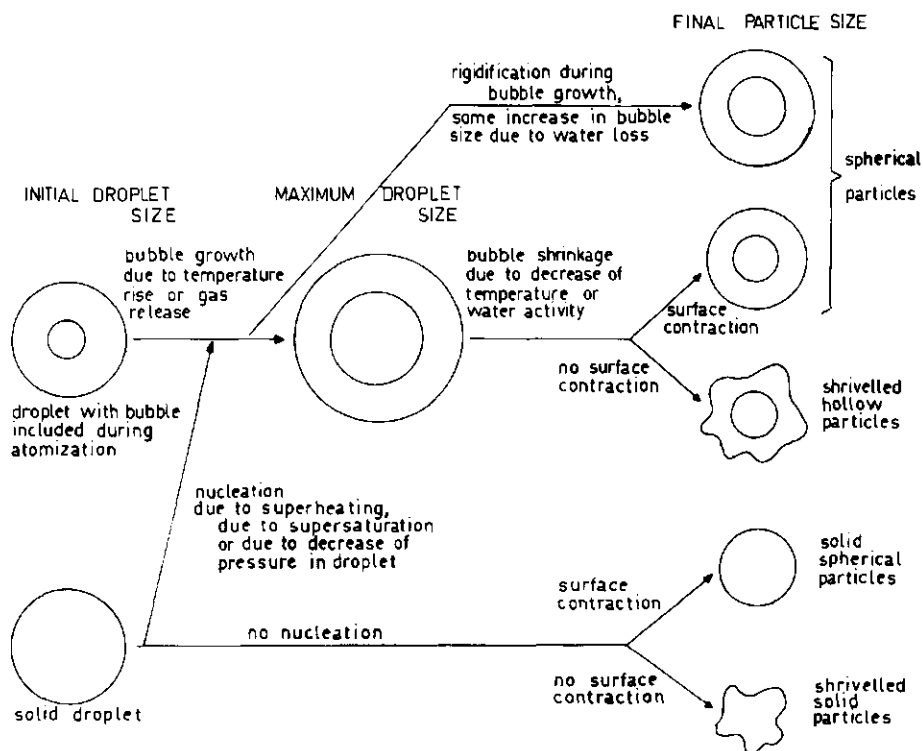
Fig. 31. Physical changes in drying droplets.

For obtaining a low density of the final product three conditions must be fulfilled:
– Bubble growth must be sufficient. This can only occur if gas is entrapped in the droplet or spontaneous nucleation, takes place. Gas can be included during atomization (Verhey, 1973). Bubble growth and nucleation can be enhanced by conditions of high inlet and outlet temperatures and a cocurrent air flow pattern as well as by the dissolution of gas into the feed liquid.
– There must be no loss of gas from bubbles due to porosity of the droplet walls or as a result of bubble collapse.
– The droplet must become rigid at a stage when the bubble is still large.
High densities will be enhanced by opposite circumstances.

Duffie & Marshall (1953) reported that an increase in air temperatures, in feed concentration or in feed temperatures can lead to a reduction of the bulk density. Their experiments were not representative for the spray drying of liquid foods, because they used a different type of raw material and the air conditions were unaffected by the evaporation from the droplets. However their results are substantiated by my calculations.

The effect of the feed temperature was less pronounced in the results of Duffie & Marshall and my calculations did not give any evidence of such an effect. In calculations in which constant inlet and outlet temperatures of the drying air were

47

assumed no significant effect of the feed temperature on the droplet inflation was found. If, however, the flow ratio between feed and air was maintained, the outlet temperature rose with increasing feed temperature (heat balance) and increased droplet inflation resulted. Furthermore, a change in the feed temperature affects the atomization process and might affect air inclusion.

Some authors found that larger droplets inflate more than smaller ones (Moore, 1967; Buckham and Moulton 1955). It is also known from spray-drying practice that cyclone powders usually have a higher bulk density than the main fraction of the spray-dried powder. The calculations do not explain such a difference if the relative amount of entrapped air is independent of the droplet size, if the Nusselt and Sherwood numbers are equal and if the conditions of the drying air at equal Fourier numbers are identical.

Differences in bulk density can partially be explained by a grinding effect of the cyclone. Furthermore, differences in relative width of the particle size distribution of cyclone and main fractions can play a role. The amount of entrapped gas could also differ for various size fractions as a result of different atomization mechanisms and the duration of the period of internal circulations.

Differences in droplet deceleration and final velocity of droplets of various size lead to different Sherwood and Nusselt numbers which could explain different droplet inflation. The differences will, however, be limited for small droplets when the Sherwood and Nusselt numbers equal 2 after very limited evaporation.

Although there is no proof, there are indications that these factors can often explain only a minor part of the effect. If so, differences in the conditions of the drying air should be responsible for the difference in inflation of the various size classes.

Fig. 3 in Section 2.4.3 indicates that for cocurrent drying, small droplets would reach higher temperatures than the larger ones. If this situation is true, the effect of size on droplet inflation would be opposite. The effect can be explained, however, by assuming a situation of gradual spray dilution. One can imagine that the time for spray dilution is sufficient for the smaller droplets to dry but not for larger droplets. Thus, for droplets that are wet inside the larger droplets would reach higher temperatures than the smaller ones and could inflate more.

Furthermore classification effects in the atomizer region can cause larger droplets to move nearer to the spray boundary and to mix with hot air at an earlier stage.

48

5 Relevance of the calculations to drying practice

5.1 Introduction

The factors which determine the drying behaviour of droplets in a spray-dryer were discussed in Chapter 2. Accordingly models were constructed to simulate this behaviour (Section 2.4) and they were applied to study the effect of some basic air circulation patterns in spray dryers on the drying process (Chapter 3) and the mutual effects between drying and droplet inflation (Chapter 4). The relevance of these calculations to the actual physical processes in spray-dryers will briefly be discussed here. This discussion will be divided into two parts:
- An attempt to visualize the model systems in actual spray-drying.
- A brief discussion of the actual droplet temperatures during spray drying and the effect on some product properties.

5.2 The idealized mixing patterns and actual spray-drying

It followed from the calculations in Chapter 3 that the mixing pattern of air and droplets in a spray dryer is of major importance for the drying history of the droplets. Unfortunately, very little is known about the actual airflow and spray dispersion in spray dryers. Therefore the following discussion will be mainly qualitative.

Three stages of the spray dispersion process can be distinguished (Fig. 32) similar to those in a free (submerged) turbulent jet (Davies, 1972). For simplicity transition stages will be neglected.
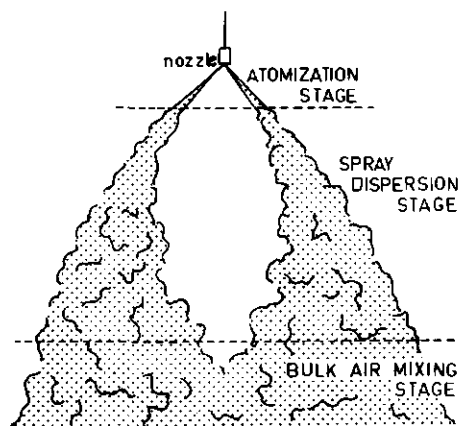
Fig. 32. Diagram of the spray dispersion process.

1 The atomization stage This stage is of relatively short duration. The liquid leaving the nozzle or centrifugal atomizer at high velocities usually forms a liquid sheet, which is unstable and which is disrupted into a large number of droplets as a result of surface tension, viscous and inertia forces. The instability mechanisms leading to the atomization have been described extensively (e.g. Marshall, 1954; Dombrowski & Munday, 1968). Vigorous transfer of momentum between the liquid and the air generates a turbulent air jet cocurrently with the droplets.

Heat and mass transfer between the liquid sheet or the droplets and the air surrounding them can take place at high rates. They are enhanced by vigorous oscillations in the liquid phase and by the high relative velocities between the droplets and the air. None of the idealized systems which we described in Chapter 3 are representative for this stage.

2 The spray dispersion stage At some distance from the atomizing device droplets move at still high velocities inside an air jet which moves cocurrently, but at a lower velocity, between the bulk of the drying air. Air from outside the jet is gradually entrained causing expansion of the jet and a decrease of the velocity. Eventually both the droplet velocity and the air velocity in the jet approach the velocity of the bulk air.

Gradual spray dispersion described in Section 3.4 could well be representative for this stage. Hence, the conditions of the air in the spray will differ greatly from the conditions of the air outside. The moisture content will be higher and the temperature will be lower due to evaporation from the droplets.

The transport of moisture out of the spray could limit the total rate of mass transfer during the spray dispersion stage.

Let us assume a flat spray of thickness $2R_{spray}$ with width and length 1, which we observe at a position fixed to stationary coordinates. Let us also assume that the conditions of the bulk of the air in the spray are determined by the evaporation from a large number of droplets and by turbulent transport of vapour to the surroundings of the spray. Let us assume stationary conditions and neglect the accumulation of water in the spray. Obviously these assumptions only make sense if the volume of the spray is small relative to the volume of the surrounding dry air and if the droplets are still far from depletion. A schematic representation of the drying spray is given in Fig. 33.

The driving forces for the water vapour transport are $\Delta\rho_{w,in}$ (from the surface of the droplet to the bulk of the spray surrounding the droplet) and $\Delta\rho_{w,out}$ (from the bulk of the spray to the surroundings of the spray). The indicated spray has a volume $2R_{spray}$ and it contains $2R_{spray} \cdot \rho_G$ kg air. With x kg atomized liquid per kg air the spray contains $x \cdot 2R_{spray} \cdot \rho_G$ kg liquid. The liquid surface in the spray is

$$A = 6x \frac{R_{spray}}{R} \frac{\rho_G}{\rho_L} \tag{45}$$

The total water evaporation from the liquid surface amounts to

$$F_{in} = 6xR_{spray} \frac{\rho_G}{\rho_L} \frac{Sh}{2} \frac{D}{R^2} \Delta\rho'_{w,in} \tag{46}$$

The moisture transfer through the (static) boundary of the spray is of the order of

$$F_{out} \approx 2 \frac{D_{eddy}}{R_{spray}} \Delta\rho'_{w,out} \tag{47}$$

50

Fig. 33. Diagram of the water vapour transport through a spray.

Fig. 34. Diagram of the geometry of a spray.

As we assumed stationary conditions and the absence of accumulation we can equate the transfer rates

$$F_{in} = F_{out} \tag{48}$$

and, hence, it follows that

$$\frac{\Delta\rho'_{w,in}}{\Delta\rho'_{w,out}} \approx \frac{D_{eddy}/R^2_{spray}}{3(Sh/2) \cdot (D_G/R^2) \cdot x \cdot (\rho_G/\rho_L)} \tag{49}$$

According to this rough estimation moisture transfer out of a spray is rate controlling if $\Delta\rho'_{w,in} \ll \Delta\rho'_{w,out}$ and, thus, if the ratio in Eqn (49) is much smaller than one. The value of this ratio will depend on the actual spraying conditions.

Let us assume atomization using a hollow cone nozzle with atomization angle 2α. The nozzle generates a spray with width β. It is reasonable to assume a constant value of β because of similar behaviour of gas jets. A schematic representation of the dimensions of the spray is given in Fig. 34. The cross sectional area of the spray at a distance l from the nozzle is given by

$$A = 2\pi l^2 \{\cos(\alpha - \tfrac{1}{2}\beta) - \cos(\alpha + \tfrac{1}{2}\beta)\} \tag{50}$$

if the atomization rate is Q kg/s and the velocity of the droplets at a distance l from the nozzle is $v_{droplet}$, the liquid load in the spray amounts to

$$x = \frac{Q}{Av\rho_G} \tag{51}$$

For small values of β the thickness of the spray can be approximated by

$$R_{spray} = l \cdot tg(\tfrac{1}{2}\beta) \tag{52}$$

51

Substitution of Eqns (51) and (52) in (49) yields

$$\frac{\Delta \rho'_{w,in}}{\Delta \rho'_{w,out}} \approx \frac{4}{3}\pi \frac{D_{eddy}}{D_G} \frac{vR^2 \rho_L}{ShQ} \frac{\{\cos(\alpha - \frac{1}{2}\beta) - \cos(\alpha + \frac{1}{2}\beta)\}}{tg^2(\frac{1}{2}\beta)} \tag{53}$$

Evaluation of Eqn (53) with: $D_{eddy} = 2.5 \cdot 10^{-3}$ m²/s; $D_G = 2.5 \cdot 10^{-5}$ m²/s; $v_{droplet} = 10$m/s; $R = 2.5 \cdot 10^{-5}$ m; $\rho_L = 1000$ kg/m³; $\rho_G = 1$ kg/m³; $Sh = 2$; $Q = 0.2$ kg/s; $\alpha = 22.5°$; $\beta = 15°$ yields:

$\Delta \rho'_{w,in}/\Delta \rho'_{w,out} \approx 0.012$

Hence, until depletion of the droplets occurs, the conditions inside the spray may well be near the adiabatic saturation conditions.

To evaluate the distance from the nozzle at which such depletion occurs Eqn (51) was evaluated with the same variables except $v = 1$ m/s (terminal velocity). It follows that $X = 0.32/R^2$ m^{-2} and for instance after approximately 2 metres the liquid load of the air is $X = 0.08$ kg/kg.

Drying air in a spray dryer could well be just saturated after evaporation of this amount of water and water droplets would just be depleted.

It may be concluded that the conditions of the air inside the spray could be close to adiabatic saturation conditions. The actual conditions will among others depend on the turbulence in the drying air and in the spray, on the droplet-size distribution and droplet load in the spray.

In my experience it takes a distance of 1–2 m and a residence time of the droplets of the order of 1–2 s in actual spray-drying before the spray is sufficiently diluted with dry air to avoid the possibility of saturated conditions. Such times are long relative to the drying times of small droplets in dry air or even air at outlet conditions (Sections 3.2 and 3.3).

Further knowledge about this subject is needed.

3 The bulk air mixing stage Finally, so much air is entrained in the spray that the droplets are well distributed over the drying air. At this stage the velocity of the droplets will be close to their final velocity. The conditions of the air are determined by the evaporation rate of the droplets and the long range mixing of the air. Both the ideally mixed air described in Section 3.2 and the perfectly cocurrent case described in Section 3.3 can be representative for this stage, the actual situation depending on the equipment design.

We must consider, however, that all droplets already dried to some extent in the previous stages and especially the smaller droplets will be nearly dry when entering the bulk air mixing stage. Furthermore, the conditions of the air differ markedly even for cocurrent flow from the initial conditions of the drying air. Hence the drying conditions will be more moderate than those described in Section 3.3 although the air flow pattern is the same at this stage.

5.3 Droplet temperatures and product properties

The representation of spray drying given in Section 5.2 can explain many of the properties of spray-dried powders. The densities of the powder particles were already discussed in Chapter 4.

52

The fact that chemical conversion and biodegradation of enzymes occurs only to a moderate extent, as well as many results on the retention of volatile trace components in drying aqueous carbohydrate solutions can be explained.

Low chemical conversions will often be caused by the cool and moist air near adiabatic saturation conditions surrounding the droplets in the dispersion stage. As a result the droplet temperatures are low until the droplets are well dispersed over the drying air.

The common opinion that 'drying is carried out at essentially the drying air wet-bulb temperature' (Porter et al., 1973) assumes the dynamic equilibrium between heat and mass flux to be responsible for the low temperatures. Although, actual temperatures (essentially (near) the adiabatic saturation temperature) are almost identical, the above assumed mechanism is wrong. The droplet is cool, not because of equilibrium between fluxes between the droplet and hot air, but because of locally cool air. By the time that the temperature of the droplet rises well above the adiabatic saturation temperature an important part of the water can be evaporated, especially for smaller droplets.

Verhey (1973) concluded from differences between the inactivation of rennin and alkaline phosphatase that most heat damage occurs in an intermediate stage when the moisture content in the interior of the droplets is already considerably lower than the initial value. Prior inactivation is limited because of low temperatures, later on inactivation is limited because of the low water activities. These results are completely in accordance with the present description of the drying process according to which most inactivation would take place immediately after the spray dispersion stage.

Differences between the formation of α and β-lactose in skim-milk powders of different particle sizes support the theory that especially the smaller droplets dry considerably during the dispersion stage. Buma (1966) concluded from the ratio between α and β-lactose that the temperature during solids formation in the small particles of the cyclone fraction was approximately 20 °C lower than that during solids formation in the larger particles of the main fraction. These results are clearly contrary to the temperature histories for cocurrent flow given in Fig. 3 but they are in agreement with the views developed above.

In general we may expect that biodegradation or chemical conversion due to heat and moist will be less for the smaller droplets both because smaller droplets dry out more in the dispersion stage and because the conditions in sprays with smaller droplets are more close to adiabatic saturation conditions. Furthermore, only the air temperatures after the dispersion stage will determine the conversion. The air will be close to outlet conditions, especially in small well mixed spray-dryers. Then the conversion will be more dependent on the outlet than on the inlet air conditions. Such results were obtained by Verhey (1973) during actual spray-drying.

Aroma volatiles can be retained in drying droplets when drying takes place such that an aroma impervious layer of low water concentration is formed rapidly (Thijssen & Rulkens, 1968) The formation of such a layer cannot be expected to take place during the spray dispersion stage, because of the slow drying taking place there. Hence, most of the aroma volatiles will be lost during the atomization

53

and the spray dispersion stages. Aroma losses can be low afterwards as a result of high Biot-numbers (Kerkhof & Schoeber, 1973).

The conditions favourable for high aroma retention will in general be contrary to those in which the biodegradation is low. So larger droplets are often favourable for aroma retention (Rulkens, 1973). This effect cannot be explained by the idealized drying systems described in Chapter 3, but only by a differing relative importance of drying in the various stages.

Changes in the viscosity of the liquid being atomized will usually cause changes of the droplet size and, hence, will affect the product properties. The example shows, however, also the limitations in the practical measures which can be taken. Very high viscosities can lead to a poor droplet distribution over the drying air and, hence, to high aroma losses and poor drying. The importance of the dispersion phenomena to the product properties is thus stressed.

For a further optimization of the quality of spray-dried powders better study of the dispersion phenomena is required. Technical improvements of the drying equipment to control the dispersion should be possible.

Summary

Properties of spray-dried powders are largely determined by the drying history of the droplets in a spray dryer. Measurement of the conditions in the drying droplets is at present impossible. Therefore, the drying was simulated with computer calculations. The physical properties of maltose solutions – considered as a model for the drying of liquid foods – served as a basis for the calculations.

A survey of the factors determining the mass transport inside a droplet and the heat and mass transfer outside is given in Chapter 2. A method is developed for the calculation of mass transfer in shrinking or swelling spherical droplets, in which a transformed diffusion equation is used. Several models for the description of heat and mass transfer in a spray dryer are discussed and the model used throughout this study is described. Results calculated with this model only deviate slightly from experimental results for single drying spheres.

The effect of mixing in a spray dryer on the drying history of droplets is indicated in Chapter 3. Perfectly cocurrent flow of the drying air with the droplets and ideally mixed drying air are considered. The situation in which droplets are dispersed very gradually in the drying air is also treated. Significant differences between the various situations are found. The drying rates and droplet temperatures being highest for perfectly cocurrent flow and lowest for gradual dispersion.

In Chapter 4 drying histories are calculated of inflating droplets in which a small amount of air is dispersed during atomization. It was found that significant inflation as a result of the partial vapour pressure of water can occur, especially for high inlet temperatures and perfectly cocurrent flow of drying air and droplets.

Finally the similarity between the described idealized mixing patterns and the actual mixing patterns in spray dryers is discussed and the product properties which are expected on basis of the calculations are compared with actual properties of spray-dried powders. It is shown that several product properties can be explained by assuming a very gradual dispersion of the droplets over the drying air, the air around the droplets being nearly saturated. There were indications that such conditions can occur in actual spray-drying during a period which is long relative to the drying times of droplets in dry air.

A survey of diffusion equations in several coordinate systems is given in Appendix A. The measurement of physical properties of supersaturated aqueous maltose solutions and especially of the diffusion coefficient over a wide range of water concentrations and temperatures is described in Appendix B. The results served as a basis for drafting the physical models.

Samenvatting

Eigenschappen van door verstuiving gedroogde poeders worden in belangrijke mate bepaald door het verloop van het droogproces in verstoven druppels. Kennis van dit verloop kan danook bijdragen tot optimalisatie van de poedereigenschappen door aanpassing van de procesomstandigheden tijdens het sproeidrogen en door verbetering van sproeidroogapparatuur. Omdat het vooralsnog onmogelijk is de condities in de druppels tijdens de droging te meten, werd in deze studie de droging gesimuleerd door middel van computerberekeningen. Hiertoe werd een rekenmodel opgesteld. Bij de berekeningen werd gebruik gemaakt van de fysische eigenschappen van maltose oplossingen. Deze oplossingen werden als modelmateriaal gekozen omdat hun drooggedrag karakteristiek geacht kan worden voor een grote groep vloeibare voedingsmiddelen.

De opbouw van het rekenmodel wordt behandeld in hoofdstuk 2. Eerst wordt een overzicht gegeven van de factoren die het warmte- en stoftransport in een druppel en de overdracht aan de buitenzijde van een druppel bepalen. Voor de berekening van het stoftransport in de druppel werd een methode ontwikkeld welke toepasbaar is voor krimpende en zwellende bolvormige druppels. Daarbij werd gebruik gemaakt van een in 'vaste-stof-coordinaten' getransformeerde diffusievergelijking. Daarna wordt aangegeven hoe de vergelijkingen voor het in- en uitwendig transport gecombineerd kunnen worden tot een rekenmodel ter beschrijving van warmte- en stoftransport in een sproeidroger. Het verder in deze studie gebruikte rekenmodel werd getoetst door vergelijking van berekende en experimentele droogresultaten voor bolvormige druppels onder laboratorium condities. De resultaten blijken goed overeen te stemmen.

In hoofdstuk 3 wordt met behulp van het rekenmodel aangegeven, welk effect de menging in een sproeidroger heeft op het verloop van de droging. Drie extreme gevallen van opmenging van druppels en drooglucht in een sproeidroger worden besproken. Een onderscheid wordt gemaakt tussen perfecte gelijkstroom van de druppels en de lucht en ideaal gemengde drooglucht. Ook wordt het geval behandeld, waarin druppels zeer geleidelijk met de drooglucht worden gemengd. De droogsnelheid en de temperatuur in de druppels blijken het hoogst te zijn bij gelijkstroom en het laagst bij geleidelijke menging.

In hoofdstuk 4 wordt berekend in welke mate druppels, waarin tijdens het verstuiven een kleine hoeveelheid lucht ingesloten is, tijdens de droging op zullen zwellen. Er werd gevonden, dat in het bijzonder bij hoge inlaattemperaturen en bij perfecte gelijkstroom van druppels en lucht een aanmerkelijke opzwelling onder invloed van de partiële waterdampspanning niet onmogelijk is. Deze opzwelling blijkt het droogproces aanmerkelijk te versnellen.

Tenslotte wordt in hoofdstuk 5 besproken in hoeverre de genoemde extreme

gevallen van opmenging van lucht en druppels karakteristiek zijn voor de meng-
ing in werkelijke drogers en voor het effect van de menging op de droging.
Daartoe worden drie stadia in het verstuivingsproces onderscheiden. Het eerste
stadium, waarin de druppels gevormd worden, kan niet door één van de drie
gevallen van menging worden gekarakteriseerd. Het tweede stadium, juist na de
vorming van de druppels kan gekarakteriseerd worden door een geleidelijke
locale opmenging van druppels met drooglucht. In het laatste stadium zijn de
druppels reeds gemengd met drooglucht en hangt de droging af van menging over
langere afstanden in de droger. Afhankelijk van het type droger zal perfecte
gelijkstroom of perfecte menging de realiteit meer benaderen. Aangetoond wordt,
dat produkteigenschappen, zoals de dichtheid van het poeder en proceseffecten
zoals de retentie van aromastoffen of het optreden van chemische of biochemische
omzettingen tijdens de droging, verklaard kunnen worden uit een zeer
geleidelijke vermenging van druppels en lucht. Daarbij kan de lucht rondom de
druppels vrijwel in evenwicht zijn met de druppels. Dergelijke omstandigheden
zouden kunnen voorkomen gedurende een tijd welke lang is ten opzichte van de
droogtijd van de druppels in droge lucht.

In appendix A wordt een overzicht gegeven van de diffusievergelijking voor
binaire systemen in een vijftal coordinaten stelsels: een stelsel ten opzichte
waarvan geen netto transport van massa plaatsvindt, een stelsel ten opzichte
waarvan geen netto molair transport plaatsvindt, een stelsel ten opzichte waarvan
geen transport van één van de componenten plaatsvindt, een stelsel ten opzichte
waarvan geen volumetransport plaatsvindt en een stelsel dat stil staat ten opzichte
van externe coordinaten. Het stelsel waarin geen netto transport van één van de
componenten plaatsvindt is in het bijzonder geschikt voor het beschrijven van
processen zoals drogen, waarbij één component in een systeem behouden blijft.

In appendix B worden diffusie-coefficienten van oververzadigde oplossingen
van maltose in water gegeven met concentraties tot 85% (w/w) en over een
temperatuurtraject van 20 tot 85 °C. Ook dichtheden en wateraktiviteiten van
deze oplossingen werden gemeten. Deze gegevens dienden als basis voor het
opstellen van het rekenmodel dat in deze studie gebruikt is.

References

Abramowitz, M. & I. A. Stegun, 1965. Handbook of mathematical functions. Dover publ. Inc., New York.

Acrivos, A. & T. D. Taylor, 1962. Heat and mass transfer from single spheres in Stokes flow. Phys. Fluids 5: 387–394.

Adler, D. & W. T. Lyn, 1971. The steady evaporation and mixing in a gaseous swirl. Int. J. Heat Mass Transfer 14: 793–812.

Antweiler, H. J., 1951. Limits of sensitivity of optical measuring methods in microelectrophoresis and microdiffusion. Microchim. Acta 36: 561–573.

Antweiler, H. J., 1952. A method for sedimentation, electrophoresis and diffusion experiments with a strong light source. An instrument for measuring diffusion constants. Chem.-Ing.-Tech. 5:284.

Arni, V. R. S., 1959. The production, movement and evaporation of sprays in spray dryers. Ph.D. thesis Univ. of Washington.

Bailey, G. H., I. W. Slater & P. Eisenklam, 1970. Dynamic equations and solutions for particles undergoing mass transfer. Br. chem. Eng. 15: 912–916.

Baltas, L. & W. H. Gauvin, 1969. Performance prediction for a cocurrent spray dryer. A.I.Ch.E.J. 15: 764–771.

Baltas, L. & W. H. Gauvin, 1969a. Transport characteristics of a cocurrent spray dryer. A.I.Ch.E.J. 15: 772–779.

Barrer, R. M., 1942. Diffusion in solids. Cambridge.

Benatt, F. G. S. & P. Eisenklam, 1969. Gaseous entrainment into axisymmetric liquid sprays. J. Inst. Fuel: 309.

Bird, R. B., W. E. Stewart & E. N. Lightfoot, 1960. Transport phenomena. Wiley, New York.

Brian, P. L. T. & H. B. Hales, 1969. Effects of transpiration and changing diameter on heat and mass transfer to spheres. A.I.Ch.E.J. 15: 419–425.

Briffa, F. E. J., 1967. Some aerodynamic aspects of atomisation. Sheffield Univ. Fuel Soc. J.: 9–15.

Briffa, F. E. J. & N. Dombrowski, 1966. Entrainment of air into a liquid spray. A.I.Ch.E.J. 12: 708–717.

Buckham, J. A. & R. W. Moulton, 1955. Factors effecting gas recirculation and particle expansion in spray drying. Chem. Eng. Progr. 51: 126–133

Buikov, M. V., 1962. Nonsteady state growth of solution droplets. Kolloid. Zh. 24: 522–529.

Buma, T. J., 1966. The physical structure of spray milk powder and the changes which take place during moisture absorption. Neth. Milk Dairy J. 20: 91–112

Carlslaw, H. S. & J. C. Jaeger, 1959. Conduction of heat in solids. Clarendon Press, Oxford.

Charlesworth, P. H. & W. R. Marshall, 1960. Evaporation from drops containing dissolved solids. A.I.Ch.E.J. 6: 9–23.

Chatterjee, A., 1964. J. Am. Chem. Soc. 86: 793.

Coulson, J. M. & J. F. Richardson, 1968. Chemical engineering. Pergamon Press, London, New York.

Cox, N. D., 1962. Rates of evaporation in spray drying. Ph.D. thesis Univ. of Wisconsin.

Crank, J., 1956. The mathematics of diffusion. Clarendon Press, Oxford.

58

Crosby, E. J. & W. E. Stewart, 1970. Vaporization of droplets in high temperature gas streams. Ind. Eng. Chem. Fundam. 9: 517.

Davies, J. T., 1972. Turbulence phenomena. Academic Press, New York.

Deryagin, B. V., V. A. Fedoseyev & L. A. Rosenzweig, 1966. Adsorption of cetyl alcohol vapor and effects of this phenomenon on the evaporation of waterdrops. J. Colloid Interface Sci. 22: 45.

Dickinson, D. R. & W. R. Marshall, 1968. The rates of evaporation of sprays. A.I.Ch.E.J. 14: 541–552.

Dlouhy, J. & W. H. Gauvin, 1960. Heat and mass transfer in spray drying. A. I. Ch. E. J. 6: 29–34.

Dombrowski, N. & G. Munday, 1968. Spray drying. In: N. Blakesbrough (ed): Biochemical and biological engineering science. Vol. 2, p. 207. Academic Press, New York.

Duda, J. L., W. L. Sigelko & J. S. Vrentas, 1969. Binary diffusion studies with a wedge interferometer. J. phys. Chem., Ithaca 73: 141.

Duffie, J. A. & W. R. Marshall, 1953. Factors influencing the properties of spray-dried materials. Chem. Eng. Progr. 49: 417–423, 480–486.

Dunlop, P. J., 1965. J. phys. Chem., Ithaca 69: 4276.

Ellerton, H. D. & P. J. Dunlop, 1967. Diffusion and frictional coefficients for four compositions of the system water-sucrose-mannitol at 25°. J. phys. Chem., Ithaca 71: 1291.

English, A. C. & M. Dole, 1950. Diffusion of sucrose in supersaturated solutions. J. Am. chem. Soc. 72: 3261–3267.

Fitts, D. D., 1962. Non-equilibrium thermodynamics. McGraw-Hill, New York.

Frazier, G. C. & W. W. Hellier, 1969. Vaporization of liquid droplets in high temperature air streams. Ind. Eng. Chem. Fundam. 8: 807.

Frössling, N., 1938. Ueber die Verdunstung fallender Tropfen. Beitr. Geophys. 52: 170–216.

Fuchs, N. A., 1959. Evaporation and droplet growth in gaseous media. Pergamon Press, London, New York.

Galloway, T. R. & B. H. Sage, 1967. Thermal and material transport from spheres. Int. J. Heat Mass Transfer 10: 1195–1210.

Gal-Or, B. & H. E. Hoelscher, 1966. A mathematical treatment of the effect of particle size distribution on mass transfer in dispersions. A.I.Ch.E.J. 12: 499–508.

Gal-Or, B., G. E. Klinzing & L. L. Tavlarides, 1969. Bubble and drop phenomena. Ind. Eng. Chem. 61(2): 21–34.

Gladden, J. K. & M. Dole, 1953. Diffusion in supersaturated solutions. II. Glucose solutions. J. Am. chem. Soc. 75: 3900–3904.

Gosting, L. J. & J. M. Morris, 1949. Diffusion studies on dilute aqueous sucrose solutions at 1° and 25 °C with the Gouy interference method. J. Am. chem. Soc. 71: 1998–2006.

Guggenheim, E. A., 1957. Thermodynamics. North Holland publ. co., Amsterdam.

Hadamard, J., 1911. Mouvement permanent lent d'une sphère liquide et visqueuse dans un liquide visqueux. C.r. hebd. Séanc Acad. Sci., Paris 152: 1735.

Heiss, R., 1968. Haltbarkeit und Sorptionsverhalten wasserarmer Lebensmittel. Springer Verlag, Berlin.

Henrion, P. N., 1964. Diffusion in the sucrose + water system. Trans. Faraday Soc. 60: 72–82.

Hidy, G. M. & J. R. Brock, 1970. The dynamics of aerocolloidal systems. Int. Rev. Aerosol Phys. Chem. vol. 1.

Hoffman, T. W. & L. L. Ross, 1972. A theoretical investigation of the effect of mass transfer on heat transfer to an evaporating droplet. Int. J. Heat Mass Transfer 15: 599–617.

Huang, W. S. & R. C. Kintner, 1969. Effects of surfactants on mass transfer inside drops. A.I.Ch.E.J. 15: 735–744.

Hughes, R. R. & E. R. Gilliland, 1952. The mechanics of drops. Chem. Eng. Progr. 48: 497–504.

Ihme, F., H. Schmidt-Traub & H. Brauer, 1972. Theoretische Untersuchung über die Umströmung und den Stoffübergang an Kugeln. Chem.-Ing.-Tech. 44: 306–318.

Ingebo, R. D., 1956. Atomization, acceleration and vaporization of liquid fuels. 6th Int. Symp. Combustion. Reinhold publ. co., New York, 1957.

Irani, R. R. & A. W. Adamson, 1960. Transport processes in liquid systems. III. Thermodynamic complications in the testing of existing diffusional theories. J. phys. Chem., Ithaca 64: 199–204.

de Juhasz, K. T., 1959. Spray literature abstracts. American Society of Mechanical Engineers.

Keey, R. B., 1972. Residence times of droplets in tall-form spray-dryer. International symposium on heat and mass transfer problems in food engineering, I.A.C. Wageningen, the Netherlands, Oct. 24–27.

Kerkhof, P. J. A. M., W. H. Rulkens & J. van der Lijn, 1972. Calculation of aroma losses from drying liquid foods. International symposium on heat and mass transfer problems in food engineering, Wageningen, the Netherlands, Oct. 24–27.

Kerkhof, P. J. A. M. & W. J. A. H. Schoeber, 1973. Theoretical modelling of the drying behaviour of droplets in spray-driers. In: A. Spicer (ed.): Advances in preconcentration and dehydration. Applied Science Publishing company, London.

Kerkhof, P. J. A. M., 1974. Correlation of process variables and aroma loss in the drying of liquid foods. 4th International congress on food science and technology. Sept. 23–27, Madrid.

Kerkhof, P. J. A. M., 1975. A quantitative study of the effect of process variables on the retention of volatile trace components in drying. Ph.D. thesis, Technical University Eindhoven, the Netherlands.

Kerkhof, P. J. A. M. & H. A. C. Thijssen, 1975b. Quantitative study of the effects of process variables on aroma retention during the drying of liquid foods. Paper presented to the A.I.Ch.E. meeting on dehydration and concentration of foods, 16–25 November 1975, Los Angeles, California, U.S.A.

Kozak, J. J., W. S. Knight & W. Kauzmann, 1968. Solute-solute interactions in aqueous solutions. J. chem. Phys., Ithaca 48: 675–690.

Kronig, R. & J. C. Brink, 1950. The theory of extraction from falling droplets. Appl. Sci. Res. A2: 142–154.

Krüger, R., 1973. Ph.D. thesis, Technical University Berlin.

Langmuir, I., 1918. The evaporation of small spheres. Physiol. Rev. 12: 368–370

Lapple, C. E. & C. B. Shepherd, 1940. Ind. Eng. Chem. 32: 605.

Levich, V. G., 1962. Physicochemical hydrodynamics, Chapter 8. Prentice Hall, London.

Lijn, J. van der, W. H. Rulkens & P. J. A. M. Kerkhof, 1972. Droplet heat and mass transfer under spraydrying conditions. International symposium on heat and mass transfer problems in food engineering, Wageningen, Oct. 17–22.

Lijn, J. van der, 1976. The constant rate period during the drying of shrinking spheres (to be published).

Longsworth, L. G., 1952. Diffusion measurements at 1°, of aqueous solutions of amino acids, peptides and sugars. J. Am. chem. Soc. 74: 4155–4159.

Longsworth, L. G., 1953. Diffusion measurements at 25°, of aqueous solutions of amino acids, peptides and sugars. J. Am. chem. Soc. 75: 5705–5709.

Luikov, A. V., 1964. Heat and mass transfer in capillary-porous bodies. Adv. Heat Transfer 1.

Luikov, A. V., 1968. Analytical heat diffusion theory. Academic Press, New York.

Marsh, B. D. & W. J. Heidegger, 1965. Mass transfer from free drops. Ind. Eng. chem. Fund. 4: 129.

Marshall, W. R., 1954. Atomization and spray drying. Chem. Eng. Progr. Monogr. Series 50(2).

Mason, A. E. & L. Monchick, 1965. Survey of the equations of state and transport properties of mois gases. Chapter 4 in: A. Wexler (ed.): Humidity and moisture. New York.

Masters, K. & M. F. Mohtadi, 1967. A study of centrifugal atomization and spray drying (1–3). Br. chem. Eng. 12: 1890–1892; 13: 88–89; 13: 242–244.

Masters, K., 1968. Spray drying—the unit operation today. Ind. Eng. Chem. 60: 53–63.

Masters, K., 1972. Spray drying. Leonard Hill books, London.

Maxwell, J. C., 1890. Collected papers Vol 11, page 625.

McDonald, A., 1951. J. Res. natn. Bur. Stand. 46: 165.

Menting, L. C., 1969. Retention of volatiles during the air drying of aqueous carbohydrate solutions. Ph.D. thesis, Technical University Eindhoven, the Netherlands.

Moore, H., 1966. Brit. Chem. Eng. 12 (1967): 87–89.

Moore, W. J., 1963. Physical chemistry. Longmans, London.

Morse, H. W., 1910. Proc. Am. Acad. Arts Sci. 45 (April 1910).

Nishijima, Y. & G. Oster, 1960. Diffusion in glycerol-water mixtures. Bull. chem. Soc. Japan 33: 1649–1651.

Okuyama, M. & J. T. Zung, 1967. Evaporation-condensation coefficients for small droplets. J. chem. Phys. 46: 1580–1585.

Parti, M. & B. Palansz, 1974. Mathematical model for spray drying. Chem. Eng. Sci. 29: 355–362.

Pennsylvanya state bibliography of sprays, 1953. The Texas Co., New York.

Perry, R. H. & C. H. Chilton (ed.), 1973. Chemical engineers' handbook, 5th edn. McGrawHill-Kogakusha, New York, Tokyo.

Pita, E. G., 1969. Heat and mass transfer in evaporating sprays. Ph.D. thesis, Univ. of Maryland.

Planovskii, A. N., M. G. Naidis, A. P. Fokin & Yu. V. Kosmodem' yanskii, 1970. Effect of polydispersity of particles on the distribution of concentration fields in spray dryers. Teor. Osn. Khim. Tekhnol. 4: 503–507; English translation 1971: 486

Porter, H. F., P. Y. McCormick, R. L. Lucas & D. B. Wells, 1973. Chapter 20 in: R. H. Perry & C. H. Chilton (ed): Chemical engineers' handbook, 5th edn. McGrawHill-Kogakusha, New York, Tokyo.

Prager, S., 1953. Diffusion in binary systems. J. chem. Phys. 21: 1344–1347.

Pritchard, C. L. & S. K. Biswas, 1967. Mass transfer from drops in forced convection. Br. Chem. Eng. 12: 879–885.

Ranz, W. E. & W. R. Marshall, 1952. Evaporation from drops. Chem. Eng. Progr. 48: 141–146, 173–180.

Resnick, W. & B. Gal-Or, 1967. Adv. chem. Eng. 7: 295.

Rowe, P. N., K. T. Claxton & J. B. Lewis, 1965. Heat and mass transfer from a single sphere in an extensive flowing fluid. Trans. Inst. chem. Engrs. 43: T14–T31.

Rulkens, W. H., 1973. Retention of volatile trace components in drying aqueous carbohydrate solutions. Ph.D. thesis, Technical University Eindhoven, the Netherlands.

Schlünder, E. U., 1964. Temperatur- und Massenänderung verdunstender Tropfen aus reinen Flüssigkeiten und wässrigen Salzlösungen. Int. J. Heat Mass Transfer 7: 49–73.

Schoeber, W. J. A. H., 1973. M.Sc. thesis, Technical University Eindhoven, the Netherlands (in Dutch).

Schoeber, W. J. A. H. & H. A. C. Thijssen, 1975. A short-cut method for the calculation dependent diffusion coefficient. Paper presented to the A.I.Ch.E. meeting on dehydration and concentration of foods, 16–25 November 1975, Los Angeles, U.S.A.

Sideman, S., 1966. Direct contact heat transfer between immiscible liquids. Adv. Chem. Eng. 6: 207–286.

Sideman, S. & H. Shabtai, 1964. Direct contact heat transfer between a single drop and an immiscible liquid medium. Can. J. Chem. Eng. June 1964: 104–117.

Sivetz, M. S. & H. Foote, 1963. Coffee processing technology. Avi publ. co., Westport, Conn.

Sjenitzer, F., 1952. Spray drying. Chem. Eng. Sci. 1: 101–117.

Sjenitzer, F., 1962. The evaporation of a liquid spray injected into a stream of gas. Chem. Eng. Sci. 17: 309–322.

Snead, C. C. & J. Zung, 1968. J. Colloid Interface Sci. 27: 25.

Stein, W. A., 1972. Berechnung der Trocknung wasserfeuchter Produkte im Sprühturm. Chem.-Ing.-Tech. 44: 1241–1246.

Tanishita, I. & A. Nagashina, 1968. Jap. Soc. mech. Engrs. Bull. 11 (48): 1161; Chem. Abstr. 70 (1969): 107853c.

Tavlarides, L. L., C. A. Coulaloglou, M. A. Zeitling, G. E. Klinzing & B. Gal-Or, 1970. Bubble and drop phenomena. Ind. Eng. Chem. 62 (11): 6–27.

Thijssen, H. A. C. & W. H. Rulkens, 1968. Retention of aromas in drying food liquids. Ingenieur (The Hague) 22 Nov. 1968: Ch 45–56

Trommelen, A. M. & E. J. Crosby, 1970. Evaporation and drying of drops in superheated vapors. A.I.Ch.E.J. 16: 857.

Tyrell, H. J. V., 1970. Diffusion in liquids. In: Sherwood (ed.): Diffusion processes. Chapter 2.1. Gordon & Breach, London, 1971.

Ueadaira, H. & H. Uedaira, 1969. Diffusion coefficients of xylose and maltose in aqueous solutions. Bull. chem. Soc. Jap. 42: 2140–2142.

Verhey, J. G. P., 1973. Vacuolevorming bij het verstuivingsdrogen. Ph.D. thesis, Agricultural University Wageningen, the Netherlands Vacuole formation in spray powder particles. III. Atomization and droplet drying. Neth. Milk Dairy J. 27: 3–18.

Vignes, A., 1966. Diffusion in binary solutions. Ind. Eng. Chem. Fund. 5: 189–199.

Von Wogau, A., 1907. Ann Physik 23: 345.

Wexler, A. & L. Greenspan, 1971. Vapor pressure equation for water in the range 0–100. J. Res. natn. Bur. Stand. 75A (3): 213

Zung, J. T., 1967. Evaporation rates and lifetimes of clouds and sprays in air. II. The continuum model. J. chem. Phys. 47: 3578–3581.

Zung, J. T, 1967a. Evaporation rates and lifetimes of clouds and sprays in air. I. The cellular model. J. chem. Phys. 46: 2064–2070.

Appendix A. The description of diffusion phenomena

A.1 Introduction

Diffusion phenomena must be described with great care. Often insufficient attention has been paid to proper definition of the frames of reference and the diffusion coefficients in the literature (Tyrell, 1970). Similarly the use of *the* diffusion equation may lead to inadmissible simplifications, if it is used in a coordinate system for which it is not valid. It is to avoid these inaccuracies that attention is paid to this subject here.

Furthermore many algorithms for the solution of diffusional problems are based on the standard form of the heat equation, i.e. they are in the form of a balance equation such as Fick's second Law. Therefore it may be advantageous to describe diffusion in such a way, that the standard form is the result. In fact this is our main target here. We shall limit ourselves to those situations where
– useful boundary conditions result,
– in a binary system the mutual diffusion coefficient may be used.

The treatment of this subject is limited to situations which allow the assumption of local equilibrium and other basic assumptions concerning the thermodynamics of irreversible processes such as the continuum concept.

By far the most common way to describe diffusion is relative to external (Cartesian) co-ordinates. An obvious reason for this is that diffusion measurements are almost exclusively performed in laboratory glassware. Diffusion fluxes so observed are described relative to vessel fixed coordinates. Among others Prager (1953) showed, that in this system the standard form of the heat equation is only obtained, if no net overall change of volume occurs upon mixing. Crank (1956) stated in more general terms, that the same form may be obtained in coordinate systems fixed to the total mass or to the mass of one component. He stated – although rather abstractly – that this is so if concentration and distance are measured in certain consistent units, i.e. if ξ be the independent variable indicating the distance, then equal increments of ξ must always include equal increments of total mass (alternatively increments of a reference component) and concentrations must be defined as amounts per unit total mass (or unit of the reference component). Here we shall elaborate on this statement to find suitable forms of Fick's laws in the various coordinate systems.

A.2 Definitions

Consider a mixture of n components. Let v_i be the velocity relative to the external coordinates, ρ_i the mass density (concentration), $\bar{v}_i$ the partial specific

volume (for further definition see e.g. Guggenheim (1957), c_i the molar density, V_i the partial molar volume and M_i the molar weight of the ith component. Then the total mass density is given by

$$\rho = \sum_{i=1}^{n} \rho_i \tag{A.1}$$

the total molar density by

$$c = \sum_{i=1}^{n} c_i \tag{A.2}$$

the mass fraction of component i by

$$\omega_i = \rho_i/\rho \tag{A.3}$$

the molar fraction of component i by

$$x_i = c_i/c \tag{A.4}$$

the number mean molecular weight of the mixture by

$$M = \rho/c \tag{A.5}$$

Now we define the mass flux relative to external coordinates

$$j_i = \rho_i v_i \tag{A.6}$$

the molar flux relative to external coordinates

$$J_i = c_i v_i \tag{A.7}$$

the mass flux relative to a plane through which no net transport of mass takes place (local centre of mass; barycentre):

$$j_i^m = \rho_i(v_i - v) \tag{A.8}$$

in which

$$v = \frac{\sum_{i=1}^{n} \rho_j v_j}{\rho} \tag{A.9}$$

the molar flux relative to the local centre of mass

$$J_i^m = c_i(v_i - v) \tag{A.10}$$

the mass flux relative to a plane through which no net transport of component r takes place

$$j_i^r = \rho_i(v_i - v_r) \tag{A.11}$$

the molar flux relative to the reference component r

$$J_i^r = c_i(v_i - v_r) \tag{A.12}$$

the mass flux relative to a plane through which no net molar transport takes place

$$j_i^* = \rho_i(v_i - v^*) \tag{A.13}$$

64

in which

$$v^* = \frac{\sum_{i=1}^{n} c_i v_i}{c} \tag{A.14}$$

the molar flux relative to the molar average velocity

$$J_i^* = c_i(v_i - v^*) \tag{A.15}$$

the mass flux through a plane through which no net transport of volume takes place (local centre of volume)

$$j_i^0 = \rho_i(v_i - v^0) \tag{A.16}$$

in which

$$v^0 = \sum_{j=1}^{n} \rho_j \bar{v}_j v_j = \sum_{j=1}^{n} c_j V_j v_j \tag{A.17}$$

the molar flux through the local centre of volume

$$J_i^0 = c_i(v_i - v^0) \tag{A.18}$$

It may be noted that definitions (A.1) through (A.10) and (A.13)–(A.15) parallel the definitions by Fitts (1962). The definitions (A.11), (A.16) and (A.17) parallel the definitions by Bird et al. (1960).

A.3 Barycentric description

Let us define the diffusion coefficient D_{ij} in the barycentric description of the diffusion flux (A.8) by

$$j_i^m = -\sum_{j=1}^{n} D_{ij} \rho \, \nabla \omega_j \tag{A.19}$$

It must be realized that this definition, although formally correct even in non-isothermal situations, only makes sense there if the Soret effect can be neglected.

For a binary system (A.19) becomes

$$j_i^m = -D_i \rho \, \nabla \omega_i \tag{A.20}$$

and it follows immediately from

$$\sum_{i=1}^{2} j_i^m = 0 \tag{A.21}$$

that

$$D_1 = D_2 \tag{A.22}$$

We shall call this the mutual diffusion coefficient and shall designate it as D without further annotation. This definition of the mutual diffusion coefficient corresponds to the definition given by Bird et al. (1960). The diffusion coefficient

65

in these coordinates given by Fitts (1962) is different from the mutual diffusion coefficient. In Section A.5 we shall prove that this definition corresponds to the definition of the mutual diffusion coefficient given by Fitts.

The statement by Crank (1956) that it is possible to arrive at a diffusion equation of the common form of Fick's second law is true and may be based on the following proof for the barycentric description.

Let us start with the continuity equation for component i.

$$\frac{\partial \rho_i}{\partial t} = -\boldsymbol{\nabla} \cdot [\rho_i v_i] + k_i \tag{A.23}$$

Summation from $i = 1$ to n gives (because no net production of mass takes place, $\Sigma\, k_i = 0$)

$$\frac{\partial \rho}{\partial t} = -\boldsymbol{\nabla} \cdot [\rho v] \tag{A.24}$$

The substantial derivative operator, describing changes in time at a point moving with a velocity $v^{(g)}$ relative to the stationary coordinates used so far is given by

$$\frac{\mathrm{D}^{(g)}}{\mathrm{D}t} = \frac{\partial}{\partial t} + v^{(g)} \cdot \boldsymbol{\nabla} \tag{A.25}$$

As we are concerned with barycentric coordinates, we shall now consider the point moving with the barycentric velocity v relative to the external coordinates. Eqns (A.24) and (A.25) may now be combined to

$$\frac{\mathrm{D}^m \rho}{\mathrm{D}t} = -\rho\, \boldsymbol{\nabla} \cdot v \tag{A.26}$$

Now we equate

$$\rho \frac{\mathrm{D}^m \omega_i}{\mathrm{D}t} = \frac{\mathrm{D}^m \rho_i}{\mathrm{D}t} - \omega_i \frac{\mathrm{D}^m \rho}{\mathrm{D}t} \tag{A.27}$$

and with (A.26) this becomes

$$\rho \frac{\mathrm{D}^m \omega_i}{\mathrm{D}t} = \frac{\mathrm{D}^m \rho_i}{\mathrm{D}t} + \rho_i\, \boldsymbol{\nabla} \cdot v \tag{A.28}$$

with (A.25)

$$\rho \frac{\mathrm{D}^m \omega_i}{\mathrm{D}t} = \frac{\partial \rho_i}{\partial t} + v \cdot \boldsymbol{\nabla} \rho_i + \rho_i\, \boldsymbol{\nabla} \cdot v = \frac{\partial \rho_i}{\partial t} + \boldsymbol{\nabla} \cdot [\rho_i v] \tag{A.29}$$

Using equation of continuity (A.23) this gives

$$\rho \frac{\mathrm{D}^m \omega_i}{\mathrm{D}t} = -\boldsymbol{\nabla} \cdot [\rho_i v_i] + \boldsymbol{\nabla} \cdot [\rho_i v] + k_i \tag{A.30}$$

or with definition (A.8)

$$\rho \frac{\mathrm{D}^m \omega_i}{\mathrm{D}t} = -\boldsymbol{\nabla} \cdot j_i^m + k_i \tag{A.31}$$

66

Supposing that the source term k_i is zero and using definition (A.20) we find

$$\frac{D^m \omega_i}{Dt} = \frac{1}{\rho} \nabla \cdot [\rho D \nabla \omega_i] \tag{A.32}$$

This diffusion equation is of the desired form. It is most useful in systems where the boundary conditions are known for a plane through which no net mass flow takes place. Although it is easy to translate Eqn (A.32) in such a way that it is expressed in terms of the molar fractions, we shall not further elaborate this case as it will seldom be used.

A.4 Reference component centered coordinates

From definitions (A.8) and (A.10) it follows directly that the mass flux relative to a reference component may be related to the mass flux relative to the local centre of mass as

$$\mathbf{j}_i^r = \mathbf{j}_i^m - \frac{\rho_i}{\rho_r} \mathbf{j}_r^m \tag{A.33}$$

For a binary system this becomes (using Eqn A.21)

$$\mathbf{j}_1^r = \frac{1}{1 - \omega_1} \mathbf{j}_1^m \tag{A.34}$$

Hence with Eqn (A.20)

$$\mathbf{j}_1^r = \frac{-D\rho}{1 - \omega_1} \nabla \omega_1 = -D\rho(1 - \omega_1) \nabla \frac{\omega_1}{1 - \omega_1} \tag{A.35}$$

Now we can write

$$\rho_r \frac{D^r}{Dt} (\rho_i/\rho_r) = \frac{D^r \rho_i}{Dt} - \frac{\rho_i}{\rho_r} \frac{D^r \rho_r}{Dt} \tag{A.36}$$

And using Eqn (A.25)

$$\rho_r \frac{D^r}{Dt} (\rho_i/\rho_r) = \frac{\partial \rho_i}{\partial t} + \boldsymbol{v}^r \cdot \nabla \rho_i - \frac{\rho_i}{\rho_r} \frac{\partial \rho_r}{\partial t} - \frac{\rho_i}{\rho_r} \boldsymbol{v}^r \cdot \nabla \rho_r \tag{A.37}$$

in which v^r is the velocity of a plane through which no net transport of the reference component occurs. Using continuity equation (A.23) and assuming the source term to be zero

$$\rho_r \frac{D^r}{Dt} (\rho_i/\rho_r) = \frac{\partial \rho_i}{\partial t} + \boldsymbol{v}^r \cdot \nabla \rho_i - \frac{\rho_i}{\rho_r} \nabla \cdot [\rho_r \boldsymbol{v}^r] - \frac{\rho_i}{\rho_r} \boldsymbol{v}^r \cdot \nabla \rho_r \tag{A.38}$$

And, hence

$$\rho_r \frac{D^r}{Dt} (\rho_i/\rho_r) = \frac{\partial \rho_i}{\partial t} + \boldsymbol{v}_r \cdot \nabla \rho_i + \rho_i \nabla \cdot \boldsymbol{v}_2 = \frac{\partial \rho_i}{\partial t} + \nabla \cdot [\rho_i \boldsymbol{v}_r] \tag{A.39}$$

Using Eqn (A.23) we obtain

67

$$\rho_r \frac{D^r}{Dt}(\rho_i/\rho_r) = -\nabla \cdot [\rho_i v_i] + \nabla \cdot [\rho_i v_r] + k_i = -\nabla \cdot [\rho_i(v_i - v_r)] + k_i = -\nabla \cdot j_i^r + k_i$$

$$\text{(A.40)}$$

Supposing that the source term be zero and substituting Eqn (A.36) in Eqn (A.40), we find the diffusion equation of the desired form

$$\frac{D^r}{Dt}(\rho_1/\rho_2) = \frac{1}{\rho_2} \nabla \cdot [\rho_2 D \, \nabla(\rho_1/\rho_2)] \tag{A.41}$$

This form is very useful for processes such as drying or sorption under such conditions that a reference component is conserved. Although the drying or sorbing body may change its volume, simple boundary conditions in terms of these coordinates can be obtained.

Eqn (A.41) may be written for a one-dimensional system as

$$\frac{D^r}{Dt}(\rho_1/\rho_2) = \frac{1}{\rho_2} \frac{\partial}{\partial x}\left\{ \rho_2 D \frac{\partial}{\partial x}(\rho_1/\rho_2) \right\} \tag{A.42}$$

Definition of the variables u, s, z as

$$u = \rho_1/\rho_2 \tag{A.43}$$

$$s = D\rho_2^2 \tag{A.44}$$

$$z = \int_0^{x'} \rho_2 \, dx \tag{A.45}$$

yields the diffusion equation more clearly in the form of Fick's second law

$$\frac{\partial u}{\partial t} = \frac{\partial}{\partial z}\left(s \frac{\partial u}{\partial z} \right) \tag{A.46}$$

Eqn (A.45) shows that equal increments of z contain equal increments of the reference component 2. Hence, in drying experiments in which the boundary conditions are usually given with respect to the reference component they are defined at fixed values of z.

A similar form of the diffusion equation can be given for cylindrical or spherical coordinates. The latter is given in Chapter 2.

By multiplying both sides of Eqn (A.41) with the suitable molecular weights we obtain the analogous equation in terms of molar densities:

$$\frac{D^r}{Dt}(c_1/c_2) = \frac{1}{c_2} \nabla \cdot [c_2 D \, \nabla(c_1/c_2)] \tag{A.47}$$

This is the form of the diffusion equation used throughout this report.

A.5 Mole centred coordinates

The molar flux relative to a plane through which no net molar flow takes place, J^*, may be expressed in terms of the mass flow relative to the local centre of mass as

$$J_i^* = \frac{1}{M_i}\left(j_i^m - \frac{\rho_i}{\rho}\sum_{j=1}^{n}\frac{M}{M_j}j_j^m\right) \qquad (A.48)$$

For a binary system we can therefore write

$$J_1^* = \frac{M}{M_1 M_2}j_1^m \qquad (A.49)$$

and combining Eqns (A.49) and (A.20) we find

$$J_1^* = -\frac{M}{M_1 M_2}D\rho\,\boldsymbol{\nabla}\omega_1 = -Dc\,\boldsymbol{\nabla}x_1 \qquad (A.50)$$

Now we can develop the Fickian form of the diffusion equation as we did for the barycentric coordinates. By dividing the continuity equation for one component (A.23) by the molar weight we obtain

$$\frac{\partial c_i}{\partial t} = -\boldsymbol{\nabla}\cdot[c_i v_i] + K_i \qquad (A.51)$$

and summation from 1 to n gives

$$\frac{\partial c}{\partial t} = -\boldsymbol{\nabla}\cdot[c v^*] \qquad (A.52)$$

And using (A.25) for at a point moving with a speed v^* relative to the external coordinates we get

$$\frac{D^* c}{Dt} = -c\,\boldsymbol{\nabla}\cdot v^* \qquad (A.53)$$

Now we equate

$$c\frac{D^* x_i}{Dt} = \frac{D^* c_i}{Dt} - x_i\frac{D^* c}{Dt} = \qquad \text{(with A.53)}$$

$$= \frac{D^* c_i}{Dt} + c_i\boldsymbol{\nabla}\cdot v^* = \qquad \text{(with A.25)}$$

$$= \frac{\partial c_i}{\partial t} + v^*\cdot\boldsymbol{\nabla}c_i + c_i\boldsymbol{\nabla}\cdot v^* = \frac{\partial c_i}{\partial t} + \boldsymbol{\nabla}\cdot[c_i v^*] = \quad \text{(using A.51)}$$

$$= -\boldsymbol{\nabla}\cdot[c_i v_i] + \boldsymbol{\nabla}\cdot[c_i v^*] = -\boldsymbol{\nabla}\cdot J_i^* \qquad (A.54)$$

Combining Eqns (A.50) and (A.54) we find the diffusion equation

$$\frac{D^* x_1}{Dt} = \frac{1}{c}\boldsymbol{\nabla}\cdot[cD\,\boldsymbol{\nabla}x_1] \qquad (A.55)$$

It is not difficult to translate this equation in terms of the mass fraction ω_1. As that form will seldom be used we shall not go into further detail.

A.6 Volume centred coordinates

So far our argument has been based on the diffusion coefficient as defined in Eqns (A.19), (A.20) and we have found for a binary system one mutual diffusion coefficient. This was so because the sum of mass fluxes relative to the local centre of mass is zero (Eqn A.21). The sum of mass fluxes relative to the local centre of volume is not zero, however. Therefore we have to find another suitable form so that the mutual diffusion coefficient can be related to measurements in volume centred coordinates.

The relation between the fluxes j_i^0 and j_i is given by

$$j_i^0 = j_i^m - \rho_i \sum_{j=1}^{n} \bar{v}_j j_j^m \qquad (A.56)$$

For a binary mixture Eqn (A.56) yields after substitution of Eqn (A.21)

$$j_1^0 = (1 - \rho_1 \bar{v}_1 + \rho_1 \bar{v}_2) j_1^m \qquad (A.57)$$

Substitution of the sum of the volume fractions equalling one

$$\rho_1 \bar{v}_1 + \rho_2 \bar{v}_2 = 1 \qquad (A.58)$$

results in

$$j_1^0 = \rho \bar{v}_2 j_1^m \qquad (A.59)$$

After substitution of Eqn (20) and using Eqns (A.58) and (A.60)

$$\bar{v}_2 \, d\rho_2 = - \bar{v}_1 \, d\rho_1 \qquad (A.60)$$

we find

$$j_1^0 = -D \, \nabla \rho_1 \qquad (A.61)$$

If no net overall change of volume occurs we may write the Fickian form as was shown by Prager (1953). This can easily be seen by substituting the continuity equation (A.23) in Eqn (A.25) yielding

$$\frac{D^0 \rho_i}{Dt} = -\nabla \cdot [\rho_i v_i] + v^0 \cdot \nabla \rho_i + k_i \qquad (A.62)$$

If $k_i = 0$ and $v^0 = $ constant which is so if there is no contraction this equation becomes

$$\frac{D^0 \rho_i}{Dt} = -\nabla \cdot j_i^0 \qquad (A.63)$$

and substituting Eqn (61) we obtain

$$\frac{D^0 \rho_1}{Dt} = \nabla \cdot [D \, \nabla \rho_1] \qquad (A.64)$$

In terms of molar fluxes we may divide (A.64) by M_1 to obtain

$$\frac{D^0 c_1}{Dt} = \nabla \cdot [D \, \nabla c_1] \qquad (A.65)$$

70

Table A.1. Expressions for the diffusion equation for binary mixtures in various coordinate systems.

Reference system	In terms of mass	In terms of moles
stationary coordinates	$\boldsymbol{j}_1 = \omega_1(\boldsymbol{j}_1 + \boldsymbol{j}_2) - D\rho\ \boldsymbol{\nabla}\omega_1$	$\boldsymbol{J}_1 = x_1(\boldsymbol{J}_1 + \boldsymbol{J}_2) - Dc\ \boldsymbol{\nabla}x_1$
	without volume contraction and net flow of volume	without volume contraction and net flow of volume
	$\dfrac{\partial\rho_1}{\partial t} = \boldsymbol{\nabla}\cdot[D\ \boldsymbol{\nabla}\rho_1]$	$\dfrac{\partial c_1}{\partial t} = \boldsymbol{\nabla}\cdot[D\ \boldsymbol{\nabla}c_1]$
barycentric coordinates	$\boldsymbol{j}_1^m = -D\rho\ \boldsymbol{\nabla}\omega_1$	$\boldsymbol{J}_1^m = -DcM\ \boldsymbol{\nabla}(x_1/M)$
	$\dfrac{D^m}{Dt}\,\omega_1 = \dfrac{1}{\rho}\boldsymbol{\nabla}\cdot[\rho D\ \boldsymbol{\nabla}\omega_1]$	$\dfrac{D^m}{Dt}\,(x_1/M) = \dfrac{1}{cM}\boldsymbol{\nabla}\cdot[cMD\ \boldsymbol{\nabla}(x_1/M)]$
mole centred coordinates	$\boldsymbol{j}_1^* = -\dfrac{D\rho}{M}\boldsymbol{\nabla}(\omega_1 M)$	$\boldsymbol{J}_1^* = -Dc\ \boldsymbol{\nabla}x_1$
	$\dfrac{D^*}{Dt}(M\omega_1) = \dfrac{M}{\rho}\boldsymbol{\nabla}\cdot\left[\dfrac{\rho}{M}D\ \boldsymbol{\nabla}(M\omega_1)\right]$	$\dfrac{D^*x_1}{Dt} = \dfrac{1}{c}\boldsymbol{\nabla}\cdot[cD\ \boldsymbol{\nabla}x_1]$
reference component centred coordinates	$\boldsymbol{j}_1^r = -D\rho_2\ \boldsymbol{\nabla}(\rho_1/\rho_2)$	$\boldsymbol{J}_1^r = -Dc_2\ \boldsymbol{\nabla}(c_1/c_2)$
	$\dfrac{D^r}{Dt}(\rho_1/\rho_2) = \dfrac{1}{\rho_2}\boldsymbol{\nabla}\cdot[\rho_2 D\ \boldsymbol{\nabla}(\rho_1/\rho_2)]$	$\dfrac{D^r}{Dt}(c_1/c_2) = \dfrac{1}{c_2}\boldsymbol{\nabla}\cdot[c_2 D\ \boldsymbol{\nabla}(c_1/c_2)]$
volume centred coordinates	$\boldsymbol{j}_1^0 = -D\ \boldsymbol{\nabla}\rho_1$	$\boldsymbol{J}_1^0 = -D\ \boldsymbol{\nabla}c_1$
	without volume contraction	without volume contraction
	$\dfrac{D^0\rho_1}{Dt} = \boldsymbol{\nabla}\cdot[D\ \boldsymbol{\nabla}\rho_1]$	$\dfrac{D^0 c_1}{Dt} = \boldsymbol{\nabla}\cdot[D\ \boldsymbol{\nabla}c_1]$

Similarly we can obtain the fickian form in stationary coordinates if v^0 is zero.

$$\frac{\partial\rho_1}{\partial t} = \boldsymbol{\nabla}\cdot[D\ \boldsymbol{\nabla}\rho_1] \tag{A.66}$$

The same equation in molar terms is obtained by dividing by M_1

$$\frac{\partial c_1}{\partial t} = \boldsymbol{\nabla}\cdot[D\ \boldsymbol{\nabla}c_1] \tag{A.67}$$

From the foregoing derivation it may be seen that the diffusion coefficient can most easily be measured if v^0 is zero or negligible. In incompressible liquids at rest relative to a measuring cell v^0 is zero if no volume contraction occurs. Even if some volume contraction occurs v^0 is usually negligible if the concentration differences in the cell are taken to be small.

A survey of the Fickian forms of the diffusion equation in the various coordinate systems is given in Table A.1.

71

Appendix B. Physical properties of model components

B.1 Properties of maltose solutions

B.1.1 Diffusion in sugar solutions

Introduction The mutual diffusion coefficients of dilute water-sucrose systems at room temperature have been studied extensively (Gosting & Morris, 1949; Longsworth, 1953; Irani & Anderson, 1960; Henrion, 1964; Chatterjee, 1964; Ellerton & Dunlop, 1967; Duda et al. 1969). The influence of the temperature on the diffusion coefficient in these systems was studied by Longsworth (1952, 1953) as well as by Gosting & Morris (1949). Both research groups studied the diffusion coefficients at 1° and 25 °C. Gosting & Morris also studied the influence of the concentration on the diffusion coefficient and found

$$1\,°C: \quad D = 2.423(1 - 0.00167\,\rho_s) \cdot 10^{-10}\,m^2/s \tag{B.1}$$

$$25\,°C: \quad D = 5.226(1 - 0.00148\,\rho_s) \cdot 10^{-10}\,m^2/s \tag{B.2}$$

In order to translate these data into terms of weight percentages we can use the expressions for the density

$$1\,°C: \quad \rho = 999.93 + 0.393 \cdot \rho_s\,kg/m^3(\rho_s < 60\,kg/m^3) \tag{B.3}$$

$$25\,°C: \quad \rho = 997.08 + 0.384 \cdot \rho_s\,kg/m^3(\rho_s < 60\,kg/m^3) \tag{B.4}$$

The expression for the diffusion coefficient at 25 °C (B.2) was slightly corrected by Chatterjee (1964)

$$25\,°C: \quad D = 5.224(1 - 0.00144\,\rho_s) \cdot 10^{-10}\,m^2/s \tag{B.5}$$

Henrion (1964) and English & Dole (1950) studied solutions of higher concentrations. Henrion at 25 °C, 50 °C and 70 °C, English & Dole at 25° and 35 °C. The latter authors found that the Gosting & Morris data for dilute systems and their own data for super-saturated solutions showed the diffusion coefficient to be linearly dependent on the weight percentage of sugar in the solution. Gladden & Dole (1953) interpreted the same data as well as their own results for glucose as a linear relationship between the mole fraction and the logarithm of the diffusion coefficient.

All these results are summarized in Fig. B.1. Although there is some variation in the results, which demonstrates the difficulty of measuring diffusion coefficients accurately, it is clear that the linear relationship between mole fraction and log D is not very accurate.

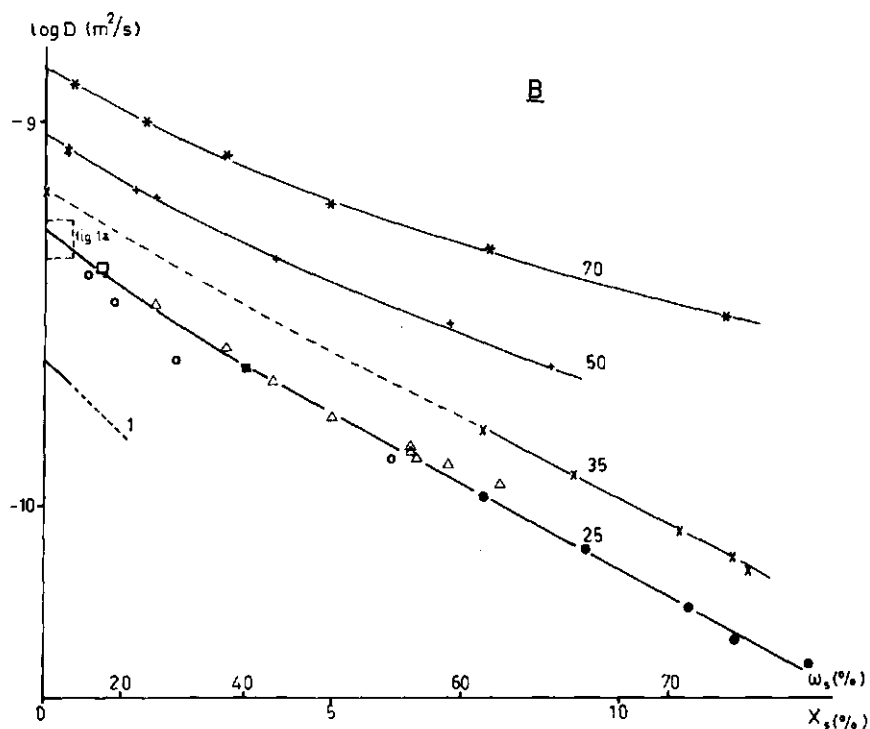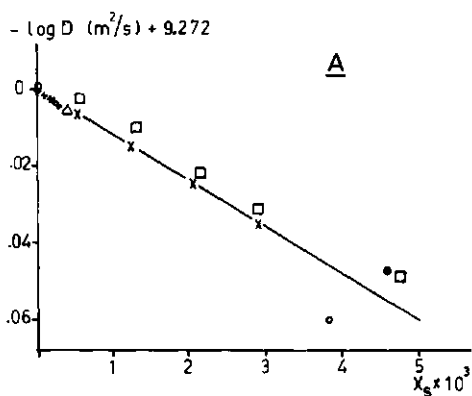Fig. B.2 summarizes the results of Longsworth (1953), for glucose, sucrose and

Fig. B.1. Diffusion coefficients of aqueous sucrose solutions as a function of the mole fraction of sucrose. (a) low concentration range, 25 °C, (b) high concentration range, various temperatures. 1 °C: —(Gosting & Morris, 1949); 25 °C: ● (English & Dole, 1950), ■ (Gladden & Dole, 1953), ○ (Irani & Adamson, 1960), △ (henrion, 1964), □ (Duda et al., 1969), +++ (Gosting & Morris, 1949; Chatterjee, 1964); 35 °C: × (English & Dole, 1950); 50 °C: + (Henrion, 1964); 70 °C: * (Henrion, 1964).
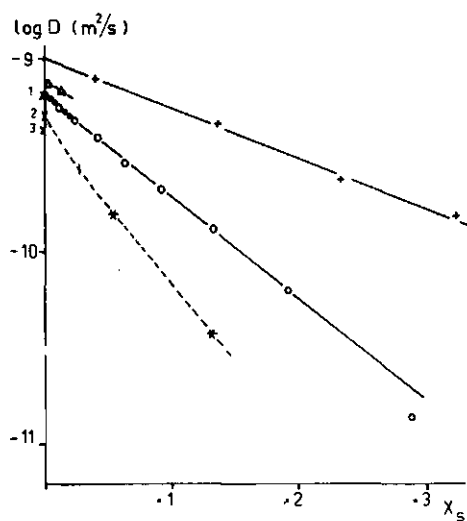
73

Fig. B.2. Diffusion coefficients of aqueous solutions of various sugars at 25 °C. (—--) sucrose see Fig. 1, ○ glucose (Gladden & Dole, 1953), ● mannitol (Dunlop, 1965), ×1, glucose, ×2, sucrose and ×3, raffinose at infinite dilution (Longswoth, 1953), + glycerol (Nishijima & Oster, 1960), * maltose (present work), △ xylose (Ueadaira & Uedaira 1969).

raffinose, of Dunlop (1965) and Ellerton & Dunlop (1967) for mannitol, of Gladden & Dole (1953) for glucose, of Nishijima & Oster (1960) for glycerol and of Ueadaira & Uedaira (1969) for xylose and maltose. The relation between mole fraction and log D as shown in Fig. B.1 has also been included. Apparently there is great similarity in diffusional behaviour among sugars of equal molecular weight. The data for the hexoses mannitol and glucose may well fit one curve. The same is true for maltose and sucrose. The data for xylose are slightly higher than those for the other monosaccharides, but this is obviously because it is the only pentose. Longsworth (1953) described the influence of the molecular weight or the apparent molal volume on the diffusion coefficient for very dilute systems:

$$1\ °C: \quad D = 11.66 \times 10^{-10}/(M_s^{\frac{1}{3}} - 1.893)\ m^2/s \tag{B.6}$$

$$D = 10.772 \times 10^{-10}/(V^{\frac{1}{3}}/10 - 1.450)\ m^2/s \tag{B.7}$$

$$25\ °C: \quad D = 24.182 \times 10^{-10}/(V^{\frac{1}{3}}/10 - 1.280)\ m^2/s \tag{B.8}$$

The sugars fit well into these relationships. For the sugars at least it seems as if similar relations may be drawn for higher concentrations too. For calculations for drying processes further data would be required.

By now we may have sufficient data for the calculation of diffusional transfer processes at room temperature and low sugar concentrations, such as dissolution, extraction or crystallization. For the purpose of calculation of the drying process, more data about higher sugar concentrations and higher temperatures would be required. The reasons for choosing maltose have been explained in Chapter 2. The choice allows us, moreover, to compare the behaviour of the disaccharides, sucrose and maltose.

Experimental For all experiments crystalline maltose ex Merck-Darmstadt was used. Solutions were made in demineralized water. To prepare supersaturated solutions the mixture was heated until a clear solution was obtained. Final

74

concentrations were determined with an Abbe refractometer using the data of Section B.1.4. The concentration differences between the solutions which were contacted for the experiments usually was about one percent by weight (wet basis). During the measurements in supersaturated solutions no crystallization took place.

Diffusion coefficients were measured in a Jamin-interferometer as designed by Antweiler (1951, 1952) and produced by Boskamp-gerätebau K. G.-Hersel bei Bonn-Germany. The optical system has been described in the articles of the designer and will not be discussed here. The same method was used by Chatterjee (1964). Our apparatus differed, however, from the versions described, in that only a small part of the interference pattern (Fig. B.3) could be seen in the scope. The total fringe-pattern could be measured by

– Moving the optical system along the cell to observe changes along the diffusional field.

– Rotating the mirrors of the optical system in such a way that the fringes would be projected at the right place in the scope.

Both movements could be read on a suitable scale. A measuring cell according to Von Wogau (1907) was used with a rectangular duct, of width 1 mm, depth (for optical path) 5 mm, height 40 mm. Two halves of the cell could slide along each other to form a boundary. The more concentrated solution was always in the lower half of the cell. At the boundary no interference pattern could be observed over a height of 1 mm because of the edges of the cell halves.

Because the refractive index varies linearly with the concentration (at least over the small concentration intervals under consideration), the solution of the diffusion equation subject to the boundary conditions of the present case may be written in terms of the refractive indices. The common form for diffusion into a semi-infinite slab with fixed surface concentration then reads

$$\frac{n(y) - n_s}{n_0 - n_s} = \mathrm{erf}\left(\frac{y}{2\sqrt{Dt}}\right); \qquad y > 0 \tag{B.9}$$
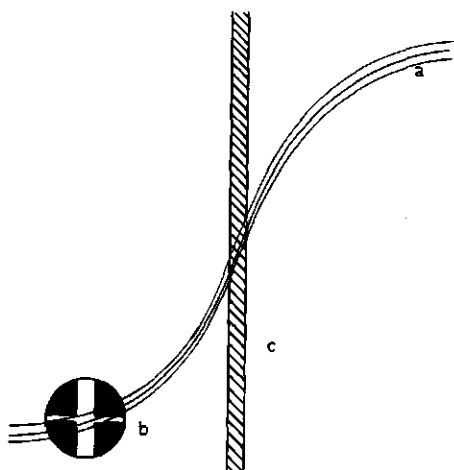

Fig. B.3. Diagram of the interference pattern and the part observed in the scope. (a) interference fringes, (b) observation in scope, (c) edges of the cell halves.

in which n_s is the (constant) refractive index at the surface of the slab (= the interface between the two sides)

$$n_s = \frac{n_0 + n_1}{2} \tag{B.10}$$

Alternatively the same distribution may be represented as

$$\frac{n(y) - n_1}{n_0 - n_1} = P\left(\frac{y}{\sqrt{2Dt}}\right) \tag{B.11}$$

which form is suitable for both sides of the distribution. $P(x)$ is here the Gauss probability integral (Abramowitz & Stegun, 1965). A distribution of this form yields a straight line on linear probability paper. The results were evaluated by plotting on this paper and drawing a regression line. The values at the end of the distribution, which show a large relative error were not considered, however. It was often found that the two sides of the distribution did not coincide although they had the same direction. This discrepancy was thought to be due to difficulties in finding the same interference line on both sides of the cell. As the diffusion coefficient can be determined from the direction of the line only, the regression was performed on a set of two parallel lines, one for each side of the cell. Corrections had to be made for initial mixing when a boundary was created

Table B.1. Effect of maltose concentration and temperature on the mutual diffusion coefficient of maltose solutions.

Concentration (%, w/w)			Temperature (°C)	$\bar{D}(m^2/s) \times 10^{10}$
c_1	c_2	$\bar{c}$		
0	0.9	0.4	28.0	5.3
0	0.9	0.4	47.0	8.5
0	0.9	0.4	66.0	12.4
51.5	52.4	52.0	20.0	1.31
52.0	53.5	52.7	28.0	1.78
51.5	52.4	52.0	39.0	2.2
52.0	53.5	52.7	47.0	2.7
51.0	53.8	52.6	56.5	4.0
52.0	53.5	52.7	66.0	4.7
51.5	53.8	52.6	74.0	6.9
51.5	53.8	52.6	85.0	8.3
73.6	74.4	74.0	20.5	0.34
72.9	74.0	73.5	28.0	0.47
73.6	74.4	74.0	39.0	0.71
73.6	74.4	74.0	47.0	0.87
73.6	74.4	74.0	54.5	1.24
73.6	74.4	74.0	66.0	1.93
73.6	74.4	74.0	74.5	2.4
73.8	74.7	74.2	85.0	3.5
84.4	85.5	85.0	66.0	0.49
85.2	86.3	85.7	85.5	1.00

76

between the cell halves. This was done using a zero time correction, which might be of the order of 1000 s. Diffusion coefficients were evaluated from the values $y - y_s$ of the regression line at

$$P = 0.7602 = P(\tfrac{1}{2}\sqrt{2}) \tag{B.12}$$

as for this value of P

$$y = \sqrt{Dt} \tag{B.13}$$

Results and discussion The influence of the temperature on the diffusion coefficient for aqueous maltose solutions with maltose concentrations of 0, 52, 74 and 82 % (w/w) is shown in Table B.1 and Fig. B.4. From the figure it can be seen that the temperature dependence may reasonably be described by the Arrhenius-type equation.

$$D = D_0 \exp(-\Delta E/RT) \tag{B.14}$$

As the slopes of the lines in the figure are proportional to the activation energy ΔE, it is found that the activation energy increases with rising sugar concentrations.

In Fig. B.5 the logarithm of the diffusion coefficient is plotted as a function of the mole fraction maltose. Both from this figure and from Figs B.1 and B.2 we get the impression that in the intermediate concentration ranges a linear dependence of the logarithm of the mutual diffusion coefficient on the mole fraction is a fairly
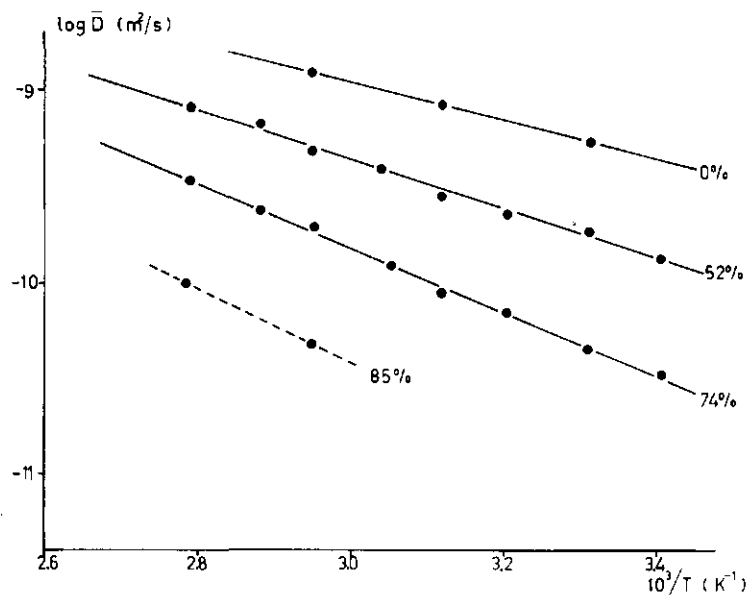

Fig. B.4. Effect of temperature on the diffusion coefficients of aqueous maltose solutions. Numbers on lines indicate maltose concentrations (%-w/w).
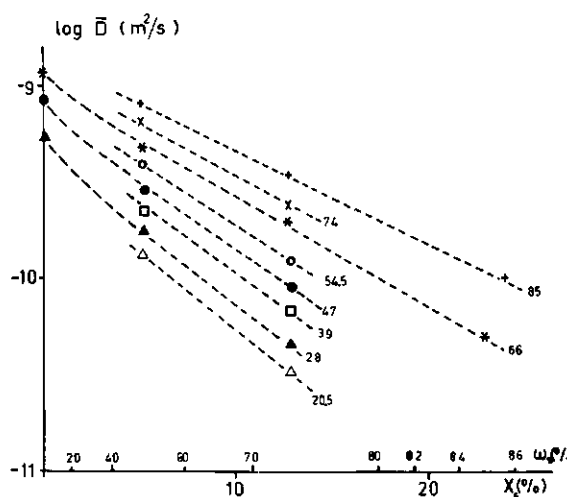
77

Fig. B.5. Effect of concentration on the diffusion coefficients of aqueous maltose solutions. Numbers on lines indicate temperatures (°C).

good fit. This relation remains true for different temperatures. Hence we can conclude that in this range the activation energy ΔE is also a linear function of the mole fraction. A similar relation was found for glucose and sucrose by Gladden & Dole (1953).

On the basis of the relations observed we have described the diffusion coefficient in the range 20–85 °C and 50–85 % (w/w) maltose by Eqn (B.15) in Table B.2. For the sake of comparison we add similar formulae for glucose and sucrose as based on Gladden & Dole (1953) and English & Dole (1950).

Extrapolation of these figures is obviously dangerous and does not necessarily provide a safe prediction of the properties of maltose solutions outside the range for which data are available. If we do extrapolate all the same, it is because for the purpose of process calculations in this study we need data which give an indication of the magnitude of the diffusion coefficient in real systems of the maltose solution type. Therefore, although these figures are based on measurements of a real system, they must be considered as purely hypothetical outside the safe range. Yet we consider them to be the best available for the given purpose.

Table B.2. Effect of composition and temperature on the diffusion coefficient for water-sugar systems.

maltose	$\log D = -7.870 - 9.40(x + 0.194)\dfrac{548-T}{T}$	(B.15)
sucrose	$\log D = -8.209 - 17.8(x + 0.121)\dfrac{447-T}{T}$	(B.16)
glucose	$\log D = -8.405 - 15.9(x + 0.147)\dfrac{397-T}{T}$	(B.17)

(B.16) based on Gladden & Dole (1953)
(B.17) based on English & Dole (1950)

78

Extrapolation with respect to temperature has only been done in a narrow range outside the field of the measurements. It was based on the Arrhenius-type Eqn (B.14) which was given already by Barrer (1942), and which is in common use for this purpose. The results shown in Fig. B.4, seem to justify the extrapolation.

Extrapolation to the lower water concentration range is much more dangerous. No figures for the diffusion coefficients at very low water concentrations are available. Only the magnitude might be comparable with that for solids, say 10^{-18} m²/s. English & Dole (1950) described the diffusion coefficient as changing linearly with the weight percentage of the sugar, but this leads to a value of zero for concentrations of the order of 80 % (w/w) sugar. Although the diffusion coefficients may indeed be very low at that concentration, absolute zero is not realistic. Gladden & Dole (1953) described the logarithm of the diffusion coefficient as changing linearly with the mole fraction and Vignes (1966) showed this relation to be true for a large number of ideal systems. For non-ideal systems Vignes included a correction factor of thermodynamic origin.

His relation reads

$$D = (D_{12}^0)^{x_1} \cdot (D_{21}^0)^{x_2} \left(1 + \frac{d \ln \gamma_1}{d \ln x_1}\right) \tag{B.18}$$

Fig. B.6 shows the values of the logarithm of the correction value on the basis of the activity measurements described in Section B.1.3. If we divide the diffusion coefficients observed by the correction factor, a relation is indeed found which may be considered to be linear. This is shown in Fig. B.7. Extrapolation of this line and of the figures for the activity coefficient to calculate the diffusion coefficient would lead to very low values $(10^{-21}$ m²/s) even for solid systems and an increase of the slope of the dotted line. On the other hand the data of Nishijima & Oster (1960)
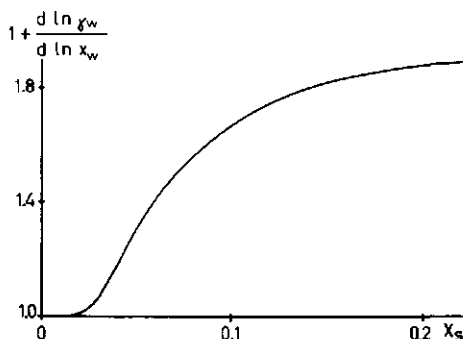

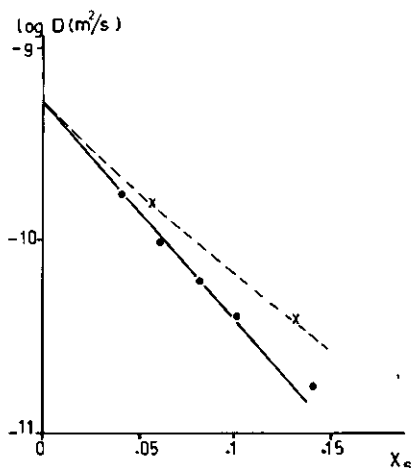Fig. B.6. Values of the correction term in Eqn (18) as a function of the mole fraction of maltose.

Fig. B.7. Diffusion coefficients for aqueous solution of maltose (– – –) and the values corrected for non-ideal behaviour (——).
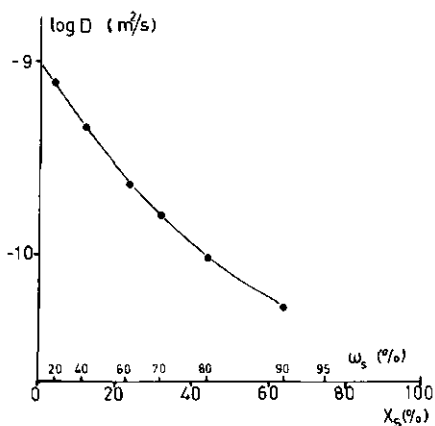
Fig. B.8. Difusion coefficients of aqueous solutions of glycerol at 25 °C (Nishijima & Oster, 1960).

for glycerol which are the only data available for a comparable system over the whole concentration range (Fig. B.8) lead us to expect a decrease of the slope of the dotted line. Obviously no choice can be made on basis of the figures available and therefore we have simply assumed a straight relation as indicated in Eqn (B.15). The result is shown in Table B.3. It must be interpreted with much caution.

B.1.2 Density of maltose solutions

The diffusion equations derived in Appendix A require data on the (molar) density of the solutions under consideration. Thus I measured the densities of supersaturated maltose solutions in the low water concentration range. Figures in the range below 50 % (w/w) maltose were given by Ueadaira & Uedaira (1969). For the
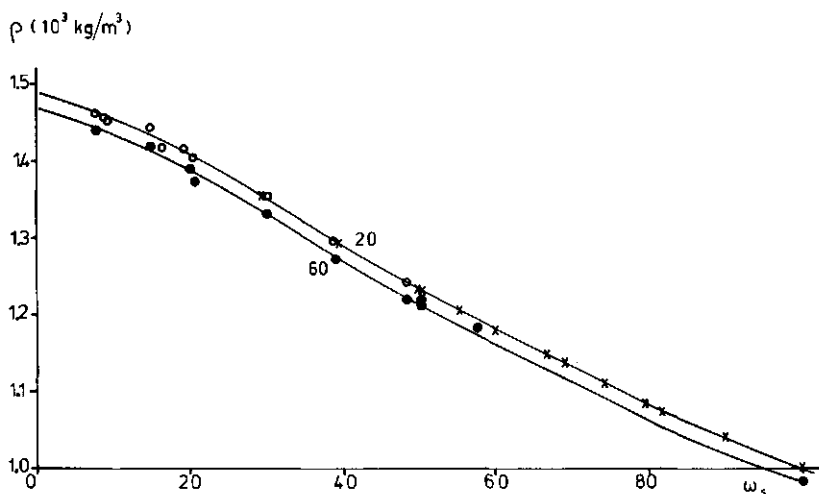

Fig. B.9. Densities of aqueous maltose solutions. 25 °C: ○ (present work) and × (Ueadaira & Uedaira, 1969) 60 °C: ● present work.

80

Table B.3. Extrapolated diffusion coefficients of aqueous maltose solutions according to Eqn (15).

| %MOIST=	MOL FR=	I=0	20	40	60	70	80	90	100 DEGREE C
100	.000	1.96x-10	3.40x-10	5.77x-10	8.97x-10	1.10x-09	1.33x-09	1.59x-09	1.88x-09
90	.006	1.73x-10	3.13x-10	5.25x-10	8.27x-10	1.02x-09	1.24x-09	1.49x-09	1.77x-09
80	.013	1.48x-10	2.73x-10	4.67x-10	7.44x-10	9.27x-10	1.14x-09	1.38x-09	1.65x-09
70	.022	1.21x-10	2.30x-10	4.03x-10	6.59x-10	8.24x-10	1.02x-09	1.24x-09	1.50x-09
60	.034	9.38x-11	1.84x-10	3.32x-10	5.54x-10	7.07x-10	8.84x-10	1.09x-09	1.33x-09
50	.050	6.60x-11	1.36x-10	2.56x-10	4.46x-10	5.74x-10	7.29x-10	9.14x-10	1.13x-09
40	.073	3.98x-11	8.40x-11	1.76x-10	3.22x-10	4.26x-10	5.53x-10	7.08x-10	8.95x-10
38	.079	3.40x-11	7.87x-11	1.59x-10	2.97x-10	3.94x-10	5.15x-10	6.63x-10	8.43x-10
36	.086	3.04x-11	6.97x-11	1.44x-10	2.71x-10	3.63x-10	4.77x-10	6.18x-10	7.89x-10
34	.093	2.60x-11	6.03x-11	1.28x-10	2.45x-10	3.31x-10	4.38x-10	5.71x-10	7.34x-10
32	.101	2.19x-11	5.25x-11	1.12x-10	2.20x-10	2.99x-10	3.98x-10	5.23x-10	6.77x-10
30	.109	1.81x-11	4.45x-11	9.75x-11	1.94x-10	2.66x-10	3.59x-10	4.75x-10	6.20x-10
28	.119	1.46x-11	3.70x-11	8.31x-11	1.69x-10	2.35x-10	3.19x-10	4.26x-10	5.61x-10
26	.130	1.15x-11	3.00x-11	6.94x-11	1.45x-10	2.03x-10	2.79x-10	3.77x-10	5.01x-10
24	.143	8.72x-12	2.37x-11	5.66x-11	1.22x-10	1.73x-10	2.40x-10	3.28x-10	4.41x-10
22	.157	6.37x-12	1.80x-11	4.48x-11	9.96x-11	1.43x-10	2.02x-10	2.80x-10	3.81x-10
20	.174	4.43x-12	1.32x-11	3.42x-11	7.49x-11	1.16x-10	1.66x-10	2.33x-10	3.22x-10
18	.193	2.90x-12	9.14x-12	2.49x-11	6.01x-11	8.49x-11	1.31x-10	1.88x-10	2.64x-10
16	.216	1.75x-12	5.91x-12	1.71x-11	4.35x-11	6.67x-11	9.96x-11	1.46x-10	2.09x-10
14	.244	9.64x-13	3.50x-12	1.09x-11	2.95x-11	4.65x-11	7.14x-11	1.07x-10	1.57x-10
12	.278	4.63x-13	1.84x-12	6.24x-12	1.43x-11	2.99x-11	4.75x-11	7.35x-11	1.11x-10
10	.321	1.78x-13	8.19x-13	3.11x-12	1.00x-11	1.72x-11	2.84x-11	4.58x-11	7.19x-11
8	.377	5.24x-14	2.67x-13	1.26x-12	4.62x-12	8.35x-12	1.46x-11	2.48x-11	4.09x-11
6	.452	1.43x-14	7.01x-14	3.73x-13	1.62x-12	3.17x-12	5.97x-12	1.09x-11	1.91x-11
4	.558	1.02x-15	9.44x-15	6.63x-14	3.67x-13	8.02x-13	1.68x-12	3.36x-12	6.50x-12
2	.721	2.95x-17	4.44x-16	4.73x-15	3.80x-14	9.81x-14	2.40x-13	5.60x-13	1.25x-12
0	1.000	6.67x-20	2.30x-18	5.05x-17	1.65x-16	2.64x-15	8.51x-15	2.57x-14	7.32x-14

81

$\bar{V}$ ($10^3 m^3$/kg)

25 °C
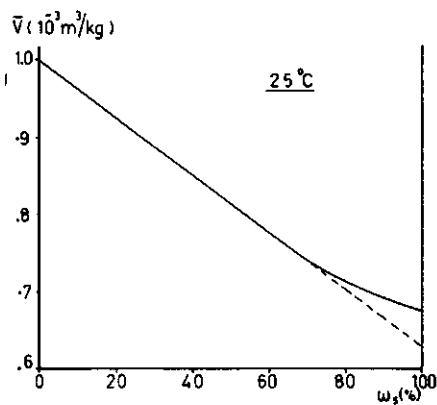
Fig. B.10. Specific volume of aqueous maltose solutions.

measurements pycnometer flasks of 50 cm³ were filled for about half with a solution of known composition and weight. At the low water concentration the solution had to be slightly heated before being transferred. One drop of the solution was used to check the concentration refractometrically (Section B.1.4). The pycnometer flasks were adjusted to volume with paraffin oil of known density, put in a thermostat bath at 25 or 60 °C (± 1 °C), de-aerated with a water aspirator and again kept for one hour at the temperature indicated. Subsequent weighing of the filled pycnometer enabled us to calculate the density of the maltose solution. Fig. B.9 shows the result. From a plot of the specific volume against the % (w/w) (Fig. B.10) it can be seen that at least for the solutions at lower maltose concentrations assumption of constant partial volumes is reasonable. For process calculations specific volumes of

18×10^{-6} m³/mole for water and
221×10^{-6} m³/mole for maltose were used.

No correction for a change with the temperature was made.

B.1.3   Vapour-liquid equilibria of maltose solutions

The rate of water loss from solutions depends on the water vapour pressure at the surface. Hence data were needed on the water activity of concentrated maltose solutions. The figures reported by Heiss (1968) were not considered to be sufficiently reliable.

Measurements were taken with two methods. At 20 °C the water activities of solutions of between 0 and 90 % (w/w) maltose were measured by equilibrating amounts of about 100 g maltose solution with air, which was continuously circulated through an Aqmel dew point meter. The water activity is given by the ratio between the saturated water vapour pressure at the dew point and the saturated water vapour pressure at 20 °C.

In a second series of measurements water activities of solutions of between 0 and 50 % (w/w) maltose were determined from the freezing point depression of these solutions. A supersaturated solution of about 80 % (w/w) maltose in water

82

was mixed with ice which was allowed to melt for varying times before the mixture was transferred to a dewar flask. After equilibration the temperature of the resulting mixture was measured accurate up to 10^{-3} K with a Boltzmann thermometer. The concentration of the equilibrium solution was measured with a refractometer (Section B.1.4). The water activity at the freezing point is given by

$$m \cdot a_w|_{\text{freezing point}} = -\frac{18}{1000}\frac{\Delta T}{K} \qquad (B.19)$$

with ΔT = observed freezing point depression

K = molar freezing point depression (1.855 K/mol/1000 g H$_2$O)

m = solute per 100 g

Although the results of the two series of measurements can strictly speaking not be compared, because they were not obtained at equal temperatures, they are both given in Fig. B.11. According to Kozak (1968) the activity figure can conveniently be represented by

$$a_w = \gamma_w \cdot x_w \qquad (B.20)$$

$$\gamma_w = \exp(A_1 x_s^2 + A_2 x_s^3) \qquad (B.21)$$

The results in Fig. B.11 fit in well with this equation, if the numerical values

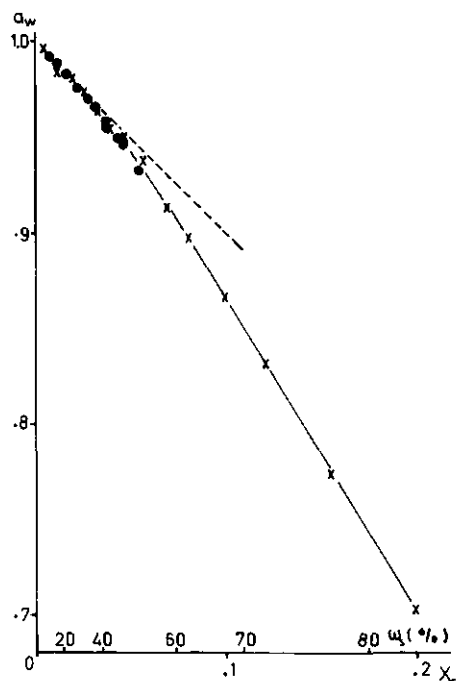$$A_1 = -4.49 \qquad (B.22a)$$

$$A_2 = 5.53 \qquad (B.22b)$$

Fig. B.11. Water activities of aqueous maltose solutions: × from measurement of the equilibrium relative humidity in the vapour phase at 20 °C, ● from measurement of the freezing point depression, (——) fit of the data by Eqns B.20–B.22.

83

are used. This relation is indicated in Fig. B.11 by the solid line. As the common experience is that the heat of sorption for sugar solutions is rather low (which is also substantiated by the absence of significant differences between the activities at 20 °C and below 0 °C) and as no accurate values were available Eqn (B.21) was used with the constants (B.22) for the estimation of the water vapour pressure over the whole temperature range of the process calculations. Both the disregard of the temperature influence and the extrapolation of the figures to low water concentrations are obviously sources of error, the size of which is difficult to estimate.

B.1.4 *Refractive indices of maltose solutions*

Maltose in crystalline form holds one molecule of water per mole maltose. During separation from a saturated solution and drying of the crystals, different amounts of water are retained. Thus the amounts of crystal water in commercial products of maltose $C_6H_{12}O_6 \cdot H_2O$ are seldom in accordance with the given formula. Determination of the water content by drying under moderate conditions does not result in removal of all crystal water. Drying water under vigorous conditions, such as by heating over P_2O_5 leads to partial decomposition of the maltose. Hence the results obtained in water analyses are somewhat arbitrary anyhow. Because of the simplicity of the method the concentrations of maltose solutions were determined throughout this work with a refractometer, using the data of McDonald (1951) as a standard. This author gives for the refractive index

$$n^{20} = 1.33299 + 1.38914 \cdot 10^{-3}\rho_s + 4.7602 \cdot 10^{-6}\rho_s^2 + 2.0933 \cdot 10^{-8}\rho_s^3$$
$$- 6.124 \cdot 10^{-11}\rho_s^4 \qquad (\omega_s < 65) \tag{B.23}$$

This equation was used over the whole concentration range and checked for higher concentration by diluting into the safe range and calculating the original concentration. This obviously gives a multiplication of the error with decreasing water contents. Both owing to this effect and because of the difficulty in handling highly viscous solutions, the error may rise to 0.5 % (w/w) at a concentration of 90 % (w/w). This error is even more marked if expressed in terms of mole fractions.

B.2 Properties of moist air

The water vapour pressures between temperatures 273 and 373 K were given by Wexler & Greenspan (1971) in the form

$$P_{sat} = \exp\left(\sum_{i=0}^{n} E_i T^{i-1} + EB \ln T\right) \qquad \text{pascal} \tag{B.24}$$

In the calculations their formula was used with $n = 2$ in which

$E_0 = -7.2465822 \times 10^3$, $E_1 = 7.7641232 \times 10^1$,

$E_2 = 5.7447142 \times 10^{-3}$, $EB = -8.2470402$.

In order to evaluate the possibility of using this formula also outside the range indicated I compared it with the formula of Tanishita & Nagashina (1968)

84

$$\frac{P}{P_{\text{crit}}} = \exp\left\{\frac{1}{T_r} \times \frac{\sum\limits_{i=1}^{5} A_i (1 - T_r)^i}{1 + \sum\limits_{j=1}^{2} B_j (1 - T_r)^j}\right\} \tag{B.25}$$

in which $A_1 = -7.69123400$, $A_2 = -26.0802370$, $A_3 = -168.170655$, $A_4 = +64.2328550$, $A_5 = -118.964623$, $B_1 = +4.16711700$, $B_2 = +20.9750680$, $T_r = T/T_{\text{crit}} = T/647.3$, $P_{\text{crit}} = 221.25$ bar.

The relative difference between the results is less than 0.03 % within the range indicated and rises to 0.1 % at 130 °C and 1 % at 200 °C. Hence, for our calculations the simpler Wexler & Greenspan formula was used.

Other physical properties of the air-water vapour system used in the calculations were
– The diffusion coefficient of water in air (Mason & Monchick, 1965)

$$D = 5.28 \times 10^{-9} T^{\frac{3}{2}} \, \text{m}^2/\text{s} \tag{B.26}$$

This diffusion coefficient was assumed to be independent of the composition. Densities of the vapour phase were calculated on the basis of the gas law

atmospheric pressure $= 10^5$ pascal

gas constant $R = 8.314$ J/mol · K

– The heat capacity of

water vapour   34.7 J/mol · K

air   28.8 J/mol · K

Air was assumed to behave as a one component system with a molecular weight of 28.8×10^{-3} kg/mol.
– The thermal conductivity of air is approximated by Taylor expansion around $T = 373$ (Mason & Monchick, 1965)

$$\lambda = 0.45 \times 10^{-2} + 0.726 \times 10^{-4} T \quad \text{J/m} \cdot \text{s} \cdot \text{K} \tag{B.27}$$

– The enthalpy change of water upon evaporation:

$$\Delta \bar{H} = 4.5 \times 10^4 - 4.05 \times 10 (T - 273.15) \quad \text{J/mole} \tag{B.28}$$

85

Appendix C. Equations for the coupled heat and mass transfer in a cellular model

Mass transport inside a droplet can be described by Eqn (25b). Diffusion and heat transport in the continuous phase can be described relative to a reference component. For this purpose we shall ignore ternary diffusion and consider air as 'one component' (ideal gas; molecular weight 28.8). Diffusion in the gas phase can then also be described by Eqn 25b

The energy equation can be written as

$$cc_p \frac{D'T}{Dt} = -\nabla \cdot \mathbf{q} + \sum_{i=1}^{n} (\bar{H}_i \nabla \cdot \mathbf{J}_i^r) \tag{C.1}$$

Stress and buoyant forces are neglected and the system is assumed to be isobaric. The total energy flux consists of a conductive, a diffusive and a thermodiffusive term and we neglect the last one

$$\mathbf{q} = \mathbf{q}^c + \mathbf{q}^d \tag{C.2}$$

In this equation we may substitute

$$\mathbf{q}^c = -\lambda \nabla T \tag{C.3}$$

$$\mathbf{q}^d = \sum_{i=1}^{n} \bar{H}_i \mathbf{J}_i^r \tag{C.4}$$

Hence,

$$cc_p \frac{D'T}{Dt} = \nabla \cdot [\lambda \nabla T] - \sum_{i=1}^{n} \mathbf{J}_i^r \cdot \nabla \bar{H}_i \tag{C.5}$$

And assuming ideal behaviour of the gas

$$\nabla \bar{H}_i = c_{pi} \nabla T \tag{C.6}$$

In a binary system the water flux is given by (Appendix A)

$$\mathbf{J}_w^r = c_r D \nabla (c_w / c_r) \tag{C.7}$$

and the flux of the reference component is zero per definition. Substituting furthermore

$$c_p = x_w c_{pw} + x_r c_{pr} \tag{C.8}$$

and using transformations 32–34 we directly find the energy equation in the transformed coordinates

$$\frac{D'T}{Dt} = \frac{c_r}{cc_p} \frac{\partial}{\partial z} \left(r^4 \lambda c_r \frac{\partial T}{\partial z} \right) + \frac{r^4 s c_{pw}}{u c_{pw} + c_{pr}} \frac{\partial u}{\partial z} \frac{\partial T}{\partial z} \tag{C.9}$$

86

The six boundary conditions to the three second order parabolic differential equations are:

1. No concentration gradient in the centre of the droplet

$$\frac{\partial u}{\partial z} = 0 \quad \text{for} \quad z = 0 \tag{C.10a}$$

2. Fluxes in both phases are equal at the vapour-liquid interface

$$s\frac{\partial u}{\partial z} = s'\frac{\partial u'}{\partial z} \quad \text{for} \quad z = Z \tag{C.10b}$$

3. Local equilibrium at the interface

$$u' = f(u, T) \quad \text{for} \quad z = Z \tag{C.10c}$$

4. The heat flux towards the interface is used to raise the temperature of the droplet and to raise the enthalpy of the evaporating water

$$r^4\left(-\lambda c_r \frac{\partial T}{\partial z} + Ls'\frac{\partial u'}{\partial z}\right) = \left(c_{pw}\int_0^Z u \, dz + c_{pr}Z\right)\frac{\partial T}{\partial t} \quad \text{for} \quad z = Z \tag{C.10d}$$

5 and 6: No exchange through the outer wall of the cell

$$\frac{\partial T}{\partial z} = 0 \quad \text{for} \quad z = Z_{os} \tag{C.10e}$$

$$\frac{\partial u'}{\partial z} = 0 \quad \text{for} \quad z = Z_{os} \tag{C.10f}$$

The coupled heat and diffusion equations were solved by an implicit finite difference method.